

**Characterization of new protein kinases of the EVH1 domain containing  
protein VASP and identification of binding partners for  
a new EVH1 domain of the Spred2 protein:  
A case study on protein interactions of EVH1 domain containing proteins**

Dissertation zur Erlangung des  
naturwissenschaftlichen Doktorgrades  
der Bayerischen Julius-Maximilians-Universität Würzburg

vorgelegt von  
**Naresh Reddy Thumati**  
aus Kodada, Indien

Würzburg, 2007

Eingereicht am: .....

Mitglieder der Promotionskommission:

Vorsitzender: .....

Gutachter: Prof. Dr. U. Walter

Gutachter: Prof. Dr. R. Benavente

Betreuer der Arbeit: Dr. rer. nat. T. Jarchau

Tag des Promotionskolloquiums: .....

Doktorurkunde ausgehändigt am: .....

### Eidesstattliche Erklärungen

Hiermit erkläre ich ehrenwörtlich, dass die vorliegende Dissertation **„Characterization of new protein kinases of the EVH1 domain containing protein VASP and identification of binding partners for a new EVH1 domain of the Spred2 protein: A case study on protein interactions of EVH1 domain containing proteins”** selbständig am Institut für Klinische Biochemie und Pathobiochemie der Universität Würzburg angefertigt wurde und dass ich keine anderen als die angegebenen Quellen und Hilfsmittel benutzt habe.

Weiterhin versichere Ich, dass die vorliegende Dissertation weder in gleicher oder ähnlicher Form noch nicht in einem andern Prüfungsverfahren vorgelegen hat und ich bisher noch keine akademische Grade erworben oder zu erwerben versucht habe.

Hiermit bewerbe ich mich erstmals um den Doktorgrad der Naturwissenschaften der Bayerischen Julius-Maximilians-Universität Würzburg

**Naresh Reddy Thumati**

Würzburg, 14.12.2007

*I dedicate this work*

*to*

*“My loving father”*

*“I bow before you having achieved what you dreamt and thought I could”*

- Yours son

## Acknowledgements

I express my heartfelt gratitude and indebtedness to Prof. Dr. Ulrich Walter for providing me an opportunity to work in his group. I thank him for his support, and help extended whenever I approached him through out my course.

I am grateful to my “Mentor” Dr. T. Jarchau for his invaluable guidance, constant enthusiasm for science that helped me to develop my scientific skills all that I own today. I admire his deep conviction to science (I call it as his passion!!). I am thankful to him for being instrumental in planning and shaping up my thesis in an unimaginable way, without whom I stand nowhere in this rapidly growing science. Words cannot replace my gratitude for his moral support when I was struggling between the hard core of my life and my dreams to have my PhD degree.

I would like to acknowledge to Dr. Christian Freund and Dr. Linda Ball for accepting and supporting me to work at FMP, Berlin. My heartfelt appreciation goes to DR. Kirill for his intellectual, humeral support and valuable time during my stay at Berlin. Also, I thank Mark for helping me in lipid interaction studies.

I thank each member of my institute especially Gunnar (Sir!!! sniff control??), Petra, Elfi, Barbara, Antonja, Leif, and many more for being good friends and made my time more lively here. I thank each and every one of my personal friends whom I can not list all in a single page here for their friendship and amicable support in crossing each and every hurdle of my life.

I am indebted to my parents Venkatravama and (late) Venkat Rami Reddy for bringing me up to here and spending their whole life just in tuning a good future for me. I am also indebted to my sister Sudha for her innocent support and love towards me. My heartfelt gratitude to my cousins: Suresh, Surender and Nagi for their everlasting love and support, especially during hard times when I lost my father. Also, I am thankful to my in-laws and other family members for their care and love towards me.

Finally, I have to acknowledge her for bearing me every second though I was never bound to the given time or word throughout my PhD. So, I take immense pleasure to acknowledge my wife for her love, caring, understanding and encouragement which boosted me towards my success.

I gratefully acknowledge the financial support by the Sonderforschungsbereich SFB 355, SFB 688 given by Deutsche Forschungsgemeinschaft (DFG) and made this project successful.

<b>TABLE OF CONTENTS</b>	<b>PAGE NO</b>
<b>1. SUMMARY (ZUSAMMENFASSUNG)</b>	<b>1</b>
1.1. Summary	1
1.2. Zusammenfassung	3
<b>2. INTRODUCTION</b>	<b>5</b>
2.1. A portrait of VASP and Spred proteins which share a conserved EVH1 adapter domain but are involved in distinct signal transduction pathways	5
2.1.1. VASP - a cytoskeletal phosphoprotein harboring an EVH1 domain	5
2.1.1.1. Domain organisation	5
2.1.1.2. VASP EVH1 domain	7
2.1.1.3. Family members	8
2.1.1.4. Signalling pathways	8
2.1.1.5. Physiological functions	9
2.1.2. Spred - an inhibitor of the Ras/Raf/MAP kinase pathway harboring a new class of EVH1 domains	11
2.1.2.1. Domain organisation	11
2.1.2.2. Spred EVH1 domain	12
2.1.2.3. Family members	13
2.1.2.4. Signalling pathways	14
2.1.2.5. Physiological functions	14
2.2. A classification scheme of EVH1 domains: portrait of a conserved domain family	15
2.2.1. EVH1 domains recognize proline-rich sequences in their binding partners in a stereo-specific manner	15
2.2.2. EVH1 domains are classified into four groups based on similarity of their sequences and recognition pattern of their ligands	17
2.2.2.1. Class 1: The Ena/VASP class	18
2.2.2.2. Class 2: The Homer/Vesl class	18
2.2.2.3. Class 3: The WASP/N-WASP class	19
2.2.2.4. Class 4: The Spred class	20
2.3. Approaches for identification and characterization of interaction partners of protein kinases and adaptor proteins	20

---

2.3.1. The role of protein interactions in biological signal transduction networks	22
2.3.2. Identification of candidate protein kinases for VASP and elucidation of phosphorylation pathways in serum stimulated cells	24
2.3.3. Identification of interaction partners for a new EVH1 domain of the Spred2 protein	26
<b>3. AIM OF THE WORK</b>	<b>30</b>
<b>4. MATERIALS AND METHODS</b>	<b>32</b>
4.1. Materials	32
4.1.1. Chemicals	32
4.1.2. Primary antibodies	33
4.1.3. Secondary antibodies	33
4.2. Methods	34
4.2.1. Cell culture	34
4.2.1.1. Solutions	34
4.2.1.2. Cell lines	34
4.2.1.3. Isolation of MCFB Cells (+/+)	34
4.2.1.4. Cell passage, counting, freezing and storage	35
4.2.1.5. Cell culture experimental set up	35
4.2.2. Protein biochemistry	37
4.2.2.1. Solutions	37
4.2.2.2. SDS- polyacrylamide gel electrophoresis (PAGE)	37
4.2.2.3. Immunoblotting	37
4.2.2.4. Protein expression and purification	38
4.2.2.5. <sup>1</sup> H NMR spectroscopy	38
4.2.3. Molecular biology	38
4.2.4. Bacterial two-hybrid system	39
4.2.4.1. Solutions	39
4.2.4.2. Preparation of different selection medium plates	40
4.2.4.3. The protocol for co-transformation	40
4.2.4.4. Plating method	41
4.2.4.5. Amplification of cDNA library	41
4.2.4.6. Library screening	42
4.2.4.7. Physical characterization of dual resistant clones	44
4.2.5. Phage display technology	45

---

4.2.5.1. Solutions	45
4.2.5.2. Helper phage amplification	46
4.2.5.3. The protocol for panning	46
4.2.5.4. Titration of phages	48
4.2.5.5. Enrichment factor	48
4.2.5.6. Amplification	49
4.2.5.7. Characterization of phagemids by colony PCR	51
4.2.6. Protein-phospholipid interaction assays	52
4.2.6.1. Solutions	52
4.2.6.2. Solid phase overlay assay	52
4.2.6.3. Preparation of multilamellar vesicles (MLVs)	53
<b>5. RESULTS</b>	<b>58</b>
5.1. Identification of protein kinases participating in serum-stimulated phosphorylation of VASP and elucidation of their order of action	58
5.1.1. Serum treatment of MCFB cells stimulates phosphorylation of VASP at Ser 157 but not at Ser-239	58
5.1.1.1. An interaction graph model describing serum-stimulated VASP phosphorylation forms a conceptual basis for experimental identification of the protein kinases involved	59
5.1.2. Serum activated PKCs, but not Rho kinases are involved in serum stimulated VASP phosphorylation at Ser-157	61
5.1.3. PKA, but not PKG is required for serum stimulated phosphorylation of VASP at Ser-157	64
5.1.4. Serum stimulated PKCs involved in VASP phosphorylation are members of the Bis I sensitive and phorbol ester regulated classical isoforms of protein kinase C	68
5.1.5. Serum stimulated VASP phosphorylation is mediated by a sequential action of classical PKC isoforms and PKA	72
5.2. In search for binding epitopes of the Spred2 EVH1 domain: Genetic screening of a cDNA expression library using a bacterial two-hybrid system	77
5.2.1. Motivation for the experimental approach chosen	77
5.2.2. Introduction to the bacterial two-hybrid system and overview of the experimental procedure	77
5.2.3. Construction of bait and target expression plasmids and establishment of the bacterial two-hybrid system for detection of EVH1 ligand interactions	80



---

5.2.4. Human brain cDNA library screening for candidate sequences harbouring binding epitopes of the Spred2 EVH1 domain and their physical and genetic characterization	83
5.2.5. Summary	88
5.3. In search for binding epitopes of the Spred2 EVH1 domain: Genetic screening using a phage display library	90
5.3.1. Motivation for the experimental approach chosen	90
5.3.2. Introduction to phage display technology and overview of the experimental procedure	91
5.3.3. Preparation and characterization of the bait fusion protein and its controls	94
5.3.4. M13 phage display peptide library screening for binding epitopes of the Spred2 EVH1 domain and physical characterization of phagemids from the isolated phage variants	96
5.3.5. Summary	99
5.4. In search for binding epitopes of the Spred2 EVH1 domain: Biochemical screening using in-vitro binding assays for non-peptidergic interactions	100
5.4.1. Motivation of the experimental approach chosen	100
5.4.2. Introduction to protein-phospholipid binding assays and overview of the experimental procedure	102
5.4.3. Preparation and characterization of the Spred2 EVH1 domain and the control proteins	103
5.4.4. Biochemical screening for phospholipid interactions of the Spred2 EVH1 domain	104
5.4.5. Summary	106
<b>6. DISCUSSION</b>	<b>108</b>
<hr/>	
6.1. Protein interactions of the EVH1 domain containing proteins VASP and Spred2	108
6.1.1. Deciphering the serum stimulated VASP phosphorylation at Ser-157	109
6.1.2. Identification of unknown binding epitopes for a new class of EVH1 domains	116
6.2. Conclusions and open questions	123
<b>7. REFERENCES</b>	<b>125</b>
<hr/>	
<b>8. ABBREVIATIONS</b>	<b>136</b>
<hr/>	
<b>9. CURRICULUM VITAE</b>	<b>138</b>
<hr/>	

## 1. SUMMARY (ZUSAMMENFASSUNG)

### 1.1. Summary

Protein interactions as mediated by catalytic or non-catalytic protein domains contribute to cellular signal transduction processes by covalent protein modification of or non-covalent binding to interaction partners. Ena/VASP homology 1 (EVH1) domains are found in different signal transduction proteins as N-terminal non-catalytic adaptor modules of ~ 115 amino acids sharing a common fold. By targeting their host proteins to subcellular sites of action they are involved in several signalling cascades which include protein phosphorylation and cytoskeletal reorganisation. In this study, protein interactions of the two EVH1 domain containing proteins VASP and Spred2 were studied according to their involvement in different and non-overlapping signal transduction pathways of the cell.

EVH1 domains were first described in the Ena/VASP protein family with the Vasodilator-stimulated phosphoprotein VASP being its founding member. As a cytoskeleton-associated protein VASP not only interacts with different proteins of the actin network but it is also a substrate for cAMP- and cGMP-dependent protein kinases. However the full complement of protein kinases targeting VASP as their substrate is still unknown. Here we used mouse cardiac fibroblast (MCFB) cells in order to study the phosphorylation status of VASP and identify new candidate protein kinases involved after serum stimulation of these cells. Using phosphosite-specific antibodies we found that serum stimulation induces a phosphorylation of VASP at Ser-157 in a time-dependent manner reaching its maximum after 90 min of stimulation. We developed an interaction graph model of possible candidate protein kinases involved. Using a pharmacological perturbation analysis with different combinations of specific protein kinase inhibitors and activators we excluded any contribution of cGMP-dependent protein kinase and Rho kinases to this process and identified a combined action of classical isoforms of PKCs and PKA in serum-stimulated VASP phosphorylation at Ser-157 positioning PKC upstream of PKA in this signalling pathway. We hypothesise that PKC receives an external stimulatory signal upon serum stimulation of MCFB cells which is passed either directly or indirectly to PKA which finally phosphorylates VASP at Ser-157.

A new EVH1 domain has been described recently in the Spred proteins (Sprouty related proteins containing an EVH1 domain) which are inhibitors of the Ras/Raf/MAP kinase pathway. Our laboratory has been involved in the elucidation of the atomic structure of the human Spred2 EVH1 domain by protein NMR spectroscopy (PDB 2JP2; 2007). A positively charged binding interface of this EVH1 domain suggests an interaction with negatively charged ligands;

however no interaction partners of this domain have been described so far. In the second part of this study, we used different genetic and biochemical screening methods to search for ligands of the Spred2 EVH1 domain. A bacterial two-hybrid system was established using a physically well characterized interaction of the VASP EVH1 domain with a panel of its ActA binding peptides as positive controls to screen a human brain cDNA expression library at different stringencies for candidate Spred2 EVH1 interaction partners. However none of the clones isolated could be genetically and physically validated to support Spred2 EVH1 specific interactions. An *in-vitro* screening of a 9-mer phage display peptide library using purified GST-Spred2 EVH1 fusion protein was performed together with a Fyn-SH3 fusion protein as a positive control. In contrast to the Fyn-SH3 domain the majority of phages isolated with the Spred2 EVH1 domain either carried no inserts or inserts with stop codons suggesting a highly non-specific interaction of the phage coat protein with the latter domain but neither the Fyn-SH3 domain nor the GST moiety. Isolation of a 13-mer proline-rich sequence was particularly surprising in this context. In order to address possible interactions of the Spred2 EVH1 domain with non-peptidic ligands protein-lipid interaction assays were performed. Quantitative binding studies to purified Spred2 EVH1 using a liposome sedimentation assay however excluded any interaction of candidate phospholipids of the phosphatidyl inositol phosphate class with the Spred2 EVH1 domain. A natively folded and thus binding-competent conformation of the purified proteins used was assessed independently by <sup>1</sup>H protein NMR spectroscopy. In summary the cumulative evidence of our genetic and biochemical screening experiments suggests that the still elusive Spred2 EVH1 ligand(s) may be formed of hydrophobic peptide epitopes larger than nine amino acids in size and carrying negative charge(s). A phosphorylation of Spred2 EVH1 binding epitopes by a post-translational modification should be seriously considered in future experiments.

## 1.2. Zusammenfassung

Proteininteraktionen, wie sie durch katalytisch oder nicht-katalytisch wirksame Proteindomänen vermittelt werden können, spielen eine wesentliche Rolle in zellulären Signaltransduktionsprozessen durch die kovalente Modifikation oder nicht-kovalente Bindung von Interaktionspartnern. Ena/VASP Homologie 1 (EVH1) Domänen finden sich als N-terminale, nicht-katalytische, etwa 115 Aminosäuren große und konserviert gefaltete Adaptormodule in vielen verschiedenen Signaltransduktionsproteinen. Indem sie ihre jeweiligen Wirtsproteine an deren subzellulärem Wirkort verankern helfen, sind sie an vielen verschiedenen Signalkaskaden wie z.B. Proteinphosphorylierungen oder Umbauprozessen des Zytoskeletts beteiligt. In diesen Arbeiten wurden Proteininteraktionen der beiden EVH1 domänen-haltigen Proteine VASP and Spred2 untersucht, die in nicht überlappenden Signaltransduktionswegen der Zelle vorkommen.

EVH1 Domänen wurden zuerst innerhalb der Ena/VASP-Proteinfamilie beschrieben, deren Gründungsmitglied das Vasodilator-stimulierte Phosphoprotein VASP ist. Als zytoskelett-assoziiertes Protein wechselwirkt VASP nicht nur mit verschiedenen Aktin-bindenden Proteinen, sondern ist auch ein Substrat der cAMP- und cGMP-abhängigen Proteinkinasen. Der vollständige Satz jener Proteinkinasen, die VASP als eines ihrer Substrate aufweisen, ist immer noch unbekannt. Hier haben wir kardiale Mausfibroblasten (MCFB) Zellen verwendet, um nach Serum-Stimulation dieser Zellen den Phosphorylierungsstatus von VASP zu bestimmen und daran beteiligte, neue Kandidaten-Proteinkinasen zu identifizieren. Mit Hilfe von Phosphorylierungsstellen-spezifischen Antikörpern konnten wir zeigen, dass eine Serum-Stimulation eine zeitabhängige Phosphorylierung von VASP an Serin 157 induziert, die ein Maximum 90 min nach Stimulation erreicht. Wir entwickelten ein Interaktionsgraphen-Modell möglicher Kandidaten-Proteinkinasen, die an diesem Prozess beteiligt sein könnten. Mit Hilfe pharmakologischer Perturbationsexperimente auf der Grundlage spezifischer Proteinkinase-Inhibitoren und Aktivatoren konnten wir einerseits eine Beteiligung der löslichen cGMP-abhängigen Proteinkinase und von Rho-Kinasen an diesem Prozess ausschliessen und andererseits die gemeinsame Beteiligung der klassischen Proteinkinase C Isoform(en) und der cAMP-abhängigen Proteinkinase nachweisen. In diesem Signalweg liegt dabei die Proteinkinase C stromaufwärts vor letzterer. Nach unserer Interpretation der Daten wird die PKC nach Serum-Stimulation der MCFB-Zellen aktiviert und aktiviert ihrerseits direkt oder indirekt die cAMP-abhängige Proteinkinase, die schliesslich VASP als proximales Substrat am Serin 157 phosphoryliert.

Eine neue EVH1 Domäne wurde kürzlich in den Spred Proteinen (Sprouty related proteins containing an EVH1 domain) beschrieben, die neue Inhibitoren im Ras/Raf/MAP-Kinase-

Signalweg darstellen. Unser Labor war an der NMR-gestützten Aufklärung der atomaren Struktur der Spred2 EVH1 Domäne beteiligt (PDB 2JP2; 2007). Die positiv geladene Bindungsfurche dieser EVH1 Domäne legt eine Interaktion mit anionischen Liganden nahe. Interaktionspartner für diese Domäne sind bisher jedoch nicht beschrieben worden. Im zweiten Teil dieser Arbeit verwendeten wir verschiedene genetische und biochemische Suchverfahren zur Identifizierung möglicher Spred2 EVH1 Liganden. Ein bakterielles Two-Hybrid-System mit der Spred2 EVH1 Domäne als Köderprotein wurde dazu etabliert unter Verwendung der physikalisch gut charakterisierten Wechselwirkung der VASP EVH1 Domäne mit ihren ActA Bindungspeptiden als eines positiven Kontroll-Interaktionspaars und zum verschiedenen stringenten Durchmustern einer humanen cDNA Expressionsgenbank aus Gehirn eingesetzt. Keiner der isolierten Klone ließ sich jedoch genetisch oder nach Sequenzierung in Hinblick auf eine Spred2 EVH1 spezifische Wechselwirkung validieren. Mittels gereinigtem GST-Spred2 EVH1 Protein wurde daher eine 9-mer Peptid-Genbank im Phage-Display-Verfahren durchgemustert unter Verwendung eines Fyn-SH3 Fusionsproteins als positiver Kontrolle. Im Gegensatz zu den Ergebnissen mit letzterer trugen die mit der Spred2 EVH1 Domäne isolierten Phagen überwiegend keine Inserts oder solche mit Stop-Codons, was eine unspezifische Wechselwirkung mit den Phagen-Hüllenproteinen dieser Domäne nicht jedoch der Fyn-SH3 Domäne oder des GST-Partners nahelegt. Die Isolierung einer 13-mer großen prolin-reichen Bindesequenz war in diesem Zusammenhang besonders überraschend. Um eine mögliche Wechselwirkung von Spred2 EVH1 mit nicht-peptidergen Liganden zu untersuchen, wurden Protein-Phospholipid-Interaktionsassays durchgeführt. Mittels quantitativer Bindungsstudien unter Verwendung der isolierten Domäne konnte eine Interaktion mit Kandidaten-Phospholipiden aus der Klasse der Phosphatidylinositolphosphate in einem Liposomen-Sedimentationsassay ausgeschlossen werden. Eine native Faltung und damit prinzipiell bindungskompetente Konformation(en) der gereinigten Proteine konnten mittels  $^1\text{H}$  Protein-NMR-Spektroskopie sichergestellt werden. Zusammengenommen lassen unsere Experimente vermuten, dass es sich bei den noch immer nicht dingfest gemachten Spred2 EVH1 Liganden um hydrophobe, negative geladene, mehr als neun Aminosäuren umfassende Peptidepitope handeln könnte. Bei deren Identifizierung in zukünftigen Experimenten sollte mit ihrer Phosphorylierung durch post-translationale Modifikationen gerechnet werden.

## 2. INTRODUCTION

### 2.1. A portrait of VASP and Spred proteins which share a conserved EVH1 adapter domain but are involved in distinct signal transduction pathways

#### 2.1.1. VASP - a cytoskeletal phosphoprotein harboring an EVH1 domain

Vasodilator Stimulated Phosphoprotein (VASP) was first characterized by Halbrügge and Walter [1] as a major cyclic nucleotide dependent phosphorylated protein in platelets and endothelial cells on stimulation with vasodilators. Referring to this observation it has been named as “vasodilator stimulated phosphoprotein”. VASP acts as a molecular adaptor associated with areas of dynamic membrane activity and is involved in cell adhesion and migration. It has binding sites for various proteins and is a well established substrate protein for protein kinase A (PKA or cAK) and protein kinase G (PKG or cGK) [2] along with other kinases as found recently [3, 4].

VASP is the founding member of Ena/VASP protein family comprising actin regulatory proteins harboring an N-terminal Ena/VASP homology 1 (EVH1) domain. VASP is expressed in almost all mammalian cell types with high levels of expression in platelets, blood vessels, spleen, stomach, intestine and lung. VASP is subcellularly highly concentrated at focal adhesions and stress fibres. Moreover, VASP localizes at cell-cell contacts of various cultured cells and is associated with highly dynamic membrane structures such as the leading edge. In both mouse and humans, the coding gene is composed of 13 exons with conserved exon-intron positions and the predicted amino acid sequences are 89% identical. The human VASP gene has been assigned to chromosome 19q13.2-q13.3, an extended region with homology to mouse chromosome 7 [5].

##### 2.1.1.1. Domain organisation

Human VASP is a 39 kDa protein containing 380 amino acids and running as a 46 kDa band in SDS-PAGE. Phosphorylation induced by vasodilator agents in intact cells or performed with purified components *in-vitro* shifts the molecular weight to an apparent molecular mass of 50 kDa [6]. VASP shows a tripartite domain organisation. In VASP, the N-terminal domain of about 115 amino acids is called Ena/VASP homology 1 domain (EVH1 domain) and the C-terminal domain is called Ena/VASP homology 2 domain (EVH2 domain) comprising about 130-190 amino acids separated by a low complexity regions including a proline-rich central region

of 60 to 90 amino acids in length (Fig.1). VASP harbors three phosphorylation sites at Ser-157, Ser-239 and Thr-278 which have been well characterized *in-vivo* and *in-vitro* [2, 7].

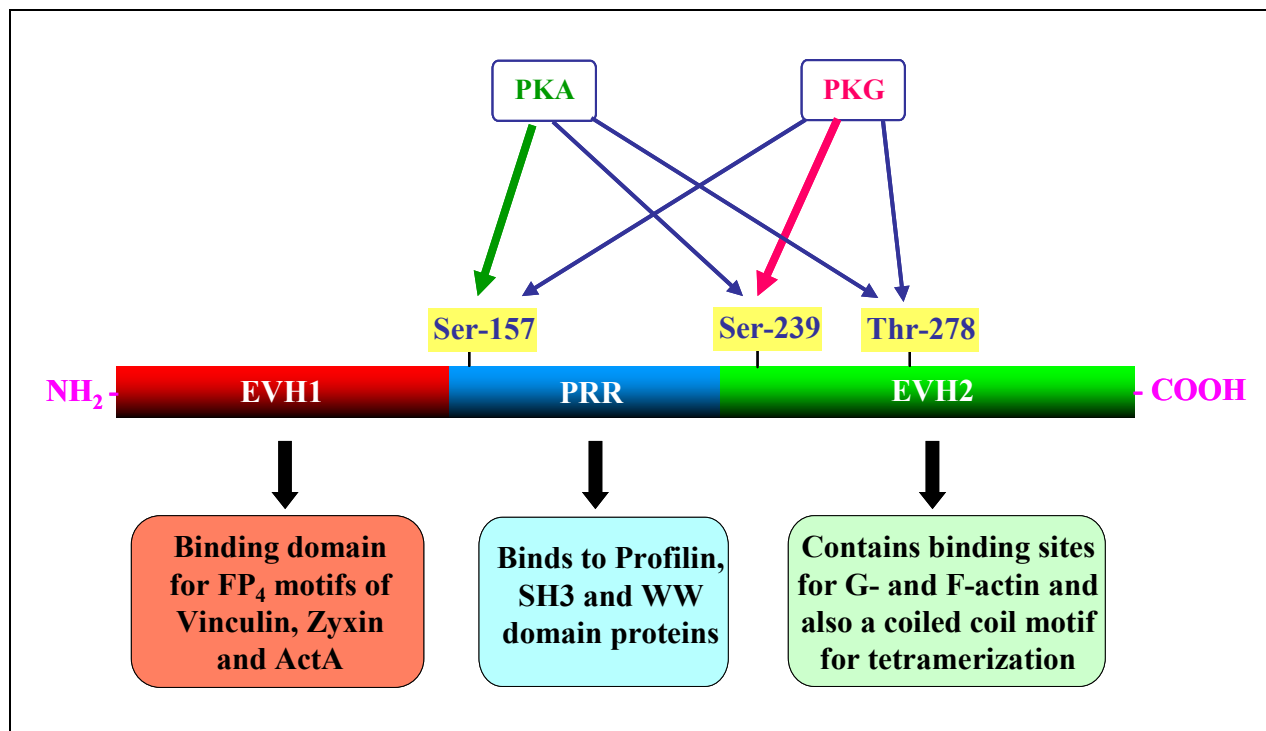


**Figure 1: Structural organization of human VASP, localization of phosphorylation sites and overview of binding partners.** EVH1 domain binds to FP<sub>4</sub> motifs, the proline-rich region (PRR) binds with SH3, WW domains and profilin and the EVH2 domain binds to G-actin, F-actin and is responsible for tetramerization. VASP is a substrate for both PKA and PKG. PKA preferentially phosphorylates Ser-157 and PKG preferentially Ser-239.

The proline-rich central region of VASP contains four copies of a GPPPPP (GP<sub>5</sub>) motif with three of them arranged in tandem. This proline-rich region binds to proteins containing Src Homology 3 (SH3) domains [8], WW domains [9] and profilin, an actin binding protein [10-12]. It is not clear which of these interactions are shared among all members of the Ena/VASP family. Profilin undergoes dimerization upon binding to the proline-rich region of VASP and promotes actin filament formation [10]. These data support a model of an action of VASP in the process of actin filament formation [13-15]. The phosphorylation sites for PKA and PKG in the central proline region of VASP do not seem to alter microfilament formation upon their phosphorylation.

The C-terminal EVH2 domain of VASP harbors three conserved blocks viz., a G-actin binding site, an F-actin binding site and a coiled coil region necessary for tetramerization [16-19]. The C-terminal oligomerization region of 45 residues is highly conserved and has been implicated in the oligomerization of individual members of Ena/VASP family. VASP behaves as tetramer and the conserved C-terminal block in the EVH2 domain is necessary and sufficient to mediate tetramer formation [16, 17]. The 1.3 Å resolution crystal structure of the tetramerization

domain reveals a parallel right-handed coiled-coil structure formed due to a 15-residue repeat in its amino acid sequence. Thus full-length tetrameric VASP adopts a “bouquet-like” quarternary structure [19]. The EVH2 domain harbors two phosphorylation sites (Ser-239 and Thr-278) which are suspected to regulate the functions of this domain [20-22]. Further characteristic functions of this domain have to be determined yet even though partial information has been disclosed including those on its role in subcellular localization and formation of multimers [11, 23].

#### 2.1.1.2. VASP EVH1 domain

The N-terminal EVH1 domain of Ena/VASP family members is necessary for binding of VASP to the focal adhesions [11, 21] at the ventral cell surface by connecting with FPPPP proline-rich motifs [24, 25] present in its binding partners vinculin [26], zyxin [27, 28] and also in the *Listeria* actin binding protein, ActA [29, 30] among others. These interactions of the EVH1 domain are likely to be important in a number of cellular processes that require regulated actin filament assembly [25] and recruitment of Ena/VASP proteins to specific sites within the cell.

The EVH1 domain structure of Ena/VASP family members has been elucidated both by X-ray crystallography [31, 32] and by NMR [24]. The EVH1 domain folds into a seven-stranded  $\beta$ -barrel with a single C-terminal  $\alpha$ -helix thus resembling a fold found in pleckstrin homology (PH), phospho tyrosine binding (PTB) and ran-binding domains (RanBD) [31-33]. VASP EVH1 domain shares structural homology with the WH1 (WASP homology 1) domain of another cytoskeletal protein Wiskott-Aldrich sndrome protein (WASP) and with N-terminal EVH1 domain of synaptic scaffold proteins (Homer/Vesl) and Sprouty related EVH1 domain containing (Spred) proteins [33] (see Chapter 2.2.2 for details).

Detailed binding studies showed that the phenylalanine and the first and final proline residues in the proline-rich FPX $\Phi$ P motifs (X = any amino acid,  $\Phi$  = hydrophobic amino acid) of VASP EVH1 binding partners are highly conserved which can not be replaced with natural amino acids without damaging the binding affinity (see Chapter 2.2.1). Recent substitution studies of these conserved residues with non-native amino acid derivatives (peptide building blocks) may open up the way for designing selective modulators of VASP function for biological studies and for the development of novel therapeutics for diseases involving pathologically altered cell adhesion or cell motility. Well characterized binding partners for the EVH1 domain of VASP which provide surface exposed proline-rich motifs to bind specifically are vinculin [34], zyxin [27] and other binding partners known so far viz., T-cell signalling Fyn-binding protein/SLP-76-associated protein (Fyb/SLAP) [35], the lipoma preferred partner LPP protein [36] and recently found paladin [37]. VASP interacts with its EVH1 domain directly with ActA, a bacterial protein from *Listeria*



*monocytogenesis* required for the recruitment and assembly of host actin filaments around the intracellular bacteria [12, 30, 38, 39].

### 2.1.1.3. Family members

Ena/VASP proteins are major constituents of signal transduction pathways regulating organization of the cytoskeleton. These proteins are a conserved family of actin regulatory proteins, which have been implicated in actin based process such as fibroblast migration [40], axon guidance and T-cell polarization, phagocytosis, migration of neutrophils and are also important for the actin based motility of the intracellular pathogen, *Listeria monocytogenesis* [12] as mentioned above. They localize to highly dynamic areas of actin reorganization, such as the leading edge of lamellipodia, the tips of filopodia; adherens type cell matrix, cell–cell junctions and other dynamic membrane regions [8, 40]. These regulator proteins of cell motility and actin assembly are found in a variety of organisms and cell types [8, 15]. VASP is the founding member of Ena/VASP family. *Drosophila* enabled (Ena), another member of this family, was discovered in a genetic screen for extragenic suppressors of *Drosophila* Abelson tyrosine kinase (D-Abl) mutants [41]. Ena has an important role in guiding axonal connections in the central and peripheral nervous system and embryonic epithelial morphogenesis of the fly [42, 43]. Later, in addition to Ena, other members of this family from vertebrates, namely Mammalian enabled (Mena), and Ena/VASP–like (EVL) protein were identified [44, 45].

Proteins of the Ena/VASP family are characterized by a common overall domain organization consisting of the conserved amino terminal EVH1 and carboxyl terminal EVH2 domains separated by a less conserved central proline-rich region as explained in Chapter 2.1.1.1 (see Fig.1) [8, 15, 46]. Mena contains two phosphorylation sites (Ser-236, Tyr-296) the first one is equivalent to the first site in VASP (Ser-157), EVL has only this site. Interestingly, *Drosophila* Ena lacks a clear equivalent of this VASP Ser-157 phosphorylation site which is only conserved among the vertebrate members of this family [8]. Phosphorylation of Mena and EVL at the position equivalent to VASP Ser-157 also induces band shifts in their mobility [15].

### 2.1.1.4. Signalling pathways

All Ena/VASP proteins are well characterized substrates of cAMP and cGMP dependent protein kinases (cAK; cGK or PKA; PKG) [7, 45], but these proteins harbor conserved and divergent sites for phosphorylation at different regions (see above). VASP harbors three phosphorylation sites viz., Ser-157, Ser-239, and Thr-278 and is one of the major substrates for

PKA and PKG (Fig.1) [2]. VASP acts thus as a major effector molecule in cyclic nucleotide dependent pathway(s) and impacts many cellular functions.

In VASP, the preferred phosphorylation site for PKA is Ser-157, which leads to the above mentioned retardation of VASP mobility during SDS-gel electrophoresis, resulting in an apparent shift in molecular weight of VASP from 46 to 50 kDa [2] indicating that this phosphorylation may cause a change in structure of the molecule and/or in SDS detergent binding to the protein. The preferred site for PKG on VASP is Ser-239 while Thr-278 is a less favoured site for both PKA and PKG, but recent studies have shown that Thr-278 is a preferred site for AMP activated protein kinase (AMPK) [3]. Phosphorylation of these later two sites does not shift the apparent molecular weight of VASP as assayed by SDS-PAGE. To date, the exact functional role of any of the three phosphorylation sites is unclear at a mechanistic level. However, a positive correlation between phosphorylation of VASP at Ser-157 and the inhibition of fibrinogen receptor (integrin  $\alpha_{IIb}\beta_3$ ) activity was reported [47]. In endothelial cells, PKG induced-phosphorylation resulted in the detachment from focal adhesions of wild type VASP, but not of mutant VASP containing Ser/Thr to Ala substitutions at all three phosphorylation sites [20, 48]. It was also hypothesized that VASP interacts with mammalian Diaphanous (mDia) protein(s) to regulate the cytoskeletal actin dynamics [21, 49]. Also, recent *in-vivo* and *in-vitro* studies have proved a role of PKC either directly or indirectly in phosphorylation of VASP [4, 50-52] which is in correlation with our studies submitted in this thesis. Also, a serine threonine kinase, AMP activated protein kinase (AMPK) was shown to be a new kinase activity phosphorylating VASP specifically at Thr-278 and effecting cell morphology [3]. Work presented in this thesis is focused on elucidating new signalling networks involved in regulation of VASP phosphorylation. However open questions still concern the molecular mechanisms by which phosphorylation effects Ena/VASP protein's function.

#### **2.1.1.5. Physiological functions**

VASP is a crucial factor in regulating actin dynamics and associated processes such as cell-cell adhesion, platelet function and actin-based motility of both cytopathogenic *Listeria* and its eukaryotic host cells. Although biochemical mechanisms emerged depicting VASP as enhancer of actin filament formation at the subcellular level increasing evidences suggest that these proteins have inhibitory functions at the cellular level in integrin regulation, cell motility and axon guidance [15, 53-55].

An important putative function of VASP is to promote actin filament assembly which depends on the ability of VASP to recruit the G-actin binding protein, profilin through its

GP<sub>5</sub> motif to strengthen the binding capacity with G-actin [12]. The G-actin binds to profilin and VASP at the leading edge of the cell and results in ruffling and extension of F-actin filaments. The control of F-actin assembly could be exerted at the level of availability of free barbed ends through nucleation, uncapping or severing by actin depolymerising factor (ADF) and the stabilization of VASP-profilin binding. AMPK mediated VASP phosphorylation at Thr-278 reduces F-actin fiber assembly and impairs stress fiber formation [3]. The direct interaction of VASP with monomeric actin [18, 56] was also suggesting the same and the phosphorylation of VASP would effect this interaction by changing the actin binding properties [20]. The effects of VASP deletion/over-expression on the motile behaviour of living cells [54, 57, 58] and actin based propulsion of *Listeria* [12, 38, 39] has given cumulative evidence for a role of VASP in cell motility. It was shown that VASP also seem to compete with capping proteins to bind at the barbed ends [59] and it enhances branched actin polymerization when ActA protein is immobilized on beads or *Listeria* [60]. VASP increases the rate of dissociation of the branch junction from immobilized ActA, which was found to be the rate-limiting step in the catalytic cycle of site directed filament branching [60].

The signalling pathways induced by vasodilators phosphorylate VASP in smooth muscles and platelets and are mediated by PKA and PKG [7]. Since both PKA and PKG signalling cascades relax smooth muscle cells and inhibit platelet activation [61, 62], it was speculated that phosphorylation of VASP by these cascades mediates the respective effects by modulating actin filament dynamics and integrin activation. At the same time, it was shown in VASP null mice studies that PKG and PKA mediated inhibition of calcium mobilization and granule secretions in platelets are independent of VASP [63] and it is a negative modulator of platelet and integrin  $\alpha_{IIb}\beta_3$  activation [64]. This suggests that the cellular role of VASP in the mediation of effects of vasodilators might be an indirect one. Phosphorylation of Ser-157 in VASP appears to correlate with their activity in cell motility [40]. It seems likely that this phosphorylation relieves either intra or inter-molecular inhibitory interactions.

Further, recent research developments are suggesting the role of protein kinase C in phosphorylation of VASP, cytoskeletal regulation and focal adhesion induction [4, 51, 52]. This interconnectivity can be elucidated by inhibiting growth hormone or serum activated kinases and looking at the phosphorylation of VASP. This approach can reveal new signalling networks that might contribute to phosphorylation of VASP.

### **2.1.2. Spred - an inhibitor of the Ras/Raf/MAP kinase pathway harboring a new class of EVH1 domains**

Spred proteins are recently described Sprouty-related proteins with an EVH1 domain (Spred) establishing a new class of EVH1 domains. They are membrane-associated suppressors of tyrosine kinases and act as negative regulators of the Ras/Raf/MAP kinase pathway upon growth factor stimulation. These proteins are involved in regulation of differentiation in neuronal cells and myocytes. All members of the Spred protein family contain an N-terminal EVH1 domain and a Sprouty-related C-terminal cysteine-rich SPR domain (Fig.2) which is responsible for translocation of Spred proteins to the plasma membrane [65].

To date, three mammalian Spreds are identified: Spred-1, Spred-2 [66], and a third isoform discovered through nucleic acid homology, called Spred-3 [67]. All Spred proteins that have been described so far localize to the plasma membrane [67]. Recent studies have disclosed the localization of Spred-1 and Spred-2 proteins in different organs and cell types which depicts their role in tissue development and organisation. Comparison of the mRNA expression profile of Spred family members in developing rat lung revealed that expression of Spred was found predominantly in mesenchymal cells [68]. The Spred-2 isoform was studied in this thesis determining its EVH1 domain structure and interacting partners.

#### **2.1.2.1. Domain organisation**

Similar to VASP, Spred proteins also show a tripartite domain organisation albeit with different elements harboring besides a conserved N-terminal EVH1 domain, a central c-Kit binding domain (KBD) and a C-terminal Sprouty-like cysteine-rich domain (SPR domain) (Fig.2) [33, 66, 67].

The c-Kit binding domain in the middle part of the Spred proteins consists of about 50 amino acids first described in Spred. This domain is not related to any previously identified tyrosine kinase interaction domain [66]. It has been shown to be responsible for the interaction with the receptor tyrosine kinases c-kit and c-fms. Spred-3 with a non-functional KBD and deletion mutants of Spred-1 in this region revealed that this internal region is involved but not essential for ERK suppression [66, 67, 69]. This raises the question of what the physiological function of this domain might be.

Similar to Sprouty proteins Spred proteins harbor a well conserved cysteine-rich SPR domain at the C terminus. In the case of Spred-2, it is required for efficient suppression of stem cell factor-induced ERK phosphorylation and suppression of hematopoietic cell development [70]. This domain is involved in binding to phosphatidylinositol 4, 5-bisphosphate [71] and for the

interaction with Raf1 [72]. A C-terminal deletion mutant of Spred-1 was shown to act as a dominant negative form and augments growth factor-induced ERK activation [66, 73]. Spred-2 with a deletion of the Sprouty domain was unable to suppress ERK activation but similar loss in Spred-1 and Eve-3 were still functional in suppressing ERK activation raising a controversial discussion [74, 75]. Therefore, future work has to be done, elucidating the physiological function of the SPR domain.

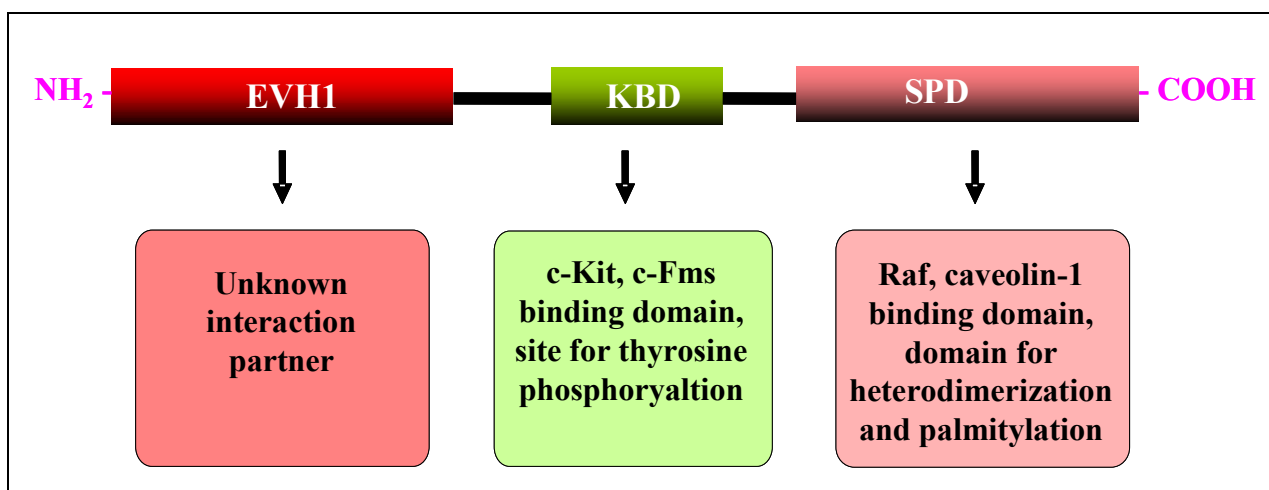


**Figure 2: Structural organization of human Spred2 and overview of binding partners.** Binding partners for EVH1 domain is not known yet, c-Kit binding domain (KBD) is a site for tyrosine phosphorylation and binds to c-Kit and c-Fms domains and the well-conserved cysteine-rich Sprouty-related domain (SPD) binds to Raf, caveolin-1 and is responsible for heterodimerization and palmitoylation.

### 2.1.2.2. Spred EVH1 domain

A new family of proteins also containing a new class of N-terminal EVH1 domains was described by Yoshimura and co-workers [66], called Spred protein. EVH1 domains of mouse and human Spred are identical, named as the human Spred-1a and mouse Spred-1 EVH1 domains. The human Spred-1 EVH1 domain is also very closely related to the other two domains with only two conservative mutations in comparison. The human Spred-3 EVH1 domain shows much less conservative mutations and an insertion [67].

The typical aromatic triad present on the surface of EVH1 domains formed by Arg-Trp-Phe in case of Spred is certainly an important factor for determining ligand specificity [33] (Table.1). The recently determined crystal structure of the Spred1 EVH1 domain from *Xenopus tropicalis* solved to 1.15 Å resolution suggests that dislocation of one of the peptide-binding groove beta-strands might narrow the putative ligand binding groove although one end of the groove shows structural flexibility. Based on these observations, it was proposed that Spred EVH1 might bind peptides that are less proline-rich than other EVH1 domain binding motifs with conformational changes indicating an induced fit [76]. The specific binding partner of the Spred

EVH1 domain is currently unknown for any of its isoforms although the limited expression patterns and non-overlapping functional roles in signal transduction of its host proteins suggest specific binding partner different from other EVH1 domain classes. Recently, the NMR structure of human Spred2 EVH1 domain which been determined in a collaborative effort of this Institute and the Structural Genomic Consortium (SGC), Oxford has been submitted to the PDB database with access code 2JP2 and can be accessed from [http://www.sgc.ox.ac.uk/structures/SPRED2A\\_2jp2.html](http://www.sgc.ox.ac.uk/structures/SPRED2A_2jp2.html) [77].

The EVH1 domains of the three mammalian Spred paralogues are functionally interchangeable [67]. Involvement of the Spred EVH1 domain in Raf inhibition was proved by the studies in which replacement of the murine Spred1 EVH1 domain with the Wiskott–Aldrich syndrome protein (WASP) EVH1 domain was not sufficient to inhibit the MAPK pathway [66]. Moreover, Eve-3 consisting only EVH1 domain is potent in inhibiting the MAP kinase pathway [75]. However, deletion of the EVH1 domain in Spred-2 ( $\Delta$ N-Spred-2) was shown to be competent to inhibit differentiation of murine haematopoietic cell lines [70]. But, sprouty domain deletion in Spred-1 shown negative dominance behaviour in EVH1 domain regulated activities [73]. These observations suggest that the different Spred proteins use different mechanisms to induce inhibition of the MAPK pathway.

### 2.1.2.3. Family members

The Spred proteins can be divided into four members as so far described in the literature including three mammalian homologous isoforms Spred-1, Spred-2, Spred-3 and a *Drosophila* founder member AE33. Recently, a splice variant of Spred-3 named Eve-3 was identified [75]. All of them bear an N-terminal EVH1 domain and Eve-3 contains merely a single EVH1 domain whereas Spred-3 lacks a functional c-Kit binding domain but maintains the inhibitory action on Raf suggesting that the KBD is not required for this action [67]. So far, four binding partners of Spred proteins were described, namely Raf1, caveolin-1, Ras, and RhoA [66, 69, 72, 78]. The former two bind to the Spred SPR domain, but the binding property of the latter two members with Spred proteins is unknown so far although their signal transduction cascades have been studied. The Spred-1 protein interacts with both Ras and Raf, probably through the Sprouty domain [66]. Spred-1 is expressed predominantly in adult brain and in some fetal tissues, suggesting a role during development [79]. Spred-2 isoform express ubiquitously in adults; especially strong expression was seen in neural tissues and different glandular epithelia, but not in fetal tissues. Spred-3 isoform was detected only in brain [67, 79], whereas Eve-3 was limited to the developing liver [75].

#### 2.1.2.4. Signalling pathways

Spred proteins were first described as suppressors of the Ras/Raf/MAPK signalling pathway [66] [80] which regulates proliferation and differentiation of cells in response to extracellular signals but they suppress ERK signalling by a different mechanism [81]. Spred proteins are potent inhibitors of a wide range of mitogenic stimuli like different growth factors, cytokines, and chemokines, but the suppressing effect seems to be restricted to the Ras/ERK/MAPK pathway [67, 73, 74, 78, 81] [80]. Endogenous Spred constitutively associates with Ras and inhibits the activation of MAPK by suppressing the phosphorylation and activation of Raf [66]. This mechanism prevents neither Ras activation nor membrane translocation of Raf, but reduces the threshold of growth factor sensitivity for differentiation [66]. In Spred-2<sup>-/-</sup> midgestation mouse embryos, Spred-2 suppresses hematopoietic processes by inhibiting MAPK activation [70] and stem cell factor or interleukin-3 stimulation of mature Spred-1<sup>-/-</sup> bone marrow-derived mast cells resulted in increased cell proliferation and MAPK activation [73]. Therefore, Spred-2 could serve as a negative regulator of embryonic [70] and Spred-1 of mature late phase hematopoiesis, respectively [73]. However, the EVH1 domain mediated protein interactions of Spred are not yet known which would disclose its role in cell signalling cascades.

#### 2.1.2.5. Physiological functions

As mentioned above, the knock-out studies uncovered the physiological functions of Spred proteins. Spred proteins are not necessary for fertility and development, and young adult mice of Spred knock-out are viable and show no apparent abnormalities [82]. However, loss of functional Spred-2 protein causes a dwarf phenotype, similar to hypochondroplasia, a common form of human dwarfism [82]. In this context, Spred-2 seems to be an important modulator of bone morphogenesis by inhibiting the fibroblast growth factor-induced MAPK pathway [82]. Similarly, Spred-1 negatively regulates allergen-induced airway eosinophilia and hyperresponsiveness without affecting helper T cell differentiation [83]. Recently, Spred-1 and Spred-2 have been shown to down regulate cell motility by suppressing activated RhoA induced stress fiber formation [78]. Furthermore as already mentioned above, Spreds seem to be important for hematopoiesis. Expression levels of Spred-1 and Spred-2 in human hepatocellular carcinoma tissue were frequently decreased compared to non-tumour tissue and their expression levels are inversely correlated with the process of invasion and metastasis [84]. Expression of Spred-1 inhibited carcinoma cell motility and proliferation *in-vivo* and *in-vitro* which is associated with ERK down regulation [84]. A specific function of Spred-3 which is expressed exclusively in brain [67] is not known yet. Physiological functions of Spred proteins are not completely known due to lack of well

characterized interaction partners. Determination of the Spred EVH1 domain binding motifs will disclose Spred proteins further regulated physiological functions.

## **2.2. A classification scheme of EVH1 domains: portrait of a conserved domain family**

Enabled (Ena)/vasodilator-stimulated phosphoprotein (VASP) homology 1 (EVH1) domains, sometimes referred to as Wiskott–Aldrich syndrome protein homology 1 (WH1) domains, are a family of small (~115 residues; ~13 kDa), non-catalytic, protein–protein interaction adaptor modules essential for their host proteins in subcellular localisation and connecting to various signalling pathways. EVH1 domains occur in single copies located exclusively at the N-termini of their host proteins (Fig.3). This conserved, unique N-terminal location appears to be a characteristic feature of EVH1 domains, which categorizes them clearly apart from structurally related domains such as RanBDs, PTB, and PH domains (Fig.3). The EVH1 domains may confer a segmental polarity to their host proteins that is required for functional or biogenetic reasons, resulting in the topological separation of this exposed terminal adaptor domain from the different types of genetically fused effector domains with which they co-exist and lodging a specific binding socket for its interaction partners [33]. In all EVH1 domains, a highly conserved cluster of three, surface-exposed aromatic side chains forms the recognition triad for their target specific proline-rich sequence ligands and classified these domains into different classes based on these interactions. The predicted phylogenetic evolutionary relationship enlighten that EVH1 domains within a class are more related than within the same species suggesting that the homology among specific sub-family members reflects similar functional and binding specificities (Fig.3). The possible divergence of a common ancestor of EVH1 domains into the different classes would probably predate the divergence of the Bilateria.

EVH1 domains mediate protein–protein interactions in a diverse range of signalling cascades, depending on their host protein and site of action [33]. The protein–protein interactions mediated by EVH1 domains are highly important for the regulation of signal transduction events, re-organization of the actin cytoskeleton, and modulation of actin dynamics and actin-based motility. Many EVH1 containing proteins are associated closely with actin-based structures and are involved in re-organization of the actin cytoskeleton. EVH1 domains are also present in proteins enriched in neuronal tissue, thus implicating them as potential mediators of synaptic plasticity, linking them to memory formation and learning.

### **2.2.1. EVH1 domains recognize proline-rich sequences in their binding partners in a stereospecific manner**



Like Src homology 3, WW and GYF domains and profilin, EVH1 domains recognize and bind specifically to core proline-rich motifs (PRMs) in peptides exposed on the surfaces of their binding partners [24, 25, 33, 85]. A small PRMs of 4–6 amino acids in the target peptides (6-12 amino acids) bind the recognition pocket on the domain surface which is unique for each class of EVH1 family due to their characteristic so called aromatic triad formed by three surface exposed amino acids (Table.1). Often, the target core PRMs occur in close tandem repeats in the sequence of the binding partner which could provide an additional mechanism for increasing binding affinity. The binding affinities of the core motifs in isolation are extremely low ( $K_d$  values in the millimolar range), but are increased to biologically significant levels by the presence of core-flanking epitopes, which make additional contacts with the domain surface [85]. The three-dimensional structures of EVH1: peptide complexes reveal the most important features of these interactions and explain the origins of specificity, ligand orientation and sequence degeneracy of target peptides in the low affinity signalling complexes (for review see [24, 33]).

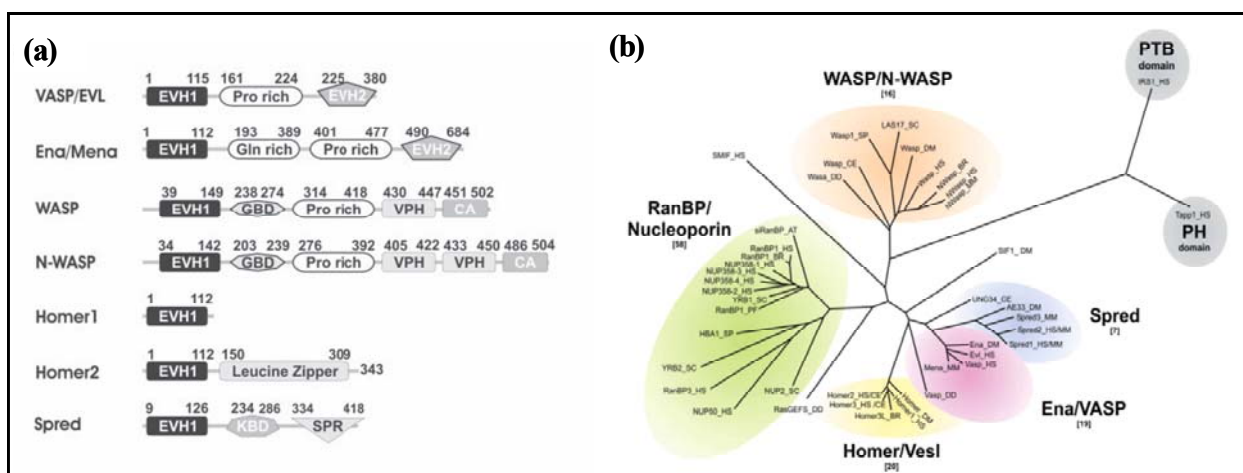


**Figure 3: Occurrence, distribution and phylogenetic classification of EVH1 domains.** (a) Domain organisation in proteins containing EVH1 domain: The EVH1 domain occur in single copies located exclusively at the N-terminus (b) Phylogenetic tree of EVH1, RanBD, PH and PTB domain sequences derived from a structure-based sequence alignment with branch lengths indicating sequence similarity. Clustering of sequences on this tree identified four distinct classes of EVH1 domains. Source: [33]

In the EVH1: peptide complexes, the surface exposed Trp side chain (Trp23; VASP numbering) is usually located at the centre of the aromatic triad and is oriented in a plane almost perpendicular to the domain surface. On one or both sides, at approximately 90° to this plane and almost parallel to the domain surface, lie the flat rings of either Tyr or Phe side chains [33]. This perpendicular arrangement of aromatic rings results in rectangular organized hydrophobic pockets on each side of the central Trp, well-suited to the recognition of peptide ligands that adopt structures close to that of a left-handed poly proline-II (PP-II) helix [33]. The FPXXP containing peptides bound by the Ena/VASP EVH1 domains and the LPPPEP region of the WIP peptide

bound by the N-WASP EVH1 domain are good examples of this. The indole proton of the central Trp forms a hydrogen bond to one of the backbone carbonyl oxygens in the peptide, which further anchors the ligand into place [33, 86]. The side chains of the peptide residues surrounding this carbonyl trunk (usually prolines) then pack closely into the rectangular shaped hydrophobic pockets on either side of the central Trp side chain. In the Ena/VASP EVH1 domains, Tyr16 and Phe79 (VASP numbering) comprise the Trp flanking aromatic residues, and the proline residues P (2) and P (5) of the Class 1 EVH1-binding motif FPPPP binds to either side of Trp23 [24, 33]. The N-terminal Phe(1) of this sequence makes a further close hydrophobic contact with the domain, which is important for anchoring the peptide and for determining the orientation of a highly symmetric ligand [85].

Variations in the geometries of the PRM binding sites give rise to the observed differences in ligand preference between the different domain sub-families. Nevertheless, they are critically placed and provide sufficient external variation to tailor the different classes of EVH1 domains to recognize highly specific target sequences [85]. This allows EVH1 domains to be used as versatile molecular adaptors by diverse families of host proteins to mediate their localization to very different signalling proteins. Recent substitution studies have incorporated peptoid building blocks (non-natural amino acids) into binding peptides derived from proline-rich regions and were able to substitute the most highly conserved residues without altering the EVH1 binding affinity to the corresponding partner [29]. This approach may open up the way for designing selective modulators for biological signalling studies and for the development of new therapeutics. Interestingly, the PRM-binding interfaces of the EVH1 domains described above have many features in common with those of the other protein interaction domains that bind specifically to proline-rich sequences viz., SH3, WW, GYF, and UEV domains, as well as the small, actin-binding, profilin protein. The described stereochemical mechanism for proline-rich peptide recognition is therefore not specific to EVH1 domains, but is rather widely used in many different types of adaptor modules involved in several signalling pathways [33].

### **2.2.2. EVH1 domains are classified into four groups based on similarity of their sequences and recognition pattern of their ligands**

EVH1 domain family proteins can be classified by a phylogenetic analysis of structural similarities based on their sequence conservation, domain co-occurrence, and ligand binding preferences. The EVH1 domains are categorised into four main groups, named after their primary host proteins viz., the Ena/VASP class, the Homer/Vesl class, the WASP/N-WASP class, and the Spred class.

### 2.2.2.1. Class 1: The Ena/VASP class

The EVH1 domains were first identified in host proteins comprising of the Ena/VASP protein family which includes *Drosophila* Ena, its mammalian orthologs (VASP, Mena, and EVL), *C. elegans* Unc-34, and *Dictyostelium discoideum* DdVASP [8, 87] (for more details, see Chapter 2.1.1.3). As explained above the domain structure of this class and the characteristic aromatic triad formed by the class-specific amino acids Tyr, Trp and Phe specifically recognizes the consensus binding motif FPX $\phi$ P (Table.1) (where  $\phi$  is a hydrophobic residue) in vinculin [26], zyxin [27, 28] the *Listeria* actin binding protein, ActA [29, 30], the intracellular axon guidance receptors in *Drosophila* and *C.elegans*, Robo [42] and SAX-3 proteins [88] respectively, the fyn-binding / SLP-76- associated protein (Fyb-SLAP) [35], the lipoma preferred partner LPP protein [36], semaphoring 6A-1 protein (SEMA6A-1) with a zyxin like carboxy terminal domain [89], and paladin [37]. Proline residues at positions (2) and (5) (FPPPP) are essential for EVH1 binding and the prolines at positions (3) and (4) (FPPPP) are highly variable [85]. Position (3) is completely non-specific and could be replaced by almost any other residue, whereas position (4) required a hydrophobic residue in order to determine EVH1 binding [24, 31, 32].

EVH1 class	Host protein	3D-structure PDB code	Aromatic Triad			Consensus ligand Motif
Class 1	VASP	1EGX	Tyr16	Trp23	Phe79	FPXXP
	Mena	1EVH	Tyr16	Trp23	Phe77	FPXXP
Class 2	Homer	1DDV	Ile16	Trp24	Phe74	TPPXXF
Class 3	N-WASP	1MKE	Ala48	Trp54	Phe104	DLPPPEPYNQT
Class 4	Spred	2JP2	Arg23	Trp30	Phe88	This study

**Table 1: The classification of EVH1 domain family members.** Summary of different classes of the EVH1 domain family featuring the highly conserved triad of aromatic amino acid residues and specific proline-rich ligand motifs are shown in the table (for details see Chapter 2.2.2). The protein database (PDB) code for the respective EVH1 domain's atomic structure is also given here.

### 2.2.2.2. Class 2: The Homer/Vesl class

The Homer/Vesl proteins are a family of synaptic scaffolding proteins that are constitutively expressed in brain and enriched at excitatory synapses representing the class 2 of EVH1 domain family [90]. The domain architecture of the Homer/Vesl family is variable. Homer 1 contains only an N-terminal EVH1 domain followed by a low complexity region. In contrast, its close relative Homer 2 consists of an N-terminal EVH1 domain, a low complexity linker region, and a leucine zipper motif at the C-terminus responsible for clustering (Fig.3) [91, 92]. In the

Homer/Vesl proteins, Ile replaces Tyr to offer a characteristic aromatic triad (Table.1) which alters the structural basis and geometry of the PRM recognition mode from that of Ena/VASP EVH1 domains, thereby recognising the class 2 specific EVH1-binding motif TPPxxF in a very different binding mode [85, 90, 93]. The two consecutive prolines and the terminal Phe of the TPPxxF motif make the closest hydrophobic contacts to the Homer EVH1 domain surface, with the exposed indole proton of Trp24 (numbering according to VASP) forming a hydrogen bond to the carbonyl oxygen of the N-terminal Thr [85, 90, 91, 93, 94].

The Homer-Vesl proteins show no obvious connection to the actin assembly machinery and are found enriched in neuronal tissue. These proteins are proposed to play a role in long-term potentiation in excitatory synapses, with implications for memory formation [95]. Homer-Vesl EVH1 domains bind selectively to PPxxF containing motifs found in the C-termini of group I metabotropic glutamate receptors (mGluRs), inositol-1, 4, 5-trisphosphate receptors (IP3Rs), ryanodine receptors (RyRs) and the Shank family proteins [92]. The EVH1 domain of Homer 1 also interacts with its own proline-rich motif in the linking region [91].

### 2.2.2.3. Class 3: The WASP/N-WASP class

The WASP/N-WASP family exhibits a more complex domain structure, comprising an N-terminal EVH1 domain (sometimes referred to as WH1 domains) [96], a short basic motif, a GTPase binding domain (GBD), a proline-rich region, and a C-terminal region containing either a verprolin homology (VPH) and cofilin-acidic (CA) domain (WASP) or two tandem VPH domains followed by a single CA domain (N-WASP) (Fig.3). The N-terminal EVH1 domain binds specifically a proline-rich sequence LPPPEPY in the WASP interacting protein (WIP), CR16 and verprolin [96]. The PRM binding triad of N-WASP is most closely related to that of Homer and conserved Tyr16 of the Ena/VASP class (equivalent to Ile16 in Homer) is replaced by Ala 48 and thus it is no longer part of the peptide binding site. Instead, a groove comprising of Trp54, Phe104 and Thr106 in the N-WASP EVH1 domain contributes to form an identical aromatic cluster for WIP peptide contact (Table.1). In contrast to the other EVH1 domains the N-WASP EVH1 domain binds a much longer proline-rich peptide, having a minimum length of 25 residues. It does not bind a 10-residue ligand of the Mena EVH1 domain from ActA, which contains a PRM (DFPPPPT) very similar to that found in the WIP peptide (DLPPPEP) [30]. It has recently been proved that this domain needs multiple recognition motifs for its functional activity [97] and binds to WIP in a reverse orientation to that observed in other classes of EVH1 domains [33, 96]. Similar to Ena/VASP proteins, the WASP family proteins are closely associated with cytoskeleton regulation. They are believed to regulate actin assembly downstream of Cdc42 and phosphatidylinositol 4, 5-

bisphosphate signalling pathways [98]. Mis-sense mutants in their N-terminal EVH1 domains result in the X-linked recessive disorder Wiscott – Aldrich syndrome (WAS), characterized by immunodeficiency, eczema, and thrombocytopenia [96].

#### **2.2.2.4. Class 4: The Spred class**

The Spred proteins possess as mentioned above a domain structure comprising an N-terminal EVH1 domain, a central c-Kit binding domain (KBD) and a C-terminal cysteine-rich Sprouty-related (SPR) domain (Fig.3) [67, 80]. As described in Chapter 2.1.2.2, a characteristic aromatic triad (Table.1) is expected to determine the specific ligand preference of this EVH1 domain class [33]. Binding studies have shown that the Spred EVH1 domain does not bind the FPPPP motif recognized by the Ena/VASP EVH1 domains and no binding partner has been identified for this EVH1 domain so far. Yet the fairly restricted tissue distribution of some Spred isoforms suggests that their binding partners may be significantly different from those of the other EVH1 domains. Recently, The SGC group (Oxford) in collaboration with our Institute has solved the NMR structure of the human Spred2 EVH1 domain and deposited it in the data base under accession code “2JP2”. The study of binding motifs for this new class of EVH1 domains is a part of this thesis work.

### **2.3. Approaches for identification and characterization of interaction partners of protein kinases and adaptor proteins**

The study of protein interactions are vital in understanding how proteins function within the cell. The ability to identify and characterize the physical and biological interactions in a living cell is essential for developing a detailed system level model of cellular functions [99]. Since 50 years, after discovering the enigma of phosphorylation, many of the signalling pathways involved in the regulation of normal cells were revealed with a major break through in the most recent interaction studies [100]. Previously interaction studies were limited to known targets in which novel protein partners or kinases were studied with specific drugs like activators and inhibitors by using biochemical and pharmacological approaches. Advancements in deciphering of the human genome and subsequent proteomics-based protein profiling studies have catalyzed resurgence in these interaction studies at a new scale using various new molecular, cellular and genetic technologies. Well known protein interaction databases based on different domain recognition motifs are now available together with the experimental data for compiling interaction data and even predicting unknown signalling interactions in a cell [101]. They are helpful to some extent in determining predictive protein interactions and giving models of the signalling network of

a specific cell type (Table.1a) [102]. Such databases are DOMINO (<http://mint.bio.uniroma2.it/domino/>), a database of interactions mediated by protein recognition modules [103], MINT (<http://mint.bio.uniroma2.it/mint/>), a Molecular Interaction database [103] and the DIP database (<http://dip.doe-mbi.ucla.edu/>), which catalogues experimentally determined interactions between proteins [104]. The success of exploring global signalling networks of a cell has shifted the research focus to an understanding of the system's level regulation of a biological system creating the new discipline of systems biology [105]. Systems biology comprises the study of the interactions between the components of biological systems, and how these interactions give rise to the function and behaviour of the cellular or even the organismic system. By revealing the molecular logic that underlies cellular processes the genomic revolution of sequencing and analysing whole genomes has now captured molecular biology into the realm of systems biology [106, 107]. Systems biology approaches also promise to improve rational decision making in drug discovery [108]. Further more the data driven modelling approaches using mathematical techniques like principle component analysis, clustering and partial least squares have addressed the huge experimental data of recent cell signalling studies to understand and help to derive algorithmic ways of analysis of cell signalling networks [109]. Thus recent advancements in interaction analysis strategies are reviewed below in context of our studies performed to determine the substrate specificity of new protein kinases for VASP and the identification of interacting peptides for the EVH1 domain of Spred proteins.

Query string	Spred binding proteins
AE331/Spred ( <i>D. melanogaster</i> )	<b>ANGEL1</b> <sup>(2,3)</sup> [Q9UNK9]
Spred1	<b>ANGEL1</b> <sup>(5)</sup> [Q9UNK9] <b>KIT</b> <sup>(1,4,5)</sup> [ P10721]; <b>HRAS</b> <sup>(6)</sup> [ P01112]; <b>ANGEL2</b> <sup>(5)</sup> [Q5VTE6] <b>RhoA</b> <sup>(6)</sup> [ P61586]; <b>PPP1CA</b> <sup>(1,3,5)</sup> [ P62136] <b>Caveolin-1</b> <sup>(6)</sup> [ Q03135]
Spred ( <i>M. musculus</i> )	<b>KIT</b> <sup>(1)</sup> [ P10721]
Spred2	<b>KIT</b> <sup>(1,4,5)</sup> [ P10721] <b>RAS</b> <sup>(4,6)</sup> [ P01112] <b>RhoA</b> <sup>(1,4,5,6)</sup> [ P61586]

**Table: Spred binding proteins as identified by interaction database searches.** The table shows a list of potential Spred binding candidates as derived from *in-silico* database and literature searches using Spred protein sequences as the query. UniProt ID of the respective hits is given in brackets. The majority of the databases did not provide any experimental evidence for the hits listed. The databases in which the hits were identified are given as follows <sup>(1)</sup>HPRD, <sup>(2)</sup>Biogrid, <sup>(3)</sup>Mint, <sup>(4)</sup>String, <sup>(5)</sup>UniHI, <sup>(6)</sup>literature search.

### 2.3.1. The role of protein interactions in biological signal transduction networks

In multicellular organisms, a multitude of different signal transduction processes are required for co-ordinating the behaviour of individual cells to support the function of the organism as a whole. Signal transduction as a key process refers to any activity by which a cell organises the transmission of a signal or stimulus from its receptors to the targets in the cytoplasm and nucleus, most often by an ordered sequence of biochemical reactions involving secondary messengers, proteins kinases and effector proteins. These signal transduction pathways are governed by an intricate web of physical and functional links between protein ligand molecules forming a signalling network. The comprehensive description of this network structure is referred to in recent days as the “interactome” of a cell [110]. Many disease processes such as diabetes, heart disease, autoimmunity and cancer arise from defects in this web of signal transduction pathways, further highlighting the critical importance of signal transduction to biology as well as medicine.

The reception of a signal on the surface of a cell often results in signal transduction cascades that include transmembrane and intracellular receptor proteins, protein kinases and phosphatases, binding proteins for secondary messengers and many intracellular protein interactions of different specificity to downstream effector molecules that finally execute the cell's response [111]. Information from the receptor-ligand complex formed by cell surface receptor and external signalling ligand activates those small molecules called secondary messengers which often constitute early steps in the signal transduction cascades. The most well-known secondary messengers include cyclic AMP and cyclic GMP, NO, calcium ion, inositol 1, 4, 5-trisphosphate (IP<sub>3</sub>), and diacylglycerol (DAG). Second messengers are often free to diffuse to other compartments of the cell, such as the nucleus, where they can influence gene expression and other processes by amplifying a signal significantly for effective transmission. Many secondary messengers elicit responses by activating protein kinases which transfers the  $\gamma$ -phosphate group from ATP to specific serine, threonine or tyrosine residues in substrate proteins by the process of protein phosphorylation [112]. This signal continues to function until protein phosphatases are activated to shut off its transmission to the targets. Protein phosphatases thus play an important role in the termination of protein phosphorylation signalling processes by hydrolytically removing the specific phosphate groups from the modified proteins. Thereby changes in the concentration of free secondary messengers could induce changes in the covalent structures of proteins. In animal cells, these cascades are mediated by two types of protein kinases: serine/threonine kinases (which phosphorylate serine and threonine amino acid side chains) and tyrosine kinases (which phosphorylate tyrosine amino acid side chains). *In-vivo* phosphorylation patterns thus transmit signals among various proteins being either phosphorylated or dephosphorylated resulting in

various changes of cellular behaviour. Many of these cascades are studied and modelled as phosphorylation networks for a computational, *in-silico* prediction of unknown substrates for different protein kinases [102, 113].

Protein-protein interactions are intrinsic to virtually every cellular process with their effects mediated by different multi-domain protein complexes. Many of the protein-protein interactions involved in signalling networks frequently make use of signalling adaptor proteins composed of conserved, non-catalytic, interacting adaptor domains and their cognate binding peptide motifs which in turn connect to specific signalling cell surface receptors and their downstream effectors [99, 112, 114]. The functional regulation of adaptor proteins is done by several mechanisms including intra-molecular interactions, conformational reorganisation, post translational modification and co-operative and combinatorial binding reactions where individual adaptor domains regulate divergent signalling networks by utilizing distinct combinations of binding partners to carry out complex developmental and physiological processes [111, 114]. Thus, the domain interacting network could be explicated by considering the modular nature of their host proteins [115]. These networks can be viewed as molecular circuits for mediating sensing and processing of stimuli. They could detect, amplify, and integrate diverse external signals to generate responses such as changes in enzyme activity, gene expression, or ion-channel activity. Specificity in protein interactions during signal transduction is regulated by different biochemical mechanism like exclusive binding of stimulating factors to the receptor complex, preferred recognition of protein kinase substrates and adaptor domain binding peptide motifs [111, 112]. Paradoxically, a similar signalling pathway often regulates very different cellular processes, for example the same signal and receptor in different cells can promote responses as diverse as proliferation, differentiation or death. Conversely, activation of the same signal-transduction component in the same cell through different receptors often elicits different cellular responses. We can anticipate that similar genetic and molecular studies in flies, worms, and mice will lead to an understanding of the interplay between different pathway components and the underlying regulatory principles controlling specificity in multicellular organisms.

One specific group of modular recognition adaptor domains, including SH3, WW and EVH1 domains play a crucial role in the assembly and regulation of many intracellular signalling complexes by a common proline rich recognition mechanism [116]. The EVH1 domain host proteins regulate a large number of transient interactions in events involving actin cytoskeleton dynamics [25] or postsynaptic signalling cascades [85] through their proline rich specific binding interactions. Knowledge of the molecular determinants of structural and



biochemical specificity of these proteins is necessary for a rational understanding of their role in signalling cascades.

Not only protein-protein interaction, but also lipid-protein interactions play a crucial role besides maintaining the structure and function of biological membranes where lipid-protein interactions are implicated in the assembly, stability and function of membrane proteins [117] [118]. Of the known adaptor domain proteins interacting with lipids, Pleckstrin homology (PH) domains [119] and Src homology3 domains [120] are well characterised for their lipid interaction and show some structural homology with EVH1 domains. Many of the EVH1 family proteins are localised to or near the cell membrane and are involved in cytoskeletal signalling cascades, but their interaction with negatively charged phospholipids has not been detected so far. The recently discovered positively charged surface of Spread EVH1 domains and their unique structure opens up the possibility of an interaction with negatively charged biological molecules.

### **2.3.2. Identification of candidate protein kinases for VASP and elucidation of phosphorylation pathways in serum stimulated cells**

The above described information has given a detailed view of how signals are transmitted from the cell surface and transduced into changes in cellular behaviour via protein kinases and protein interactions. The combination of biochemistry, structural biology and genetics has developed different tools like immunodetection studies with polyclonal and monoclonal antibodies for phospho and non-phospho forms of the target proteins, NMR studies, transgenic and knock out studies which are very helpful in characterizing the functional role of these protein molecules in different signalling pathways. Despite the close structural relationship among different signalling molecules such as protein kinases, recent studies suggest that activators and inhibitors selective for specific subclasses can be designed to activate or block the responses of these molecules thus up- or down-regulating these signalling pathways. Such up- and down-regulation of signalling pathways could be studied by looking at a specific end substrate or target molecule participated in that pathway. These activators and inhibitors are thus useful pharmacological tools to trace out the order and role of signal transduction molecules in a specific pathway. Recently, the development of peptide inhibitors for specific kinase isozymes has been started depending on the structural variations of isozymes. Especially, protein kinases are the most exploited targets in pharmacological studies due to the key roles of these enzymes in many human diseases including cancer [121]. Recently, the *in-silico* virtual screening of large scale chemical databases with different docking procedures for protein kinase inhibitors depicts their demand in drug designing [122]. Transgenic methodologies have also provided further evidence for

involvement of biological molecules in regulation of signalling pathways. Knock out models are thus well known tools for elucidation of signalling pathways. In some cases like studies of VASP, even though a knock out model may not show any apparent gross phenotype, there might be alterations at the cellular level in the signalling molecule's recruitment for signal transduction. Hence, knock out technology is a valuable approach to elucidate the role of specific molecules in a particular signalling pathway complementary to pharmacological and biochemical studies.

Activation of cyclic nucleotide dependent signalling pathways regulates the phosphorylation of VASP via PKA and PKG (see Chapter 2.1.1.4). Inhibition of PKA and PKG activity by cyclic AMP and cyclic GMP antagonists thus down regulates the phosphorylation of VASP which can be detected by using monoclonal or polyclonal phosphorylation site-specific anti-VASP antibodies [48, 123]. Furthermore, it is possible to activate cyclic nucleotide dependent signalling pathways by adenylyl and guanylyl cyclase activators or agonists thus modulating the phosphorylation of VASP. Also, external stimulation of cells by growth hormones or serum proteins may interconnect and regulate not only the cyclic nucleotide dependent signalling pathways but also other cascades that directly or indirectly phosphorylate VASP by protein kinases participating in cytoskeletal regulation and focal adhesion induction. The interconnectivity of these pathways can be elucidated by either inhibiting or activating various candidate protein kinases including growth hormone or serum activated protein kinases followed by assaying the phosphorylation status of VASP.

As versatile molecular tools for these signalling assays that address the extent and function of VASP phosphorylation after different stimuli and activation of specific kinases, specific antibodies had been developed. A polyclonal anti-VASP antiserum for detecting phospho and non-phospho VASP based on the mobility shift from 46 kDa to 50 kDa in SDS gel electrophoresis [6] and more specifically, monoclonal antibodies for the individual phosphorylation sites of VASP had been raised and characterized previously namely, anti-phospho-Ser-157 VASP (5C6 mAB) and anti-phospho-Ser-239 VASP (16C2 mAB) monoclonal antibodies [48, 124]. Immunohistochemical experiments are also possible with these mABs to find out the role of these phosphorylation sites in localization of VASP to its various binding partners. They are also very useful tools to differentiate among PKA and PKG action as assayed by VASP phosphorylation in signal transduction pathways known to engage these protein kinases in relation to different stimuli. It is possible with these phosphorylation site-specific mABs to trace out the involvement of effective phosphorylation at these acceptor sites by various protein kinases which may have direct or indirect actions on VASP as a substrate. Genetic tools like site-specific mutations are advanced techniques that can also be used to dissect the function of individual phosphorylation sites in VASP. De-phospho mutant

VASP proteins consisting of serine substituted by alanine at both phosphorylation sites namely Ser-157-Ala and Ser-239-Ala are convenient tools to evaluate the function of these VASP phosphorylation sites on the cell's behaviour [3]. Clarification of the complex relationship between secondary messengers (especially cyclic nucleotides), protein kinases and cytoskeleton-associated proteins (like VASP, WASP and others) may lead to future diagnostic and therapeutic implications for haemostasis, cardiovascular diseases and cancer.

### 2.3.3. Identification of interaction partners for a new EVH1 domain of the Spred2 protein

A substantial proportion of intracellular signalling pathways and physical interaction complexes in a cell are mediated by short peptide binding domains like EVH1 domains and their multidomain scaffold, anchoring or adaptor proteins [112]. Many of these non-covalent interactions are of relatively low affinity and with a transient impact on signal transduction. Comprehensive characterization of their interacting peptides and substrate specificity is critical for understanding the mechanisms and signalling networks involved in many cellular functions.

As described by Fields et al many types of physical, molecular biological and genetic screening approaches are available to identify binding partners of a protein or a domain [125, 126]. The conventional approaches of protein interaction-motif detection can be distinguished into three categories viz., affinity-elution methods, genomic library screening (both *in-vivo* and *in-vitro*) methods and synthetic peptide library screening methods. Of the affinity-elution approaches, protein affinity chromatography is a popular method where cell extract proteins are passed over a bait protein immobilized to a column matrix and the bound ligands are eluted after washing off unbound extract proteins [126]. Immunoprecipitation and tandem affinity purification (TAP)-tag-based co-precipitation experiments represent further powerful tools to isolate proteins of interest and their associated interaction partners from cell extracts using the immobilized N- and C-terminally tagged bait protein in a batch-type protocol [125, 127, 128]. Prey proteins co-purified by these affinity-chromatography based approaches are subsequently identified by immunodetection or mass spectrometry. The recent advances in mass spectrometry have allowed the molecular characterization of large protein complexes and even an analysis of protein interaction networks on a proteomic scale [129].

One of the most commonly used genetic systems today is the two-hybrid system, which was originally described by Fields and Song in yeast [130-134]. Two-hybrid systems are extremely powerful approaches of detecting protein-protein interactions *in-vivo* in a heterologous host organism. The two-hybrid system approach is mostly employed in yeast or *E. coli*, though it has also been developed for mammalian cells [135]. The modular domain organisation of certain

transcription factors forms the genetic basis for two-hybrid systems which use transcriptional activity of a reporter gene suitable for screening or selection as a measure of productive protein-protein interactions. The modular nature of these site specific transcriptional activators consists of a DNA binding domain and a transcriptional activation domain which could be fused with bait and target proteins to be tested in the genetic system for their interaction [126, 136-139]. We decided to use an *in-vivo* genetic library screening approach based on a bacterial two hybrid system to search for the Spred EVH1 domain binding epitopes. The coding sequence of the bait protein, human Spred2 EVH1 domain was cloned to a respective plasmid vector to express the recombinant DNA binding domain as a fusion protein to genetically screen proteins fused to a transcriptional activator domain of RNA polymerase for binding epitopes. Thus selected epitope guides in disclosing the interacting protein of the Spred2 EVH1 domain through a genomic sequence blast search. After completion of many genome studies for various organisms including human, by application of two-hybrid systems in yeast or bacteria *in-vivo* screening of libraries of genes or fragments thereof identified recognition motifs which interact with a protein of interest [126, 140-144]. Complete protein-protein interactions network thus determined by identification of the domain recognition motifs in a given cellular proteome, referred to as the “interactome” would thus be the next milestone along a deeper understanding of cellular signalling networks of the cell [145] [110, 146, 147].

The *in-vitro* peptide library screening for specific domain interaction based on exposing libraries of peptides on the surface of phages is a complementary and orthogonal tool in screening for peptide or even antibody binding motifs [148, 149]. Since the last few years, advances in molecular biology allowed this phage display technology to dominate even hybridoma technology to serve as an advanced tool in antibody engineering [150] [151, 152]. Phage display technique uses an *in-vitro* selection method in which a peptide or protein is genetically fused to a coat protein of a bacteriophage resulting in the display of the fused protein on the exterior of the phage virion which contains its gene thus providing a link between phenotype and genotype for selection of desirable peptides from large collections of variants [153]. The phage display screening process occurs in several repetitive cycles of affinity selection and subsequent amplification of enriched phage populations by host bacteria. This is opposed to other methods described above which comprise only single selection rounds [154]. One of the most advanced features of phage display is to make large sized libraries of mutants for a given protein, particularly focused to a limited region of the protein so that a small number of amino acid residues can be mutated [155, 156]. Despite the relatively large size of libraries that can be constructed by phage display, the randomization of more than six residues ( $\approx 6 \times 10^7$  variants) often already exceeds the

ability to construct a complete library with all possible combinations of sequences [157]. Phage display libraries screened for peptide binding adaptor domains contain few fixed amino acids, which are often indispensable for binding and the rest of the residues is randomized by maintaining a number of “degenerated” positions. Completely randomized 9mer peptide phage display libraries (X9mer) have gained more popularity for selecting affinity ligand motifs from a set of peptides [158]. Phagemids containing one of the genes encoding the fusion capsid protein, beside a resistance gene and the large intergenic region of the phage (IR) have all necessary elements for DNA replication and packaging required to clone and express proteins/peptides of interest as capsid fusion proteins in *E. coli* (Fig.19) [153]. To display peptides or proteins on viral particles using this phagemid system, bacteria have to be infected further with packaging-defective helper phages. These helper phages supply an almost complete viral genome *in trans*, but its large IR region is engineered with the DNA-packaging function impaired. In the absence of a helper phage the phagemid is propagated as a plasmid. While after infection of the phagemid-harboring *E. coli* cells with them, both the fusion version of a capsid protein from phagemid and the wild type copies of all capsid proteins from the helper phages are expressed. Phage assembly of all fusion and wild type capsid proteins together thus forms encapsulated phage virion particles which are extruded from the host cells and can be harvested for screening. The protein of interest immobilized on a solid phase is incubated with this phage display library to allow binding between the protein and the appropriate phages by a special *in-vitro* selection procedure called “bio-Panning” (Fig.20) [159]. Phage display has been shown to be a successful tool for selection of short proline rich motifs (6-15 amino acids) for peptide binding adaptor domains like SH3 domain, EVH1 domains, WW domains and for refining of designed proteins with only a small part of the protein being subjected to the evolution at each step [154]. Therefore, phage display peptide library screening was used as a second experimental approach for binding epitope identification of the Spred2 EVH1 domain in the studies submitted by this thesis.

Complimentary to phage display biochemical methods which are based on screening of chemically synthesised peptide libraries have been utilized extensively to identify binding sites or refine recognition motifs of many proteins. SPOT synthesis, the highly parallel chemical synthesis of biological molecules on cellulose membranes by position specific application of defined building blocks in each synthesis cycle [160, 161], has therefore become a widely used tool for studying biological molecular recognition *in-vitro*. These tests are important tool in biochemical identification of the protein-ligand binding interactions and enable to generate an enormous sequence diversity of custom peptide libraries for mapping applications. SPOT technology was originally developed as a system for easily determining the amino acid sequence of peptide

antigens. Peptide sequences corresponding to the specificity of an antibody are identified by conventional enzyme linked or autoradiographic detection methods. Such technology has since progressed to include a variety of new applications for research in the areas of peptide chemistry, molecular biology, cell biology and immunology for studies like protein-protein and protein-phospholipid interactions, phosphorylation studies, nucleic acid binding and combinatorial peptide library screening [162]. Thus, it has been utilized successfully for epitope mapping (also known as peptide walking) [27, 30], alanine scanning [163], substitution analysis [24, 30],[164], screening of potential peptide ligands derived from genomic sequences [165] or mutational analysis of binding domains [166]. Ligand molecules other than peptides like phospholipids are also capable of being screened with similar SPOT methods by spotting and immobilizing the target molecules on a solid phase membrane. Incubation of the spotted membrane with the protein of interest determines complex formation with the interacting molecules and further solid phase studies using fine-tailored ligand forms reveal the chemical details for binding of these pairs [120]. Experiments like the whole interactome scanning experiment (WISE) uses a selective combinatorial approach of SPOT scans and phage display screening to reveal all the peptides in a proteome that have the potential to bind to any domain of interest [115, 167].

The preferred binding motifs for individual domains identified by the methods described above can be used to blast genome data for identification of the proteins holding these binding sequences. Finally, such information aims at exploring the proteome of a whole organism for the candidate binding partners and thus forming network models of multi protein complexes. Hence, understanding and identification of specific motifs and the recognition code of individual domain classes gives an interactome of the complete signalling network for a cell. As recognition motif specificity is an important basis for signal transduction regulation, determination of such specific motifs for every adaptor domain is an essential step in finally describing a functional global interactome.

### 3. AIM OF THE WORK

Ena/VASP homology (EVH1) domains are found in different signal-transduction proteins as N-terminal non-catalytic, adaptor modules of ~ 115 amino acids sharing a common fold. By targeting their host proteins to subcellular sites of action EVH1 domains are involved in protein-protein interactions in a diverse range of signalling cascades several of them include protein phosphorylation. These interactions takes place through a recognition pocket formed by a highly conserved cluster of three surface exposed aromatic side chains in EVH1 domains with proline rich specific sequences of the target proteins.

EVH1 domains were first described in the name giving Ena/VASP protein family with the Vasodilator-stimulated phosphoprotein VASP being its founding member. Several EVH1 binding proteins of VASP have been described being responsible for localisation of VASP to different regions of the cytoskeleton including the microfilaments and focal adhesions. As a cytoskeleton associated protein VASP has been found to be a substrate of cAMP- and cGMP-dependent protein kinases and implemented in regulation of cytoskeletal reorganisation. Besides cyclonucleotide dependent protein kinases however many other protein kinases are known to be involved in regulation of cytoskeletal remodelling in particular during serum stimulation of cells. Using a combined cell biological and pharmacological approach, in the first part of this thesis several candidate protein kinases are analysed with regard to their specificity towards VASP as a substrate of phosphorylation during serum stimulation of cells. Specifically the following topics were addressed:

1. Analysis of the effect of serum stimulation on VASP in terms of its phosphorylation.
2. Identification of the candidate protein kinases participating in serum stimulated VASP phosphorylation and elucidation of their order of action involved in these pathways.

A new EVH1 domain has been described in the recently discovered Spred proteins (Sprouty related proteins containing an EVH1 domain) which are membrane-associated suppressors of tyrosine kinases and act as proximal negative regulators of the Ras/Raf/MAPK signalling pathway. This new EVH1 domain harbours a characteristic recognition pocket different from all the other EVH1 domains suggesting binding to unique ligand(s) which have not been discovered so far. Using different screening methods in combination with *in-vitro* binding assays to candidate ligands, in the second part of this thesis a search for ligands of the Spred EVH1 domain was performed. Specifically, the following topics were addressed:

1. Genetic screening of a cDNA expression library using an *in-vivo* interaction cloning approach for candidate sequences harbouring binding peptide motifs of the Spred EVH1 domain
2. Genetic screening of a phage display library using an *in-vitro* affinity selection approach for oligopeptide binding motifs of the Spred EVH1 domain.
3. Biochemical screening using *in-vitro* binding assays for studying the interaction of the Spred EVH1 domain with phospholipid candidate ligands.



## 4. MATERIALS AND METHODS

### 4.1. Materials

#### 4.1.1. Chemicals

3-AT .....	Sigma,
8-pCPT-cGMP.....	Biolog
Adenine HCL.....	Sigma,
Antibiotic & Antimycotic solution (100 X).....	Sigma
Bisindolylmaleimide I (Bis I) .....	Calbiochem
Bisindolylmaleimide V (Bis V) .....	Calbiochem
Dimethyl Sulfoxide (DMSO).....	Calbiochem
Dulbecco's Modified Eagle Medium (DMEM).....	Invitrogen
Falcon tubes .....	BD-biosciences
Foetal Calf Serum (FCS).....	Biospa
Forskolin .....	Calbiochem
Glutathione Sepharose <sup>®</sup> 4B matrix.....	Amarsham
GSH.....	Amarsham
H 89.....	Calbiochem
His drop out supplements.....	BD-biosciences
Insulin-Transferrin Sodium selenate (ITS) growth supplements .....	Sigma
M9 salts .....	Q biogen
PEG.....	Fulka
Phorbol 12-Myristate 13-Acetate (PMA).....	Sigma
Phosphate Buffer Saline (PBS).....	Biochrome AG
Ro-31-8220.....	Calbiochem
RPMI 1640 Medium.....	PAN
Thiamine HCL.....	Sigma
Trypsin EDTA.....	PAN
Trypsin.....	Invitrogen
Y-27632.....	Calbiochem

All the standard chemicals of highest purity were obtained from Sigma, Calbiochem and other chemicals were of analytical grade.

#### 4.1.2. Primary antibodies

Name	Antigen	Type	Origin	Supplier	Dilution
M4	VASP	Polyclonal	Rabbit	immunoGlobe (cat# 0016-05)	1:3000
5C6	VASP epitope with Ser-157P-VASP	Monoclonal	Mouse	Nanoo tools (cat# VASP 5C6)	1:100
16C2	Ser-239P-VASP epitope-KVpSKQE	Monoclonal	Mouse	Nanoo tools (cat# VASP 16C2)	1:100
Anti PKG	cGMP dependent protein kinase 1 $\alpha$	Polyclonal	Rabbit	-	1:1500
Anti GST	-	Polyclonal	Rabbit	Santa cruz biotechnology (cat# sc-33613)	1:5000
Anti Spred EVH1	-	Polyclonal	Rabbit	-	1:5000
Anti VASP EVH1	-	Polyclonal	Rabbit	-	1:5000
Anti $\lambda$ cI	N-terminal polypeptide (aa 21–36)	Polyclonal	Rabbit	Stratagene (Cat#240110)	1:5000

**Table 2: Primary antibodies used in the experiments.** The information known about recognition motif, type, supplier's details and dilution used in the experiments are described in the table for each primary antibody.

#### 4.1.3. Secondary antibodies

Name	Label	Supplier	Dilution	Detects
Goat-anti -Rabbit Ig	Horse Radish Peroxidase	Amersham biosciences NA 934V	1:5000	M4, anti PKG, Anti Spred EVH1, Anti VASP EVH1, Anti GST, Anti $\lambda$ cI
Goat-anti- Mouse Ig	Horse Radish Peroxidase	Amersham biosciences NA 931V	1:5000	5C6 and 16C2

**Table 3: Secondary antibodies used in the experiments.**

## 4.2. Methods

### 4.2.1. Cell culture

#### 4.2.1.1. Solutions

**Phosphate buffer saline (PBS):** 8.19 g/L NaCl, 0.2 g/L KCl, 1.45 g/L Na<sub>2</sub>HPO<sub>4</sub>, 0.2 g/L KH<sub>2</sub>PO<sub>4</sub>, pH 7.4

**Earl's buffer:** 6.8 g/L NaCl, 0.4 g/L KCl, 0.125 g/L NaH<sub>2</sub>PO<sub>4</sub>, 1 g/L Glucose, 0.05 g/L Phenol Red, 2.45 g/L Tris, pH 7.5

**Sample buffer:** 0.062 M Tris HCl (pH= 6.8), 2% (w/v) SDS, 10% (v/v) Glycerol, 10% (v/v) β-Mercaptoethanol, 0.001% (w/v) Bromophenol Blue

#### 4.2.1.2. Cell lines

Wild type Mouse Cardiac Fibroblast Cells (MCFB (+/+)) were used as the biological model for all the experiments to look for serum stimulated VASP phosphorylation. Cardiac fibroblasts localize at the connecting regions of tissues to organs and blood vessels. These cells were preferred as they express high levels of VASP, commonly used for cytoskeletal studies and are easy to handle in cell culture laboratory and a well established methodology is available in our laboratory [58]. Mouse mesangial cell lines (+/+) were also used for positive control experiments to rule out any cell specific activity in serum stimulated VASP phosphorylation.

#### 4.2.1.3. Isolation of MCFB Cells (+/+)

Two months old mice of both sexes were anaesthetised with ether. Hearts were excised, submerged in cold PBS and cut into pieces (2-3 mm size) with tissue chopper. The pieces were washed with Earl buffer and cells were dissociated with 1mg/ml collagenase/dispase for 30 min at 37°C in incubator. When the tissue pieces sank in Earl buffer, the tissue pieces that had sedimented were discarded and the supernatant containing the isolated cells was taken out and spinned down at 800xg for 5 min to isolate cardiac fibroblast cells. The pelleted cells were resuspended in DMEM, 10% FCS and transferred to a 25 cm<sup>2</sup> culture flask to grow at 37°C in the incubator. Later, the cells were trypsinized for every 3 days, (0.1% Trypsin), counted (CASY®1 cells counter, Schärfe system, Germany) and transferred to a new flask at a density of 5 x 10<sup>3</sup> cells/cm<sup>2</sup>. After continuous growth of the cells in the same medium for 3 to 4 weeks, the isolated

cells from this culture spontaneously became immortalized and then started to grow in 6 cm petri dishes with the same nutrient medium [168].

#### 4.2.1.4. Cell passage, counting, freezing and storage

The cells grow up to 80% confluence in 6-cm dish with DMEM and 10% FCS within 3 days. Then medium was drained out from the dish and cells were washed twice with warm PBS. Then trypsinized by adding 0.1% Trypsin in PBS for 3 to 4 min and incubated at 37°C in incubator until the cells adopted rounded shape. The trypsinized cells were resuspended in DMEM with 10% FCS and  $1.5 \times 10^5$  cells were replated on 6 cm dishes containing 5 ml of DMEM with 10% FCS. Passages from 20 to 40 of this cell line were preferred to use for signal transduction experiments. Mouse mesangial cells (+/+) were cultured in 7.5 cm<sup>2</sup> cell culture flask in RPMI 1640 medium containing 20% FCS, 0.1% ITS growth supplements and 10% antibiotic and antimycotic solution (100X). Cell passaging was carried out for mouse mesangial cells also as described above with the help of warm PBS-EDTA and Trypsin-EDTA after cells were grown to 80% confluent. Cells from passages 4 to 10 were preferably used for the experiments because these cells showed faster growth during these passages.

A 100 µL volume of cell suspension was diluted in 10 mL of PBS and counted with CASY® 1 cell counter (Schärfe system, Germany) as described by the manufacturer. Trypsinized cells were collected in warm DMEM with 10% FCS, then counted and pelleted by centrifugation at 5000xg for 5 min at room temperature. The pellet was resuspended in freezing medium (DMSO + 10% FCS) to a final concentration of  $10^6$  cells/mL, and aliquoted into 1 mL cryotubes. The aliquots were frozen for 48 hours at - 80°C and then stored in liquid nitrogen.

#### 4.2.1.5. Cell culture experimental set up

MCFB cells (+/+) were plated at  $1 \times 10^4$  cells per well in six well plates, and grown up to 80% confluent in DMEM containing 10% FCS (Fig.4). Then the medium was drained and cells were washed twice with warm PBS to counter the effect of any remaining serum. To these cells only DMEM was added and kept for starvation overnight in order to synchronise these cells in the same phase of cell cycle. Some of the synchronised quiescent cells were stimulated with 10% FCS and/or activators PMA (1 µM) and Forskolin (10 µM) (see Table.6) depending on the experimental question to be solved for the respective stimulated signalling pathway's effect on VASP phosphorylation. Synchronised cells were also separately incubated with specific inhibitors namely Y-27630 (10 µM), Ro-31-8220 (10 µM), and Bis I (10 µM) and H 89 (10 µM) (see

Table.6) for 30 min before stimulating with respective activators either individually or in combination (PMA, Forskolin and 10% serum). In all the experiments, after incubating the cells with specific activators for respective incubation periods (4 hours for FCS, 8 min for PMA and 30 min for Forskolin), cells were washed twice with cold PBS and then cell lysates were collected in sample buffer containing 10%  $\beta$ -mercaptoethanol with the help of a cell scraper. Overnight starved cells without any stimulation were collected as unstimulated controls and Bis V was used as a negative control for the inhibition activity of Bis I. DMSO was used as a solubilisation vehicle in all the experiments that treat the cells with the above mentioned activators and inhibitors. The collected samples were boiled immediately at 100°C for 5 min and stored at -20°C.

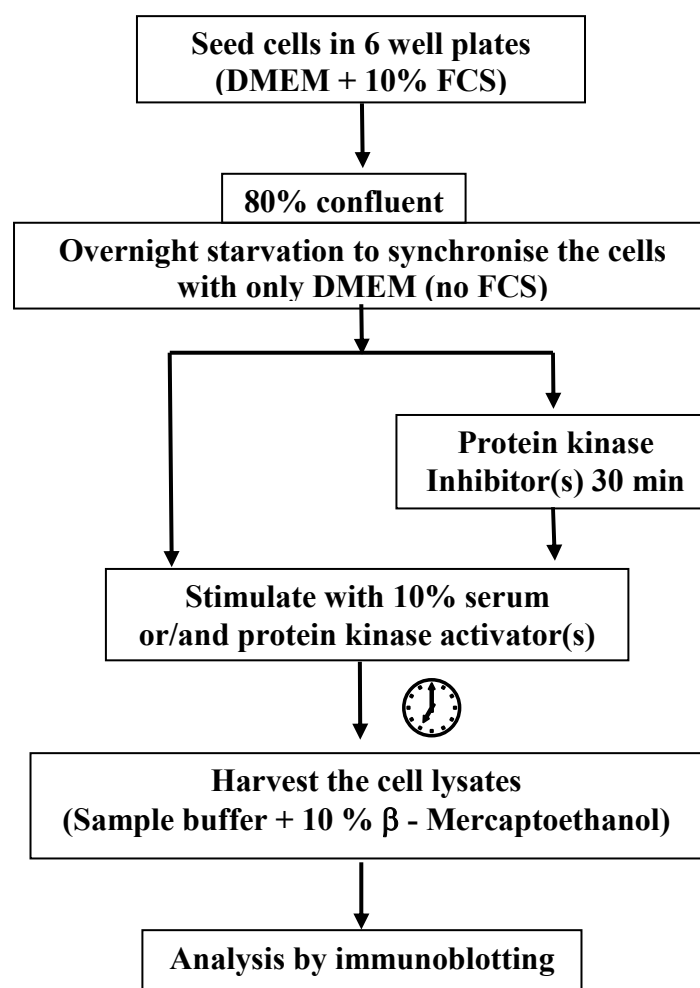


**Figure 4: Scheme of the general experimental set up used in the cell culture work.** MCFB cells (+/+) were grown in a six well plate with DMEM and 10% serum until they grow up to 80% confluence. Then the cells were starved for overnight using only DMEM medium without FCS for synchronization of cells. These synchronized cells were used for the experiments with activation or inhibition of different protein kinases. Before stimulating the cells with serum or/and a specific activator, some of the cells were incubated for 30 min with a single protein kinase inhibitor or a combination of different ones which are needed to inhibit the corresponding pathways in that experiment. Details are given in the figure legends in the results section. After incubation for the respective time period, the cells were lysed in sample buffer containing 10%  $\beta$ -mercaptoethanol and boiled for 5 min at 100 °C before storing at -20 °C. These samples were used for immunoblotting experiments for detecting VASP phosphorylation.

## 4.2.2. Protein biochemistry

### 4.2.2.1. Solutions

**Stacking gel buffer:** 0.5 M Tris HCl, 0.4% (w/v) SDS (pH 6.8 )

**Resolving gel buffer:** 1.5 M Tris HCl, 0.4% (w/v) SDS (pH 8.8)

**Electrode buffer (1X):** 3 g/L Tris base, 14.4 g/L Glycine, 1 g/L SDS

**Sample buffer (2X):** 0.062 M Tris HCl (pH= 6.8), 2% (w/v) SDS, 10% (v/v) Glycerol, 10% (v/v)  $\beta$ -Mercaptoethanol, 0.001% (w/v) Bromophenol Blue

**Acrylamide 4x solution (mix= 37.5:1):** 29.22% Acrylamide, 0.78% Bis-acrylamide

**Transfer Buffer:** 25 mM Tris base, 150 mM Glycine, 10% (v/v) Methanol (pH 8.3)

**10% Ammonium per sulfate (APS):** 1 gm in 10 mL H<sub>2</sub>O

### 4.2.2.2. SDS- polyacrylamide gel electrophoresis (PAGE)

Sodium dodecyl sulfate polyacrylamide gel electrophoresis (SDS-PAGE) was performed using 9% (w/v) polyacrylamide separating gels [169]. Cell lysates collected in sample buffer containing 10%  $\beta$ -mercaptoethanol after cell treatment experiments were loaded into the slots of the gel and separated with a voltage of 100 volt until the samples reached the resolving gel and then separated under 150 volt for the rest of the experiment.

#### Composition for 9 % SDS poly acrylamide gel electrophoresis:

<b>Resolving gel (total volume= 8 mL)</b>	<b>Stacking gel (total volume= 3 mL)</b>
Acrylamide 4x solution..... 3.0 mL	Acrylamide 4x solution.....0.52 mL
Resolving gel buffer.....2.5 mL	Stacking gel buffer .....1 mL
H <sub>2</sub> O.....3.7 mL	H <sub>2</sub> O .....2.48 mL
TEMED.....40 $\mu$ L	TEMED.....10 $\mu$ L
10% (w/v) APS .....100 $\mu$ L	10% (w/v) APS .....40 $\mu$ L

### 4.2.2.3. Immunoblotting

Proteins resolved on SDS-PAGE were transferred to Nitrocellulose transfer membrane (PROTRAN BA83; pore size = 0.2  $\mu$ m) in a Semi Dry Transfer Device (Fast Blot B33, Biometra, Germany) by transfer buffer at 260-280 mA current for 1 hour, according to manufacturer's description. After transfer, the membranes were stained with Ponceau solution (0.1% (w/v) Ponceau in 5% (v/v) CH<sub>3</sub>COOH) for 2-3 min and then washed with tap water. Ponceau solution would stain all the proteins present on the membrane. So, it could be helpful to

confirm the perfect transfer of protein from SDS gels to the membrane. Subsequently, the membranes were incubated with blocking solution for one hour (4% (w/v) milk powder in PBS + 0.025% (v/v) Tween-20 + 0.15% (v/v) Triton X-100). After blocking the non-specific binding sites on the membranes, they were incubated with the respective primary antibodies freshly diluted in solution containing 4% (w/v) milk powder with PBS (Table.2) for one hour. Membranes were then washed 3 times 15 min each with PBS + 0.025% (v/v) Tween-20 + 0.15% (v/v) Triton X-100 and incubated for 45 min with the specific secondary antibody (Table.3) diluted at 1:5000 in 4 % (w/v) milk with PBS. Then the membranes were again washed twice with PBS + 0.025% (v/v) Tween-20 + 0.15% (v/v) Triton X-100 for two times 15 min each and then finally with PBS only for 15 min. The washed membrane was exposed to scientific imaging film (KODAK X-Omat AR film, XAR-5) after incubating it in developer solution (Amersham biosciences, Cat# RPN 2106V2) for a minute, according to the manufacture's instructions of the Enhanced Chemiluminescence (ECL) method. Developer solution is a highly sensitive chemiluminescent substrate system utilizing a novel acridine-based chemistry and horse radish peroxidase, which is tagged with secondary antibody, to generate a light signal that is normally detected on exposing the film.

#### 4.2.2.4. Protein expression and purification

The GST-Spred EVH1 protein used in this study was expressed and purified from the pGEX-4T2-hSpred2 (1-124) construct available in our laboratory. The expression, purification and cleaving the GST tag from the Spred2 EVH1 domain was performed as described in [170]. The purified GST-Spred2 EVH1 protein and Spred2 EVH1 protein were analysed on SDS gel electrophoresis after purification and stored at +4°C.

#### 4.2.2.5. <sup>1</sup>H NMR spectroscopy

The GST-Spred2 EVH1 protein expressed and purified in our laboratory was tested for its biological activity and native folding conformation before using in the interaction studies. A 100 μM protein sample in PBS was mixed with 1:10 (v/v) ratio of D<sub>2</sub>O and natively folded conformation of the protein was analysed in Bruker XWIN-NMR Spectrophotometer (available at FMP, Berlin).

#### 4.2.3. Molecular biology

The plasmid isolation during this total study was performed by using the mini-prep (for small scale), midi-prep (for medium scale) maxi-prep (for large scale) kits supplied by Qiagen sample and assay technologies. The volume of o/n culture and procedure was followed as given in the product manual. For pBT and pTRG origin plasmids, low-copy number plasmid isolation

protocols were employed. The isolated plasmid's mass determination was done by using spectrophotometer ( $A_{260}$ ) and standard mass rulers on the Agarose gel electrophoresis after linearising the plasmid. The standard enzymes supplied by Fermentas life sciences and New England Biolabs were used for restriction enzyme digestion analysis and followed their standard protocol of enzyme digestion. For cloning experiments, the quick ligation kit provided by New England Biolabs was used and the ligation mixtures were performed in 1:3 and 1:5 ratios of vector and insert was used.

#### 4.2.4. Bacterial two-hybrid system

##### 4.2.4.1. Solutions

**M9 media additives:** Solution I and solution II were prepared separately as shown below by mixing the components listed in the order. Solution II was added to solution I to get M9 media additives prior to use.

**Solution I:** 10 mL of 20% glucose (filter sterilized)  
5 mL of 20 mM adenine HCl (filter sterilized)  
50 mL of 10× His dropout amino acid supplement (autoclaved)

**Solution II:** 0.5 mL of 1 M  $MgSO_4$  (autoclaved)  
0.5 mL of 1 M Thiamine HCl (filter sterilized)  
0.5 mL of 10 mM  $ZnSO_4$  (autoclaved)  
0.5 mL of 100 mM  $CaCl_2$  (autoclaved)  
0.5 mL of 50 mM IPTG (filter sterilized)

**10x M9 salts** (Qbiogene #3037-032): 112 gm of 10X M9 salts were dissolved in 1 L deionised water and autoclaved.

**M9+ His-dropout broth:** 50 mL of 10× M9 salts, 67.5 mL M9 media additives and 380 mL of sterile deionised water were mixed to prepare M9+ His-dropout Broth. It can be store at 4°C for up to one month and brought to room temperature prior to use.

**1 M 3-AT stock solution:** 840.8 mg of 3-AT was dissolved in 10 mL of DMSO

**SOB medium:** 20.0 gm of tryptone, 5.0 gm of yeast extract and 0.5 gm of NaCl were dissolved in deionised water to a final volume of 1 L and sterilized by autoclave. 10 mL of filter-sterilized 1 M  $MgCl_2$  and 10 mL of filter-sterilized 1 M  $MgSO_4$  were added to the autoclaved solution to get SOB medium.

**SOC medium:** Freshly prepared 2 mL of filter-sterilized 20% (w/v) glucose was added to 98 mL of SOB medium (autoclaved) to get SOC medium prior to use.



**LB agar:** 10 g of NaCl, 10 g of tryptone, 5 g of yeast extract and 20 g of agar were dissolved in 1 L of deionised water and autoclaved to sterilize. Then, poured into plates after adding respective antibiotic to the medium.

#### 4.2.4.2. Preparation of different selection medium plates

The following methods and calculations were used to prepare different types of screening medium plates for B2H system experiments.

##### **Non-selective screening medium (also called as No 3-AT medium) (for 750 mL):**

1. 11.25 gm of Bactoagar added in 570 mL deionised H<sub>2</sub>O in 1 L flask and autoclaved.
2. After cooling the agar to 70°C, 75 mL of 10× M9 salts solution was added.
3. After cooling the agar mixture to 50°C, 101.25 mL of M9 media additives, 0.75 mL of Chloramphenicol (25 mg/mL) and 0.75 mL of Tetracycline (12.5 mg/mL) were added and poured into petri dishes. The plates were wrapped in aluminium foil and stored in dark place at 4°C.

##### **Selective screening medium (also called as 3-AT medium):**

The selective screening medium was prepared as non-selective screening medium. After adding both antibiotics, required volume of 1 M 3-AT stock was added to get the desired concentration of 3-AT in the screening medium plates and poured into petridishes.

#### 4.2.4.3. The protocol for co-transformation

1. BacterioMatch II validation reporter strain competent cells (Stratagene, cat # 200192) were thawed and gently mixed by tapping the tube. Then, 100 µL aliquots of competent cells were prepared in required number of pre-chilled 14 mL BD falcon tubes (one aliquot for each bait and target test pair co-transformation reaction). It is critical to use 14 mL BD falcon polypropylene round-bottom tubes for this procedure.
2. 1.7 µL of the β-ME was added to 100 µL aliquot of cells and the tubes were swirled gently.
3. The tubes were incubated on ice for 10 minutes with swirling for every 2 minutes.
4. Then respective bait and target plasmid DNA was added to reaction tubes and incubated on ice for 30 minutes with gently swirling after the first 15 minutes of incubation.
5. After incubation, the tubes were swirled gently and heat-pulse shock was given to cells by keeping tubes in 42°C water bath for 35 seconds.
6. Then incubated the tubes on ice for 2 minutes and added 0.9 mL of pre-warmed SOC medium to each tube.

7. Incubated tubes at 37 °C with continuous shaking at 225 rpm for 90 minutes and then cells were collected by centrifugation at  $2000 \times g$  for 10 minutes.
8. Discarded the supernatant and the cells were washed by resuspending the cells in 1 mL of room temperature M9+ His-dropout broth to remove the rich medium.
9. The cells were collected as described in step.7 and gently discarded the supernatant. Then resuspend the cells in a fresh 1 mL volume of M9+ His-dropout broth.
10. Then incubated the cells at 37°C with shaking at 225 rpm for 2 hours. This allows the cells to adapt to growth in minimal medium prior to plating
11. Plated the co-transformation reaction mixtures on the appropriate non-selective and selective screening medium plates with the help of sterile glass beads and incubated at 37°C for colony growth.

#### 4.2.4.4. Plating method

All the plates were brought to the room temperature before plating transformation mixture to avoid moisture on the surface of the plates which hinders the bacterial cell growth. A 20  $\mu$ L volume of co-transformation reaction mixture without any dilution and 20  $\mu$ L and 200  $\mu$ L aliquots of 1:100 diluted co-transformation reaction mixtures were plated on non-selective screening medium plates in triplicates. A 200  $\mu$ L volume of co-transformation reaction mixture without any dilution was plated on desired concentration of 3-AT medium plates in triplicates.

#### 4.2.4.5. Amplification of cDNA library

Name of the library: Human brain cDNA expression plasmid library (Stratagene, Cat # 982262)

Cloning details: Uni-directionally cloned into pTRG Vector at XhoI and EcoRI sites

Host strain: XL-1 Blue MRF` Kan cell;

Primary colonies:  $1.65 \times 10^6$  cfu; estimated titer given by Stratagene:  $2.5 \times 10^8$  cfu / ml

The glycerol stock of human brain cDNA expression plasmid library was completely thawed on ice and 1:10 dilution aliquot were prepared for 200  $\mu$ L volume with SOC medium. Remaining original library stock was immediately re-frozen for future usage. A pool of 248  $\mu$ L of SOC medium and 2  $\mu$ L volume of 1:10 diluted cDNA library glycerol stock ( $\approx 50,000$  cfu) was plated on each 150 mm LB-tetracycline agar plate and spreaded the mixture evenly over the surface of the agar using a sterile glass beads. The number of plates required in the experiment depends on the number of colonies to be grown in order to harvest the amount of plasmid required for library screening. But it should be at least one time more than the complexity of library so that the amplified library plasmid pool consists of total complexity of the cDNA library. We amplified

cDNA library by streaking on 50 plates (150 mm plate). The total number of colonies grown on these 50 plates would yield nearly 250  $\mu\text{g}$  of cDNA plasmid library which can be isolated using maxi-prep plasmid isolation kit ( $\approx 50,000$  colonies/plate and each colony contains nearly  $1 \times 10^5$  cells). The plates were incubated at  $30^\circ\text{C}$  for 24 hours. Prolongation of incubation time (up to 30 hours) could increase the recovery of plasmids containing longer cDNA inserts.

Gently scraped all of the bacterial clones to one edge of the 150 mm plate by using a wide, sterile scraper (may be a sterile cell scraper works out better) and the dense paste was transferred from the edge of the plate into the chilled, sterile container having a small amount of SOC medium. The amplified library clones from all the plates were pooled into the same sterile container by performing the same procedure for all the plates and cells were resuspended by pipetting up and down repeatedly with enough SOC medium. The volume of resuspended cells was measured and 2  $\mu\text{L}$ , 5  $\mu\text{L}$  volumes of the resuspended amplified library were plated on LB Tetracycline plates to estimate the titer of the amplified library (cfu/mL) by incubating them at  $30^\circ\text{C}$  for 24 hours. The cDNA library plasmid DNA was isolated from the pooled bacteria using Qiagen maxi-prep kit. The mass of the isolated cDNA library pool was determined by spectrophotometer and the cDNA library insert present in the isolated cDNA library pool was analyzed by digesting with XhoI and EcoRI enzymes. As the insert is a pool of cDNA library, we could observe a smear with different sizes of strands all together after linearising on agarose gel. The mass of cDNA library plasmid was also estimated with reference to a mass ruler used on agarose gel to cross check the mass estimated from spectrophotometer.

#### 4.2.4.6. Library screening

Pilot co-transformation experiment was performed to find out the the number of co-transformation reactions required to cover the complete amplified cDNA library in library screening experiment. The recombinant pBT bait vector [i.e. pBT-Spred2 (1-124)] and the pTRG-cDNA library plasmid were co-transformed into BacterioMatch II screening reporter competent cells (Stratagene, Cat # 200190). After evaluating the results from the pilot co-transformation experiment, the number of co-transformation reactions to be performed during library screening to cover the complete complexity of cDNA library was determined. Then, a large scale cDNA library screening was performed by transforming pBT-Spred2 (1-124) and pTRG-cDNA library plasmid DNA for those many of 500  $\mu\text{L}$  volume transformation reactions using BacterioMatch II screening reporter competent cells. A negative control plasmid pair (pBT-Spred2 (1-124) and pTRG empty plasmid) were also co-transformed in the experiment.

The following protocol was used to perform co-transformation for large scale library screening:

1. Pre warmed SOC medium to 42°C.
2. Required number of aliquots each of 500  $\mu$ L volume of the BacterioMatch II screening reporter competent cells were thawed on ice and gently mixed the cells by tapping the tube. After thawing, each 500  $\mu$ L volume of cells was transferred into pre-chilled 14 mL BD Falcon tubes. Note: It is critical to use 14 mL BD Falcon polypropylene round-bottom tubes for this procedure.
3. Added 8.5  $\mu$ L of the  $\beta$ -ME to each tube and incubated the tubes on ice for 10 minutes by swirling for every 2 minutes.
4. To each tube, 200 ng of the pTRG-cDNA library and 200 ng of pBT-Spred2 (1-124) plasmids were added and swirled the tubes gently to mix. Incubated the tubes on ice for 30 minutes by swirling the tubes gently after the first 15 minutes of incubation.
5. After 30 min, swirled the tubes gently again and given heat shock to the reactions at 42°C for 55 seconds and incubated the tubes on ice for 2 minutes and then 2.5 ml of pre-warmed SOC medium (at 42°C) was added to the tubes.
6. Transferred each of the cell suspensions from each falcon tube into separate 50 mL conical bottom tubes for outgrowth and incubated the at 37°C with shaking at 225 RPM for 90 min.
7. The cells were spun down at 2000  $\times$  g for 10 minutes and the supernatant was discarded gently by taking care to avoid disturbing the pellet.
8. In order to remove residual rich medium, the cells were washed twice by resuspending the cells in 3 mL of room temperature M9+ His-dropout broth and collected the cells as described in step.6.
9. After washing steps, the cell pellets were resuspended in 1.5 mL of M9+ His-dropout broth and incubated at 37°C with shaking at 225 rpm for 2 hours. This allows the cells to adapt growth in minimal medium prior to plating.
10. The adapted outgrowth cultures from step. 9 were pooled together into one tube and swirled the tube to mix well. The final reaction volume after pooling all the co-transformation reactions is 7.5 ml.

During the adaptation period in step.9, agar plates were labeled and the surface moisture was dried. A 100  $\mu$ L volume of 1:100 dilutions of reaction mixture from step.10 in M9+ His d/o broth was plated on 100 mm non-selective screening medium plates (no 3-AT plates) in triplicates to determine the co-transformation efficiency as well as the total number of colonies screened was determined from these plates. The rest of the reaction pool was plated in 300  $\mu$ L aliquots onto 150 mm 3-AT selective screening medium plates of desired 3-AT concentration for

the library screening. For negative control pair, 100  $\mu$ L of undiluted reaction mixture from step.10 was plated on non 3-AT and 3-AT plates in triplicates. All the plates were incubated at 37 °C and observed colony growth at every 24 hours. The colony growth with different time points was noticed to study their difference in behavior. Depending on the need of the experiment, 3-AT resistant colonies were replica plated on to higher 3-AT concentration selection medium plates by using sterile tooth picks.

The colonies from the 3-AT screening medium plates were replicated onto dual selective screening medium (5 mM 3-AT + Streptomycin) plate and LB-Tetracycline/Chloramphenicol plate by using sterile tooth picks for secondary screening and colony preservation respectively. The positive control co-transformants of pBT-LGF2 / pTRG-Gal11<sup>P</sup>, pBT-VASP / pTRG-ActA (332-344)W plasmid pairs and negative control co-transformants were also included on the same plates on the dual selective screening medium to confirm the effectiveness of the plates. The plates were incubated at 37°C for 24 hours and then transferred to room temperature to incubate for additional 15–18 hrs in a dark location. The growth pattern of the colonies was recorded.

#### 4.2.4.7. Physical characterization of dual resistant clones

The identified dual resistant colonies from the secondary screening medium were further characterized for the target plasmid insert coding sequences by colony PCR and enzyme digestion. The replica colony of the positive colony was picked from the maintenance plate and dissolved in 25  $\mu$ L of sterile water by pipetting up and down. Then stirred the tube gently with stirrer and cooked for 5 min at 45°C. Then centrifuged the sample at high speed for 2 min and 3  $\mu$ L of the supernatant was used as DNA template in the PCR reaction. The pTRG-Gal11<sup>P</sup> was used positive control in colony PCR.

Forward primer (5'-3') = **TGGCTGAACAACCTGGAAGCT**

Reverse primer (5'-3') = **ATTCGTCGCCCGCCATAA**

#### PCR reaction mixture (for 20 $\mu$ L volume):

<b>Reaction component</b>	<b>Volume</b>
Template DNA =	3 $\mu$ L
Forward primer (10 $\mu$ M) =	0.5 $\mu$ L
Reverse primer (10 $\mu$ M) =	0.5 $\mu$ L
dNTP mix (2.5 mM) =	1 $\mu$ L
Taq polymerase (New England biolabs) =	0.5 $\mu$ L
NEB 10X reaction buffer =	2 $\mu$ L
H <sub>2</sub> O =	12.5 $\mu$ L

**PCR programme:**

Process	Temperature	Time	Number of cycles
Initial denaturation	94°C	2 min	-
Denaturation	94°C	30 sec	30 cycles
Annealing	50°C	30 sec	
Extension	72°C	90 sec	
End	12°C	-	-

The amplified PCR reaction product was analysed on 1% agarose gel electrophoresis and the colonies having target insert coding sequence in the target plasmid were identified by finding the respective amplified product. From such positive colonies, the target plasmid was isolated by physically separating from the bait plasmid using antibiotic selection facility. The total plasmid was isolated from the positive colony by mini-prep plasmid isolation kit from 2 mL overnight cultures. The isolated total plasmid was transformed in to the BacterioMatch II validation reporter strain competent cells and co-transformants were plated on LB-tetracycline plates. After overnight incubation of the plates at 37°C, the colonies grown were replica plated on to the LB-Chloramphenicol plate (which selects the cells carrying bait plasmids) and incubated at 37°C for overnight. The cells which were grown on LB-tetracycline plates but not on LB-Chloramphenicol plates were identified as the colonies carrying only the target plasmid and isolated target plasmid. The isolated target plasmid was analysed by enzyme digestion with EcoRI and XhoI and the cleaved insert target coding sequences were analysed on 1% agarose gel electrophoresis. The positive target plasmids identified from colony PCR were sequenced for further study and also used for the panel of genetic assays.

**4.2.5. Phage display technology****4.2.5.1. Solutions**

**PBS buffer:** 140 mM NaCl, 2.7 mM KCl, 20 mM Na<sub>2</sub>HPO<sub>4</sub>, pH = 7.3

**PBS + 0.1% Tween 20:** 0.1 mL Tween 20 + 1 litre PBS buffer

**0.1 M Glycin:** Dissolved 1.1 gm glycine in 100 mL distilled water and adjusted pH to 2.2

**2 M Tris:** Dissolved 24.2 gm Tris HCl in 100 mL distilled water and adjusted pH to 1.1

**20% PEG + 2.5 M NaCl:** Dissolved 200 gm PEG (PEG-6000 from Fulka # 81253) and 146 gm NaCl in 1 litre distilled water

**2YT medium:** Dissolved 31 gm of 2YT cock tail powder (Roth # X966.2) in 1 litre Millipore water and autoclaved after adjusting the pH to 7.4.

#### 4.2.5.2. Helper phage amplification

One litre fresh culture of *E. coli* XL-1 blue MRF' cells grown up to 0.5 OD<sub>600</sub> in presence of 1:500 dilution of Tetracycline (10 mg/mL) at 37°C with continuous shaking was infected with 100 µL of helper phages (VCSM13 Interference-Resistant Helper Phages, Stratagene, cat # 200251) and further incubated for 30 min. After two hours of incubation, 1:333 dilution of Kanamycin (35 mg/mL) and 1:500 dilution of Tetracycline (10 mg/mL) were added to suppress the un-infected cells and then incubated for overnight at 30°C with continuous shaking. The overnight grown turbid culture was centrifuged at 10,000 RPM for 10 min and the supernatant was collected in to fresh bottles. The supernatant was incubated with 1/4<sup>th</sup> its volume of 20% PEG + 2.5 M NaCl solution [171] in ice to chill down the solution until a transparent cloudy smear appears due to dense phage particles in PEG solution. The chilled dense solution was centrifuged at 10,000 RPM for 30 min at 4°C to pellet down the phage particles. The pellet was dissolved in a small volume of PBS (3 to 4 mL) and collected into a fresh eppendorf tube. The solution was mixed by pipetting up and down to dissolve the pellet uniformly and centrifuged at high speed for 5 min to get rid of the cell lysate particles. The supernatant was collected in fresh tubes and added 20% PEG + 2.5 M NaCl solution at the rate of 150 µL/1 mL volume of supernatant. Then incubated on ice for 30 min and centrifuged to pellet down the particles at high speed for 5 min in table top centrifuge. The supernatant was discarded and centrifuged again for few seconds to remove the supernatant completely. The pellet was dissolved in PBS in a small volume and centrifuged for 5 min at high speed in table top centrifuge. The clear white supernatant is the amplified helper phage solution which was collected in a fresh sterile tube and preserved at -20°C by adding 30% (v/v) of the sterile 100% glycerol.

#### 4.2.5.3. The protocol for panning

1. 65 µL of 80% of Glutathione Sepharose<sup>®</sup> 4B matrix (i.e. ≈ 50 µL) was taken in a fresh 1.5 mL eppendorf tube and centrifuged at 3000 RPM for 30 sec by using table top centrifuge
2. The pellet was dissolved in 1 mL PBS + 0.1 % Tween 20 to wash out ethanol after discarding the supernatant very carefully and centrifuged for 5 sec at high speed
3. Repeated step 2
4. Repeated step 2 again with only PBS.
5. The supernatant was removed carefully by leaving few drops to make sure that the pellet was not disturbed and thus the volume of slurry at this stage is 50 to 60 µL after removing the ethanol. Then, added 60 µL of only PBS to it for preparing 50 % diluted matrix and dissolved uniformly which results in 50 % slurry and 50 % PBS in total solution.

6. The total slurry was made into two parts of each  $\approx 60 \mu\text{L}$  fresh 1.5 mL eppendorf tubes and labelled them as aliquot 1 and aliquot 2 (Aliquot 1 was used for query test and aliquot 2 was used for negative control panning).
7. Added 0.4 mg of GST fusion protein i.e. GST-Spred2 EVH1 to aliquot 1 and 0.25 mg of GST alone (as negative control) to aliquot 2.
8. Both the aliquots were incubated at  $4^\circ\text{C}$  for 10 min after vortexing the tubes thoroughly to mix protein and matrix uniformly and then centrifuged at 3000 RPM for 30 sec.
9. The supernatant was discarded carefully and the pellets were washed for 5 times by dissolving each time in 1 mL PBS + 0.1% Tween 20 followed by centrifugation to get rid of the unbound protein remained in between the beads.
10. After final wash, the pellets were dissolved in  $25 \mu\text{L}$  of PBS + 0.1 % Tween 20 and the total volume would be  $50 \mu\text{L}$  (including  $25 \mu\text{L}$  of matrix with bound protein and  $25 \mu\text{L}$  PBS + 0.1 % Tween 20).  $10 \mu\text{L}$  of slurry (i.e.  $5 \mu\text{L}$  of matrix) was collected from each aliquot and prepared SDS sample by adding  $10 \mu\text{L}$  of 2X SDS buffer and heating at  $100^\circ\text{C}$  for 5 min. This SDS sample would be useful to determine whether the protein is bound to the beads to further quantify the same.
11. The remaining matrix slurry volume of both aliquots was increased from  $40 \mu\text{L}$  to  $400 \mu\text{L}$  by adding the following components

Component	End con / proportion	Final composition (for $400 \mu\text{L}$ )
Matrix	-	$40 \mu\text{L}$
BSA (50 mg/mL)	5 mg/ml	$40 \mu\text{L}$
PBS + 0.1% Tween 20	Half of the final volume	$200 \mu\text{L}$
PBS	Rest of the volume	$120 \mu\text{L}$

12.  $50 \mu\text{L}$  of M13 phage display X9 library (titre:  $2 \times 10^{11}$  Pfu/ml) was added to each of the  $400 \mu\text{L}$  of matrix and incubated at  $4^\circ\text{C}$  with  $360^\circ$  rotation for overnight.
13. After overnight incubation, the samples were centrifuged for 30 sec at 3000 RPM in table top centrifuge and discarded the supernatant carefully without disturbing pellet.
14. The pellet was then dissolved in 1 mL PBS + 0.1% Tween 20 and centrifuged for 30 sec at 3000 RPM in table top centrifuge
15. Step 14 was repeated for two more times and the pellet was dissolved in 1 mL PBS + 0.1% Tween 20 and incubated for 1 hour at room temperature.
16. steps 13, 14 and 15 were repeated for two more times.



17. After final incubation, the solution was centrifuged and supernatant was discarded. The pellet was dissolved in only PBS and centrifuged for 30 sec at 3000 RPM in table top centrifuge. The supernatant was discarded carefully without disturbing the pellet.
18. The pellet was dissolved completely in 350  $\mu$ L of 0.1 M glycine (pH = 2.2) and incubated for 20 min at room temperature.
19. Then centrifuged for 30 sec at 3000 RPM at table top centrifuge and collected the supernatant in new tube.
20. 20  $\mu$ L of 2 M Tris was added to the collected supernatant to neutralize the solution and stored at 4°C. This is the eluted bound phages of the respective protein during this panning round. At the end of each panning round, we got the elute phages against both query protein and negative control (i.e. GST alone) which were titrated to estimate the total number of phages eluted in each panning round.

#### 4.2.5.4. Titration of phages

Titration of phages was performed after every panning round and amplified to estimate the titre (pfu/mL) of the phages. The phages to be titrated (either elute phages or amplified phages) were diluted by serial dilution method up to desirable dilution by taking 45  $\mu$ L of fresh 2YT medium and 5  $\mu$ L of phages from previous dilution. 50  $\mu$ L of fresh 0.5 OD<sub>600</sub> *E. coli* XL-1 blue MRF' culture was added to the 50  $\mu$ L volume of all phage dilutions. The cells were incubated with phages for infection at 37°C for 10 min and then centrifuged for 3 min at 5000 RPM to pellet down the infected cells. Then, 50  $\mu$ L of the supernatant was discarded and the pellet was dissolved in the rest of the supernatant. Each of these infected cells were plated on LB-AMP at 37°C for overnight. A control was also made by plating 50  $\mu$ L of cells without any phage infection. The number of colonies grown from every dilution were normalised to one dilution factor and the average colony count gives titre value of the phage sample tested. The following formula was used to calculate the titre of the phages tested.

$$\text{Phage titre (pfu/mL)} = \text{Number of colonies} \times 10^X \text{ dilution factor} \times 1000 / 45$$

#### 4.2.5.5. Enrichment factor

The enrichment factor was calculated after determining the titre of elutes of GST fused protein and GST alone from a panning round. Enrichment factor of a panning round gives the rate of the bound phages enriched against the GST fused protein in that round.

$$\text{Enrichment factor} = \text{Net outcome for GST fusion protein} / \text{Net outcome for GST alone}$$

(Net outcome = Number of bound phages eluted/ Number of phages given as input in the panning round)

#### 4.2.5.6. Amplification

Amplification was performed with enriched positive phage population given from a panning round against GST fusion protein. We used different protocols for the amplification of enriched positive phages without losing the consistency of phage representation.

##### Protocol 1:

1. 2 mL of 0.5 OD<sub>600</sub> culture of *E. coli* XL-1 blue MRF' was infected with 100 µL of eluates of GST fusion protein and incubated at 37°C for 15 min with continuous shaking.
2. 6 mL of fresh 2YT medium, 3.2 µL Ampicillin (100 mg/mL), and 16 µL of Tetracycline (10 mg/mL) was added and incubated for one hour at 37°C with continuous shaking.
3. After incubation, 4.8 µL of Ampicillin (100 mg/mL) was added to increase the specific selection for recombinant phage infected cells and incubated for one hour with continuous shaking.
4. After incubation, the cells were super infected with 100 µL of helper phages (VCSM13 Interference-Resistant Helper Phage from Stratagene, cat # 200251) and incubated at 37°C for 30 min with continuous shaking.
5. After incubation, the super infected culture volume was increased to 500 mL by adding fresh 2YT medium along with 460 µL of Ampicillin (100 mg/mL) and 920 µL of Tetracycline (10 mg/mL) and incubated for 2 hours at 37°C with continuous shaking.
6. After incubation, the culture looked turbid due to growth of super infected cells. Then 1: 500 dilution of Kanamycin (35 mg/mL) was added and incubated overnight with continuous shaking at 37°C. The super infected cells do not grow fast and sometimes we do not see any turbidity even after many hours of super infections. In such cases, we used 1:1000 dilution of Kanamycin (35 mg/mL) and incubated overnight.
7. The overnight grown turbid culture was centrifuged at 10,000 RPM for 10 min. The supernatant was collected and 1/4<sup>th</sup> of its volume of 20% PEG + 2.5 M NaCl solution was added to the supernatant. This was incubated on in ice to harvest the amplified phages at least for 2 hours. We observed a transparent cloudy smear due to dense phage particles in PEG solution.
8. After dense solution was centrifuged at 10,000 RPM for 30 min at 4°C to pellet down the phage particles.

9. The pellet was dissolved in small volume of PBS ( $\approx 1.5$  mL) uniformly and transferred into a fresh eppendorf and centrifuged at high speed for 5 min to get rid of the un-dissolved particles. The supernatant was collected in a fresh tube.
10. 20% PEG + 2.5M NaCl solution was added at the rate of 150  $\mu$ L/ mL of the supernatant and incubated on ice for 30 min.
11. After incubation, the solution was centrifuged to pellet down the phage particles at high speed for 5 min. The supernatant was discarded and centrifuged again for few seconds to discard the remnants of the supernatant.
12. The pellet was dissolved in PBS and centrifuged for 5 min at high speed. The supernatant was collected in a fresh tube which is the amplified phage sample and preserved at  $-20^{\circ}\text{C}$  by adding 30% (v/v) of the sterile 100% glycerol.
13. Amplified phages were titrated to know the titre of the phages amplified in this amplification process.

**Protocol 2:**

1. 500 mL fresh culture of *E. coli* XL-1 blue MRF' was grown up to 0.5 OD<sub>600</sub> in presence of 1:500 dilution of Tetracycline (10 mg/mL) and then infected with 100  $\mu$ L of eluates of GST fusion protein. The infected culture was incubated at  $37^{\circ}\text{C}$  for 30 min with continuous shaking.
2. After incubation, 200  $\mu$ L Ampicillin (100 mg/mL) and 1 mL of Tetracycline (10 mg/mL) was added and incubated for one hour at  $37^{\circ}\text{C}$  with continuous shaking.
3. After incubation, 300  $\mu$ L of Ampicillin (100 mg/mL) was added and again incubated for one hour with continuous shaking.
4. After incubation, the cells were super infected with 100  $\mu$ L of helper phages (Technical name: VCSM13 Interference-Resistant Helper Phage from Stratagene, cat # 200251) and 1 mL Ampicillin (100 mg/mL), 1 mL of Tetracycline (10 mg/mL) were supplied. Then incubated at  $37^{\circ}\text{C}$  for 2 hours with continuous shaking.
5. Rest of the method was same as in protocol 1, from step.6 onwards.

**Protocol 3:**

1. 2 ml fresh culture of *E. coli* XL-1 blue MRF' grown up to 0.5 OD<sub>600</sub> in presence of 1:500 dilution of Tetracycline (10 mg/mL) was infected with 100  $\mu$ L of elute phages of GST fusion protein and incubated at room temperature for 15 min without shaking
2. Then, 6 mL of fresh 2YT medium, 2  $\mu$ L Ampicillin (100 mg/mL), 8  $\mu$ L of Tetracycline (10 mg/mL) were added and incubated for 1 hour at  $37^{\circ}\text{C}$  in a water bath without shaking.
3. After incubation, 4.8  $\mu$ L of Ampicillin (100 mg/mL) was added and incubated for 1 hour with continuous shaking.

4. After incubation, the cells were super infected with 100  $\mu$ L of helper phages and incubated at room temperature for 30 min without shaking.
5. After incubation, the 8 mL culture of super infected cells was upgraded to 500 mL by fresh 2YT medium along with 500  $\mu$ L of Ampicillin (100 mg/mL) and 1 mL of Tetracycline (10 mg/mL) and incubated for 2 hours at 37°C with continuous shaking.
6. Rest of the method was same as in protocol 1, from step.6 onwards.

**Protocol 4:**

1. 25 mL fresh culture of *E. coli* XL-1 blue MRF' was grown up to 0.5 OD<sub>600</sub> in presence of 1:500 dilution of Tetracycline (10 mg/mL) was infected with 100  $\mu$ L of elute phages of GST fusion protein and incubated at 37°C for 30 min without shaking.
2. 100 mL of fresh 2YT medium, 125  $\mu$ L Ampicillin (100 mg/mL) and 125  $\mu$ L of Tetracycline (10 mg/mL) were then added and incubated at 37°C with continuous shaking until OD<sub>600</sub> of the culture reaches 0.5.
3. 100  $\mu$ L of helper phages was used to super infect and incubated at room temperature for 30 min without shaking and then incubated with shaking at 37°C for 30 min.
4. These cultures were centrifuged and the cells were resuspended in 500 mL of fresh 2YT medium, 0.75 mL Ampicillin (100 mg/mL), 1.5 mL of Tetracycline (10 mg/mL) and 1.5 mL Kanamycin (35 mg/mL) and grown overnight with continuous shaking at 37°C.
5. Isolation of amplified phages was performed as described in protocol 1, from step.7 onwards

**4.2.5.7. Characterization of phagemids by colony PCR**

Colony PCR was performed to determine the phagemids carrying insert coding sequences from the phage population eluted in the panning rounds against query GST fusion protein. The respective phage infected cells plated on LB-Ampicillin plates for selecting single colonies. Colony PCR was performed to identify the amplified insert coding regions in the phagemids.

1. Single colony was picked by using a sterile yellow tip and dissolved in 15  $\mu$ L of sterile water by pipetting up and down and vortexing.
2. 5  $\mu$ L of the cells were collected in a fresh tube for back up.
3. Rest of the sample was boiled at 100°C for 5 min to lyse the cells and centrifuged at high speed for 5 min to pellet down the cell debris.
4. The supernatant was used as template for colony PCR.

Forward primer (5'-3'): TACCCTCGTTCCGATGCTG

Reverse primer (5'-3'): GCTGAGGCTTGCAGGGAG

**PCR reaction mixture:**

Reaction component	Volume
Template DNA	3 $\mu$ L
Forward primer (50 $\mu$ M)	0.3 $\mu$ L
Reverse primer (50 $\mu$ M)	0.3 $\mu$ L
dNTP mix (2.5 mM)	2 $\mu$ L
Taq polymerase (New England biolabs)	0.18 $\mu$ L
NEB 10X reaction buffer	1.5 $\mu$ L
H <sub>2</sub> O	7.7 $\mu$ L
Total reaction volume = 15 $\mu$ L	

**PCR programme:**

Process	Temperature	Time	Number of cycles
Initial denaturation	94°C	2 min	-
Denaturation	94°C	20 sec	30 cycles
Annealing	65°C	20 sec	
Extension	72°C	20 sec	
End	4°C	-	-

The amplified PCR products were analysed on 2% agarose gel. An empty and recombinant phagemids were used as positive and negative control in PCR reaction. Loading both of those amplified products together on a 2% agarose gel gives a double band of very low molecular weight difference ( $\approx$  50 kDa) which could help us to identify positive and negative phagemids.

**4.2.6. Protein-phospholipid interaction assays****4.2.6.1. Solutions**

**Washing solution (TBS-T):** 10 mM Tris, 150 mM NaCl, 0.1% (v/v) Tween-20, pH 8.0

**Blocking solution (TBS-T + 3% BSA):** 3 g fatty acid free BSA + 100 mL TBS-T

**MLV buffer (Liposome buffer):** 100 mM NaCl, 10 mM MOPS, pH = 7.2

**LUV buffer (Sucrose buffer):** 176 mM sucrose, 10 mM MOPS, pH = 7.2

**4.2.6.2. Solid phase overlay assay**

PIP Strip™ membranes (Echelon, cat # P-6001) containing phospholipids spotted onto Hybond-C membranes were used for phospholipid membrane screening in solid phase overlay

assay to identify Spred2 EVH1-phospholipid interactions. GST-ADAP SH3-N fusion protein was used as positive control for phospholipid membrane screening experiments.

**1. Blocking:** Blocked the membrane with TBS-T+ 3% BSA solution and gently agitated for one hour at room temperature.

**2. Add protein of interest:** Discarded blocking solution and incubated the membrane with 10  $\mu\text{g}/\text{mL}$  GST-Spred2 EVH1 fusion protein in fresh blocking solution for overnight at 4 °C with shaking.

**3. Washing:** The membrane was washed three times with TBS-T with gentle agitation for 10 min each.

**4. Anti-GST antibody:** Incubated the membrane for 2 hours at RT with anti-GST polyclonal antibody (dil 1:1,000 (v/v)) in blocking solution.

**5. Washing:** as in step 3

**6. Anti-rabbit HRP antibody:** Incubated the membrane for 1 hour at RT with anti-rabbit IgG-HRP (dil 1:10,000 (v/v)) in blocking solution.

**7. Washing:** as in step 3

**8. Detection:** The protein bound phospholipids were detected using enhanced chemiluminescence (SuperSignal West Pico, PierceIllinois). The membrane was incubated in developer solution (solution A = 2 mL and solution B = 50  $\mu\text{L}$ ) for few minutes and drained off before exposing the membrane in scientific image illuminator which detects the signal and produces an electronic image in computer.

#### 4.2.6.3. Preparation of multilamellar vesicles (MLVs)

The synthetic lipids phosphatidylcholine (PC), phosphatidylserine (PS), which contain palmitic and oleic acid esterified at the *sn*-1 and 2 positions of the glycerol backbone, PI(4)P (Cat No. 840045) and PI(4,5)P<sub>2</sub> (Cat No. 840046) were purchased from Avanti Polar Lipids. PI (3) P, PI (5) P, and PI (3, 5) P<sub>2</sub> (Cat No. P-3016, P-5016, P-3516 respectively) were obtained from Echelon Inc. To prepare MLVs, PC, PS and different phosphoinositides (PIPs) were dissolved in chloroform or chloroform: methanol: water solutions (as per product description by supplier) in desired ratios as shown in the Table.4. This was dried on a rotating evaporator to get the require liposome composition. Liposomes (4 mM) were prepared in the proportion of 52 mol% PC, 46 mol% PS and 2 mol% of the mono-PIs or 54 mol % PC, 44 mol % PS and 2 mol% of the bis-PIs [172].

Total volume of vesicle Stock = 1200  $\mu\text{L}$  (Enough for two binding assay experiments)

End concentration of phospholipid in the liposome vesicle stock = 4 mM

	POPC	POPS	PI(X)P DiC16*	PI(3,5)P2, DiC16	PI(4,5)P2, Di 18:1
Con. Stock ( $\mu\text{g}/\mu\text{L}$ )	20	20	1	1	1
MW	760.1	784	956.96	1080.9	1074.17
<b>POPC:POPS</b>					
Portion (%)/ mol	50.0 %	50.0 %			
Vol. Stock ( $\mu\text{L}$ )	91.2	94.1			
Mass ( $\mu\text{g}$ )	1824.2	1881.6			
<b>POPC:POPS:PI(3)P</b>					
Portion (%)/ mol	52.0%	46.0%	2.0%		
Vol. Stock ( $\mu\text{L}$ )	94.8	86.6	91.8		
Mass ( $\mu\text{g}$ )	1897.2	1731.0	91.8		
<b>POPC:POPS:PI(4)P</b>					
Portion (%)/ mol	52.0%	46.0%	2.0%		
Vol. Stock ( $\mu\text{L}$ )	94.9	86.6	96.1		
Mass ( $\mu\text{g}$ )	1897.2	1731.1	96.1		
<b>POPC:POPS:PI(5)P</b>					
Portion (%)/ mol	52.0%	46.0%	2.0%		
Vol. Stock ( $\mu\text{L}$ )	94.9	86.6	91.9		
Mass ( $\mu\text{g}$ )	1897.2	1731.1	91.9		
<b>POPC:POPS:PI(3,5)P2</b>					
Portion (%)/ mol	54.0%	44.0%		2.0%	
Vol. Stock ( $\mu\text{L}$ )	98.5	82.8		103.8	
Mass ( $\mu\text{g}$ )	1970.2	1655.8		103.8	
<b>POPC:POPS:PI(4,5)P2</b>					
Portion (%)/ mol	54.0%	44.0%			2.0%
Vol. Stock ( $\mu\text{L}$ )	98.5	82.8			103.1
Mass ( $\mu\text{g}$ )	1970.2	1655.8			103.1

X = monophospho lipids

**Table 4: Composition of the liposome vesicles.** The phospholipids of different phosphorylation sites were mixed along with the respective amounts as shown in the table to get the 4 mM end vesicle stock concentration. The ratio/mol were calculated to compose the liposomes such that the overall surface charge of the liposome is equilibrated.

1. The phospholipids were dissolved in chloroform or methanol as per the supplier's description to achieve desired concentration and kept on ice.
2. The glass tubes were washed with methanol and chloroform each two times thoroughly by vortexing to rinse the sides perfectly. After washing, few drops of chloroform was added to the tube for easy pipetting of phospholipids.
3. By using glass Hamilton syringe, phospholipids were mixed in the appropriate ratio as shown in the table.4 to prepare MLVs

Note: After mixing the phospholipids together in glass test tube, they should be colourless. If phospholipid mixture looks like white cloudy, it can be dissolved further by adding few drops methanol further.

4. The organic solvents were carefully evaporated by using rotating vacuum pump for 1 hour. The evaporation was extended further for few phospholipids when the solvent was not completely evaporated. If the evaporation is not taking place at all for any phospholipids in such cases we left them over night for evaporation to get rid of solvents completely or used nitrogen stream to remove rest of the solvent.
5. The multi lamellar vesicles were resuspended in 400  $\mu\text{L}$  of LUV buffer and incubated for 30 min in a dark place at RT by closing the test tubes with parafilm.
6. Then the volume was split into two equal halves (200  $\mu\text{L}$  each) which is the final required amount for one phospholipid-protein sedimentation assay as per our experimental plan (used safe lock eppendorf tubes for MLVs).
7. MLVs were made by passing through five cycles of freezing (liquid nitrogen) and thawing (37 °C water bath) and then final round of frozen MLVs were stored at -80°C.

#### **4.2.6.4. Preparation of large unilamellar vesicles (LUVs)**

1. MLVs of required phospholipids were thawed by keeping on ice for few minutes.
2. During thawing MLVs, mini-extruder (Avantis, cat # 610000) was assembled as per the instructions given at <http://www.avantilipids.com/ExtruderAssembly.html> (Fig.5). Four filter supports (Avanti #610014) and one polycarbonate membrane (100 nm diameter, Avanti # 800309) was used in the mini extruder for our experiments.
3. Once the MLVs solution is fully thawed the sample was loaded into one of the gas-tight Hamilton syringes and carefully placed it into one end of the mini-extruder.
4. The empty gas-tight syringe was placed into the other end of the mini-extruder. Note: Make sure that the empty syringe plunger is set to zero and the syringe will be filled automatically as the MLVs are extruded through the membrane.
5. the plunger of the filled syringe gently pushed until the solution was completely transferred to the alternate syringe through the extruder.
6. The plunger of the alternate syringe was pushed gently to transfer the solution back to the original syringe.  
Note: The MLVs suspension should begin to show transparent colour after passing through the extruder.
7. Repeated steps 5 & 6 for 4 times.
8. Taken care to fill the final extrusion in the alternate syringe (the receiver in the step 5) at the end of extrusion to reduce the chances of contamination with larger particles or foreign material.



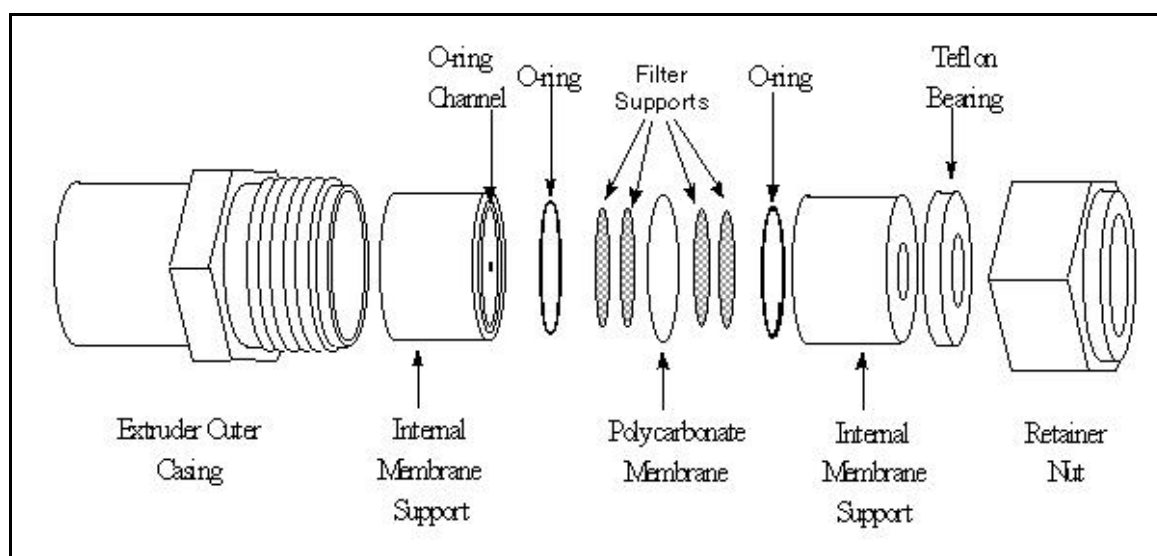


**Figure 5: The design of mini-extruder.** The mini-extruder for the preparation of LUVs is made up of extruder casings on both sides and a bi-layer of filter supports to the polycarbonate membrane to support the pressure created during extrusion. The content and arrangement of components of the mini-extruder is depicted in this diagram.

9. The filled syringe was removed from the extruder and injected the LUVs solution into a clean eppendorf tube.
10. The extruder was cleaned by passing the LUV buffer for 5 times before using for a new LUVs preparation.
11. The volume of the extruded LUVs was measured and filled with the rest of the volume with MLV buffer to get final volume of 1400  $\mu\text{L}$  (it gives nearly 1:8 dilution) to exchange the suspension buffer.
12. The LUVs were centrifuged at 45,000 RPM at 10° C for one hour in Beckman TLA-45 rotor.
13. The supernatant was discarded by leaving 50  $\mu\text{L}$  in the tube to avoid pellet damage.
14. The pellet was dissolved in required volume of MLV buffer by considering 50  $\mu\text{L}$  already left in the tube to get final phospholipid concentration of 4 mM.

#### 4.2.6.5. Liposome sedimentation assay

1. Binding assays were performed with 2  $\mu\text{M}$  of ultra purified and natively folded Spred2 EVH1 protein. The protein was added to LUVs of serial dilutions in a total reaction mixture volume of 500  $\mu\text{L}$  as shown in the table.5. The ADAP SH3-C protein was used as a positive control for protein-phospholipid sedimentation assay.
2. The binding assay mixtures were incubated at RT in dark place for 30 min.
3. Then centrifuged at 45,000 RPM for 1 hour at 10° C in ultracentrifuge to sediment the bound protein-phospholipid interacting complex.

4. The supernatant was removed immediately and protein amount present in the supernatant was determined by tryptophan fluorescence emission in a luminescence spectrophotometer. Also, the equivalent aliquots of supernatant and pellet samples were analysed by SDS-PAGE to detect the protein present in the respective proportions.
5. The reaction mixture without liposomes (zero concentration reaction mixture) is used as the blind value giving the protein concentration maximally to be present in the supernatant if no binding at all occurs in other reaction mixtures.

End con of phospholipid ( $\mu\text{M}$ )	0	100	300	600	900	1600
Liposome, LUVs (4 mM) to be taken in $\mu\text{L}$	0	12.5	37.5	75	112.5	200
MLV buffer (in $\mu\text{L}$ )	490	477.5	452.5	415	377.5	290
Protein (End con = 2 $\mu\text{M}$ ) Stock = 0.1 mM	10 $\mu\text{L}$	10 $\mu\text{L}$	10 $\mu\text{L}$	10 $\mu\text{L}$	10 $\mu\text{L}$	10 $\mu\text{L}$

**Table 5: The composition of sedimentation assay reaction mixture.** The LUVs of different phospholipid compositions were incubated with query protein in presence of MLV buffer in the proportions as shown in the table. The reactions were performed at different concentrations of liposomes to assay the binding affinity quantitatively against the query protein. The reaction mixture without phospholipid would show a base line interaction behaviour since one of the interaction partner is missing. This would serve as a negative control in our experiments.

## 5. RESULTS

### 5.1. Identification of protein kinases participating in serum-stimulated phosphorylation of VASP and elucidation of their order of action

#### 5.1.1. Serum treatment of MCFB cells stimulates phosphorylation of VASP at Ser-157 but not at Ser-239

Serum stimulation of cells is known to induce several signalling cascades including those involved in regulation of the cytoskeleton. Many protein kinases are serum sensitive and effect components of the cytoskeleton. However, not much is known about the role of serum on phosphorylation of the cytoskeletal protein, VASP. Hence we have examined the effects of serum stimulation on the phosphorylation status of VASP. Overnight starved quiescent Mouse Cardiac Fibroblast (MCFB) cells (+/+) were stimulated with 10% serum and assayed in cell lysates for alterations in VASP at different time points according to the general experimental scheme as given in Chapter 4.2.1.5. Western blot analysis by using polyclonal anti-VASP antiserum M4 after protein separation on SDS-PAGE showed that serum stimulation induced phosphorylation of VASP as indicated by a shift in apparent molecular weight from 46 kDa to 50 kDa (Fig.6a) which was not seen in unstimulated quiescent cells. The M4 antiserum detected also a non-specific 80 kDa band in western blots which served as a loading control in our experiments. It was found that serum stimulation of VASP phosphorylation was time dependent and was prominent as early as 90 min after serum stimulation (Fig.6b) and persisted even after 10 hours (Fig. 6c). The shift in the apparent molecular weight of VASP from 46 kDa to 50 kDa detected by polyclonal M4 antiserum indicates a phosphorylation of VASP at Ser-157 [2]. Similar results were seen also in mouse mesangial cells (+/+) confirming that the observed activity is not cell specific (Fig.6d). Thus the results clearly establish that there is a phosphorylation event occurring at Ser-157 of VASP during stimulation of cells by serum. The site specificity of VASP phosphorylation can be determined with the use of monoclonal antibodies directed against the three known phosphorylation sites of the VASP molecule (see Chapter 2.3.2.3).

To find out the identity of the VASP phosphorylation sites engaged after serum stimulation, lysates of serum stimulated cells were analyzed at different time points for the status of individual phosphorylation sites. This was done using monoclonal antibodies 5C6 and 16C2 which are specific for the individual phosphorylation sites Ser-157P and Ser-239P on VASP, respectively [124]. Western blots with 5C6 and 16C2 showed that serum stimulated VASP phosphorylation only at Ser-157 but was not found at Ser-239 (Fig. 7a and b). These experiments confirmed that

phosphorylation of VASP induced by serum stimulation was confined to Ser-157. The effect of serum stimulation on the regulation of Thr-278, the third phosphorylation site of VASP, could not be determined due to a lack of specific antibodies for this site, however recently published research articles proposed working antibodies also for this phosphorylation site [3].

These experimental results show that serum stimulation preferentially induces VASP phosphorylation at Ser-157 which causes the shift in molecular weight from 46 kDa to 50 kDa as detected by anti-VASP antiserum M4.

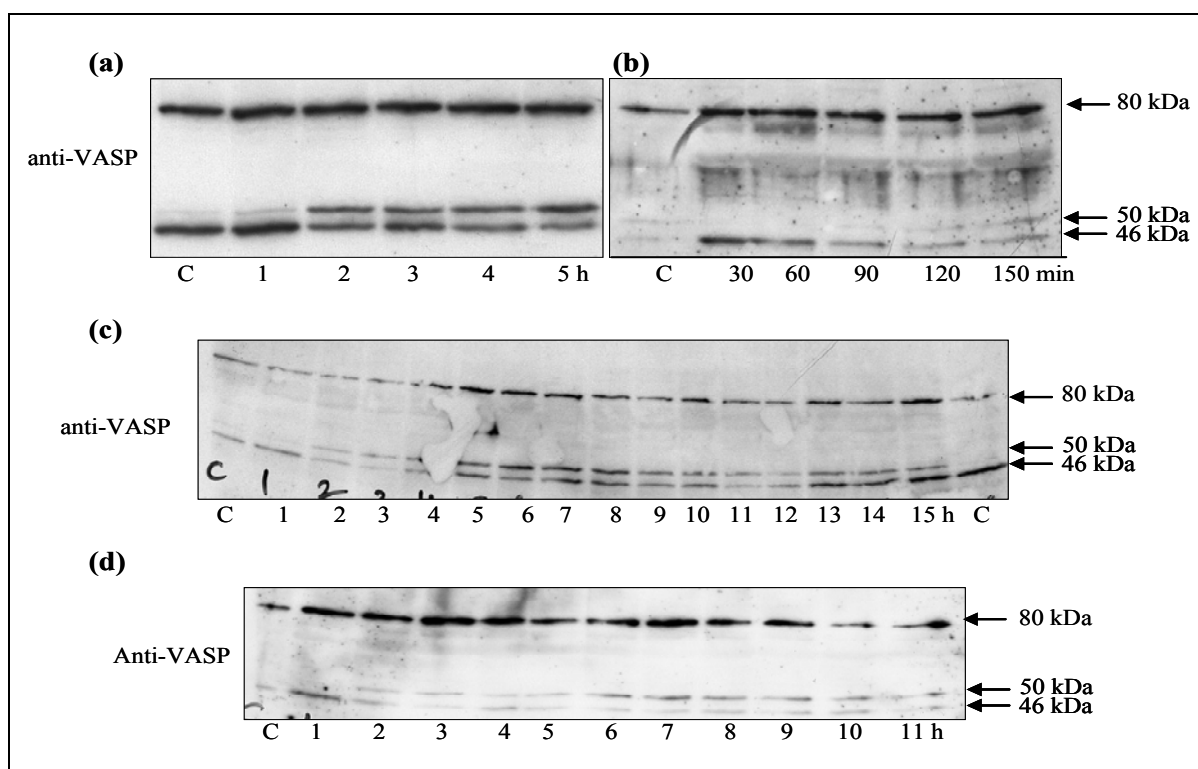


**Figure 6: Serum treatment of cells stimulates VASP phosphorylation.** Overnight starved MCFB cells (+/+) were stimulated with 10% FCS and VASP phosphorylation was studied at different time periods with an interval of one hour (Fig. a and c) and 30 min (Fig. b) each, by immunoblotting using M4-antiserum. Similar experiments were also carried out using Mouse mesangial cells (+/+) (Fig. d). In all the blots, 46 kDa and 50 kDa bands represent non-phospho and phospho forms of VASP respectively and an upper band at 80 kDa is also recognized by the M4 anti-VASP antiserum, which serves as a loading control. Blots shown are representative of four independent experiments. In all blots, C represents control samples which are unstimulated cell lysates.

#### 5.1.1.1. An interaction graph model describing serum-stimulated VASP phosphorylation forms a conceptual basis for experimental identification of the protein kinases involved

To summarize the major pathways expected to be involved in serum stimulated VASP phosphorylation at Ser-157 a graph model of the interaction network which addresses its candidate players and their possible interactions was developed (see Fig.8). This directed interaction graph was organized into three major hierarchical layers of protein interactions modelled at different resolution (and represented by three different background shadow colours in

the diagram) that correspond to the major relay stations of the signal transduction cascades under study viz., an input signal by external stimulation of the cell, an intermediate processing of the signals by signal transduction and signal exchange and finally a targeted output signal as detected by a change in the molecular properties of the effector protein VASP. The key players like stimulators/receptors, candidate protein kinases, and the substrate protein involved in this signal transduction network are represented as nodes. The direct or indirect interaction pathways between these nodes either already known or inferred from the literature as described in other biological contexts are represented by directed edges (unbroken or broken arrows respectively) in this interaction map. The top node at the external layer of this interaction map represents the serum added to the cells and is considered here as a collection of unspecified stimuli which by binding to an array of cell surface receptors initiate signalling processing. Arrows labelled as *a*, *b*, *c*, *d*, *e*, *f* refer to different serum-stimulated intracellular pathways leading to the activation of an intermediate network of protein kinases which are represented as nodes in the next layer of interaction in our interaction map. These candidate protein kinases do have the propensity to downstream phosphorylate VASP (either directly or indirectly as labelled by unbroken or broken arrows respectively with numbering 1, 2, 3 and 4 according to the protein kinase specified) or to be engaged in phosphorylation reactions among each others (labelled by unbroken arrows with apostrophized numbers; for the sake of clarity only nearest-neighbour interactions are shown in the diagram). VASP phosphorylation represents the bottom node in the convergent final layer of the directed interaction graph. The alphanumerical coding of nodes and edges described here will be used throughout the following text while referring to the experimental results in this part of the thesis.

Specifically, stimulation of cells with serum intracellularly activates many cytoskeleton-associated protein kinases like MAP kinases (arrow '*a*' in Fig.8), protein kinases C (arrow '*b*' in Fig.8) or Rho kinases (arrow '*d*' in Fig.8) which are known to play an important role in cytoskeletal reorganization. Of these kinases, we hypothesized based on literature knowledge that Rho kinases and PKCs may be new candidate protein kinases responsible for mediating serum-derived signals involved in VASP phosphorylation. Such a phosphorylation event might be either the result of a direct interaction with VASP as a proximal substrate for these candidate protein kinases or the result of an indirect one involving other protein kinases of the network. Also indirect phosphorylation pathways might finally be expected to involve phosphorylation of VASP through the cyclic nucleotide dependent protein kinases (PKA and PKG) which are well-known to use VASP as one of their direct substrates. Hence PKA and PKG are also considered as member nodes of the inter-connecting network layer in our directed interaction graph model. The nodes of the

protein kinase network are further labelled in the diagram of Fig.8 by those antagonistic or agonistic drugs (specified for the respective kinase and their mode of action on this target) which will be used as pharmacological tools to study experimentally the structure of this network in the following perturbation experiments with MCFB (+/+) cells. Basically identification of candidate protein kinases involved will be achieved by looking at VASP phosphorylation in the presence of different combinations of activators or inhibitors complemented by appropriate controls of drug specificity.

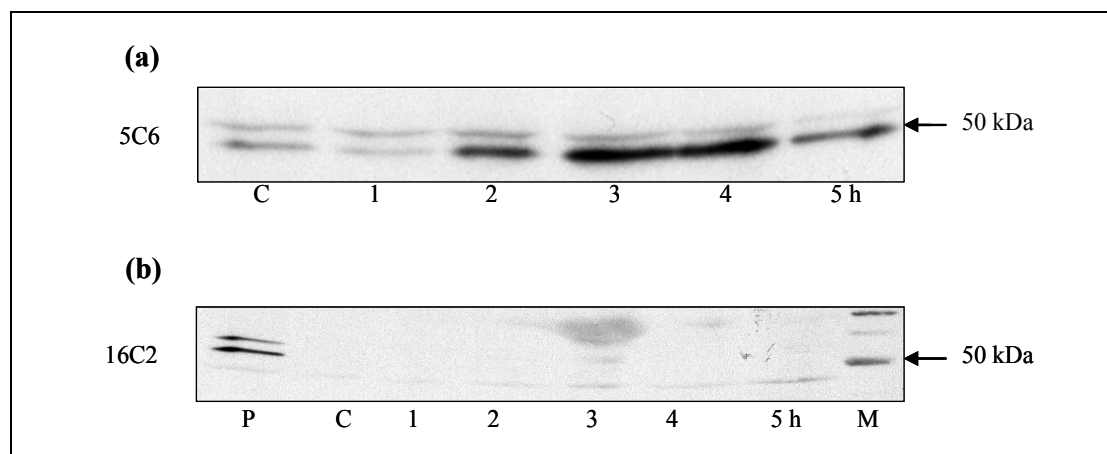


**Figure 7: Serum stimulated VASP phosphorylation occurs at Ser-157.** In serum stimulated MCFB cells (+/+) after different time periods, VASP phosphorylation at Ser-157 (Fig. a) and Ser-239 (Fig. b) was probed using respective monoclonal antibodies 5C6 and 16C2. In Fig a and b, *C* represents unstimulated cell sample and in Fig. b, *P* represents endothelial cells lysates which were used as positive control samples. Blots shown are representative of three independent experiments. In Fig. a, an extra positive band with a molecular weight larger than 50 kDa appeared which remained unchanged in intensity during time course of the experiment. Its nature is currently unclear.

### 5.1.2. Serum activated PKCs, but not Rho kinases are involved in serum stimulated VASP phosphorylation at Ser-157

It is shown above that VASP is phosphorylated at Ser-157 on stimulation of cells by serum and we subsequently looked for the type of protein kinases that are involved in this process. In general serum stimulation regulates many cytoskeleton-associated protein kinases that are responsible in different signalling pathways for cytoskeletal remodelling as shown in the interaction network map described above. Of these kinases, PKC and Rho kinases and their respective signalling pathways are of great importance in serum-mediated alterations of the cell cytoskeleton. VASP is known to participate in such cytoskeletal alterations as a key player. Although there are many protein kinases activated during serum stimulation, we focused our experiments initially on Rho kinase and PKC in view of the fact that only these kinases might have some indirect interactions with VASP. Both of these kinases and VASP for instance are known to participate in focal adhesion formation. These kinases might mediate direct or indirect phosphorylation of VASP during serum stimulation although VASP has so far been known to be

phosphorylated by cyclic nucleotide-dependent kinases only while studying other conditions of cellular stimulation.

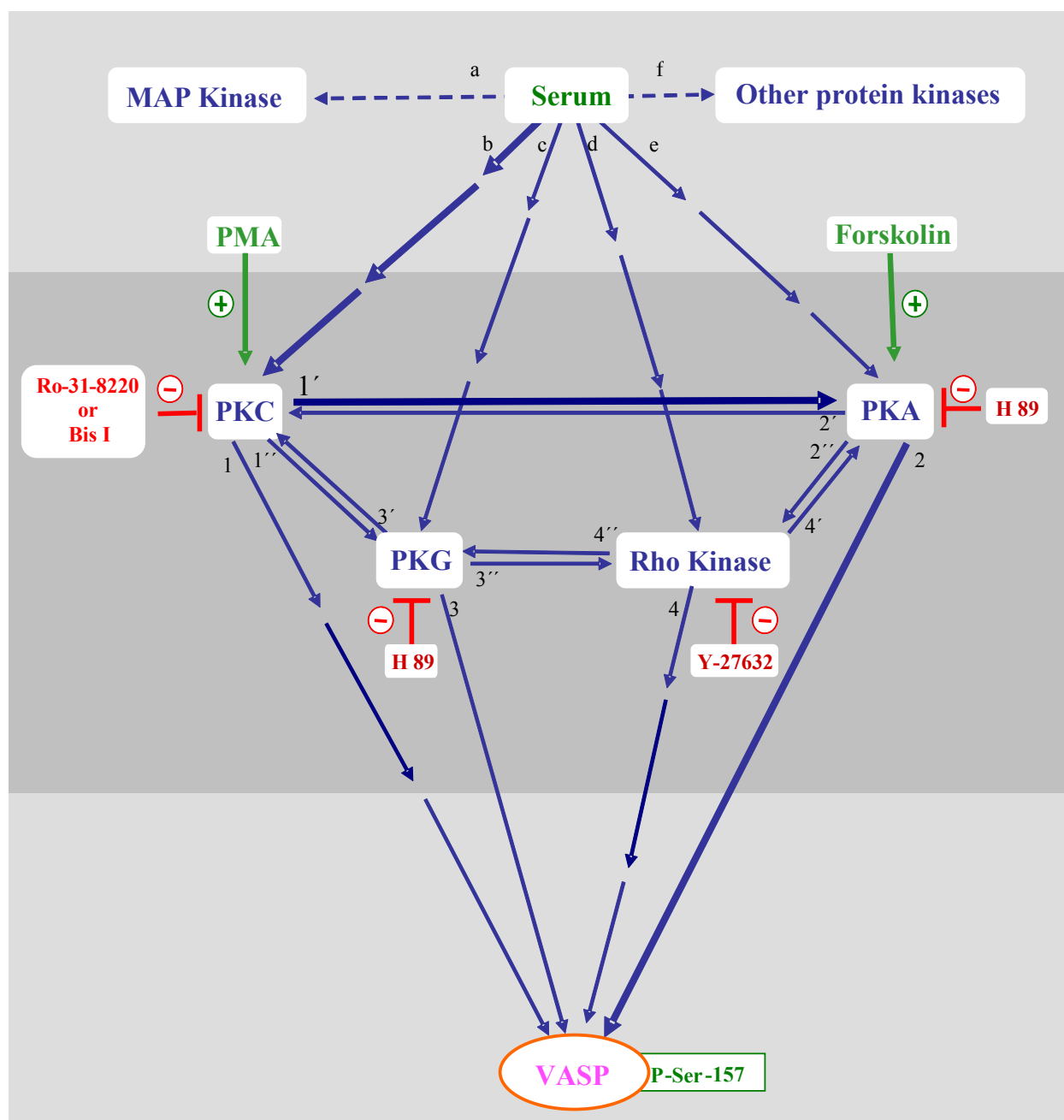


**Figure 8: Representation of an interaction graph model compiling possible pathways involved in serum stimulated VASP phosphorylation.** In the above interaction graph, the following notation was used: arrows labelled as *a, b, c, d, e, f* consider different serum stimulation pathways leading to an activation of the respective kinases. Possible pathways down-stream of serum activated PKC, PKA, PKG and Rho kinase are represented by arrows labelled with numbers *1, 2, 3* and *4* (and apostrophes) respectively. The same nomenclature was used throughout the whole text of this thesis. A set of activator (green) and inhibitor (red) shown at each node are used to modulate the respective kinase activity experimentally.

We first tested for an involvement of PKCs and Rho kinases in serum stimulated VASP phosphorylation by treating quiescent cells with Ro-31-8220 (10  $\mu$ M) and Y-27632 (10  $\mu$ M), inhibitors of PKCs and Rho kinases respectively (see Table.6), prior to the stimulation with

serum according to the general experimental scheme shown in Chapter 4.2.1.5. The samples were analyzed by western blot using M4 antiserum. The results were shown in Fig. 9a. Control lanes 1 and 2 show the unstimulated and serum stimulated samples respectively and thus support the phosphorylation of VASP at Ser-157 in this experiment. In the same western blot, in presence of the PKC inhibitor (see pathways [1], [1'], [1''] in Fig.8) there was no phosphorylation of VASP upon serum stimulation as seen in lane 4, while with the Rho kinase inhibitor (see pathways [4], [4'], [4''] in Fig.8) VASP phosphorylation still occurred at Ser-157 as seen in lane 3. In presence of both inhibitors together lane 5 shows a result which is in line with the results observed in lane 3 and 4. Taken together these experiments suggest that PKCs mediates serum stimulated VASP phosphorylation, but Rho kinases do not. According to the interaction map presented in Fig.8, PKC may mediate this process either by a pathway [1] or by the other possible pathways using further the intermediate protein kinases PKA or PKG labelled as [1'+2] or [1''+3] in Fig.8 resulting finally in the phosphorylation of VASP at Ser-157. Insensitivity of VASP phosphorylation to the action of the Rho kinase inhibitor Y-27632 suggests that pathways [4], [4'] and [4''] are not involved in serum stimulated VASP phosphorylation. The detailed role of PKC in phosphorylation of VASP during serum stimulation however can not be elucidated from this type of experiments and will be addressed later on.

To confirm the specificity of the inhibitors used, positive control experiments were done to determine whether these substances might unspecifically interrupt known cyclic nucleotide-dependent protein kinase mediated signalling pathways that induce VASP phosphorylation. In principle the inhibitors used that have been described to inhibit PKC and Rho kinase might also interact with the activity of other protein kinases like PKA and PKG which are known to phosphorylate VASP independently of serum stimulation. To address this question, the quiescent cells were incubated with the above mentioned inhibitors at the same concentration for 30 min and then stimulated with an adenylate cyclase activator which finally activates PKA (Forskolin) or a PKG specific activator (8-pCPT-cGMP). The cell lysates were analyzed by western blot using M4 antiserum and assayed for phosphorylation of VASP. The results showed VASP phosphorylation by treatment of the cells with PKA and PKG activators also in the presence of each of the inhibitors as it was observed without inhibitors (compare lanes 3 and 4 with lane 2 in Fig.9b. Data are not shown for PKG activity). These data rule out that the inhibitors of PKC and Rho kinase are unspecifically interrupting PKA- and PKG-mediated signalling pathways leading to VASP phosphorylation and thus suggest that they act according to their described specificity also under the experimental conditions used here.



Compound	Activity	Concentration used	Reference
Y-27632	A highly potent, cell-permeable and selective <b>inhibitor</b> of Rho-associated protein kinases (K <sub>i</sub> = 140 nM)	10 μM	[173]
Ro-31-8220	Competitive and selective <b>inhibitor</b> of protein kinase C (IC <sub>50</sub> = 10 nM)	10 μM	[174]
Bis I	Acts as a competitive <b>inhibitor</b> for the ATP-binding site of PKC (K <sub>i</sub> = 10 nM)	10 μM	[175]
Bis V	Negative control compound for protein kinase C inhibition studies (IC <sub>50</sub> > 100 mM)	10 μM	[176]
H89	A highly selective cell-permeable potent <b>inhibitor</b> of protein kinase A (K <sub>i</sub> = 48 nM)	10 μM	[177, 178]
PMA	<b>Activator</b> of protein kinase C <i>in-vivo</i> and <i>in-vitro</i> at nM concentrations. Also <b>inhibitor</b> of PKC during long-term treatment.	1 μM	[179, 180]
Forskolin	<b>Activator</b> adenylate cyclase resulting in increased cAMP levels and activation of PKA (EC <sub>50</sub> = 4 mM)	10 μM	[177]

**Table 6: Drugs used in the pharmacological perturbation experiments.** Both activators (shown in green colour) and inhibitors (shown in red colour) used in this work are listed here. Their mode of action and the concentrations of the compounds used in the experiments are listed in the table.

### 5.1.3. PKA, but not PKG is required for serum stimulated phosphorylation of VASP at Ser-157

The above experiments have shown that VASP is phosphorylated at Ser-157 on serum stimulation and that in this phosphorylation PKC is involved. It is therefore necessary to further elucidate if PKC mediated VASP phosphorylation after serum stimulation is dependent on other well known protein kinases which have already been found to phosphorylate VASP in a well defined manner (see interaction graph model in Fig.8). In general, PKA and PKG are major protein kinases linking cyclic nucleotide-dependent signal transduction with the cytoskeleton. Even though PKG preferentially phosphorylates VASP at Ser-239, it can also phosphorylate Ser-157 (see Chapter 2.1.1.4) [2]. As serum stimulation via PKC also mediates phosphorylation of Ser-157 on VASP, it became an important issue to determine whether PKC phosphorylates VASP at Ser-157 without any involvement of PKA and PKG (see pathway [1]) or whether its effect depends on PKA or PKG either directly or indirectly (see pathways [1'+ 2] and [2'+ 1] or [1''+ 3] and [3'+ 1] in the interaction network model summarized in Fig.8).

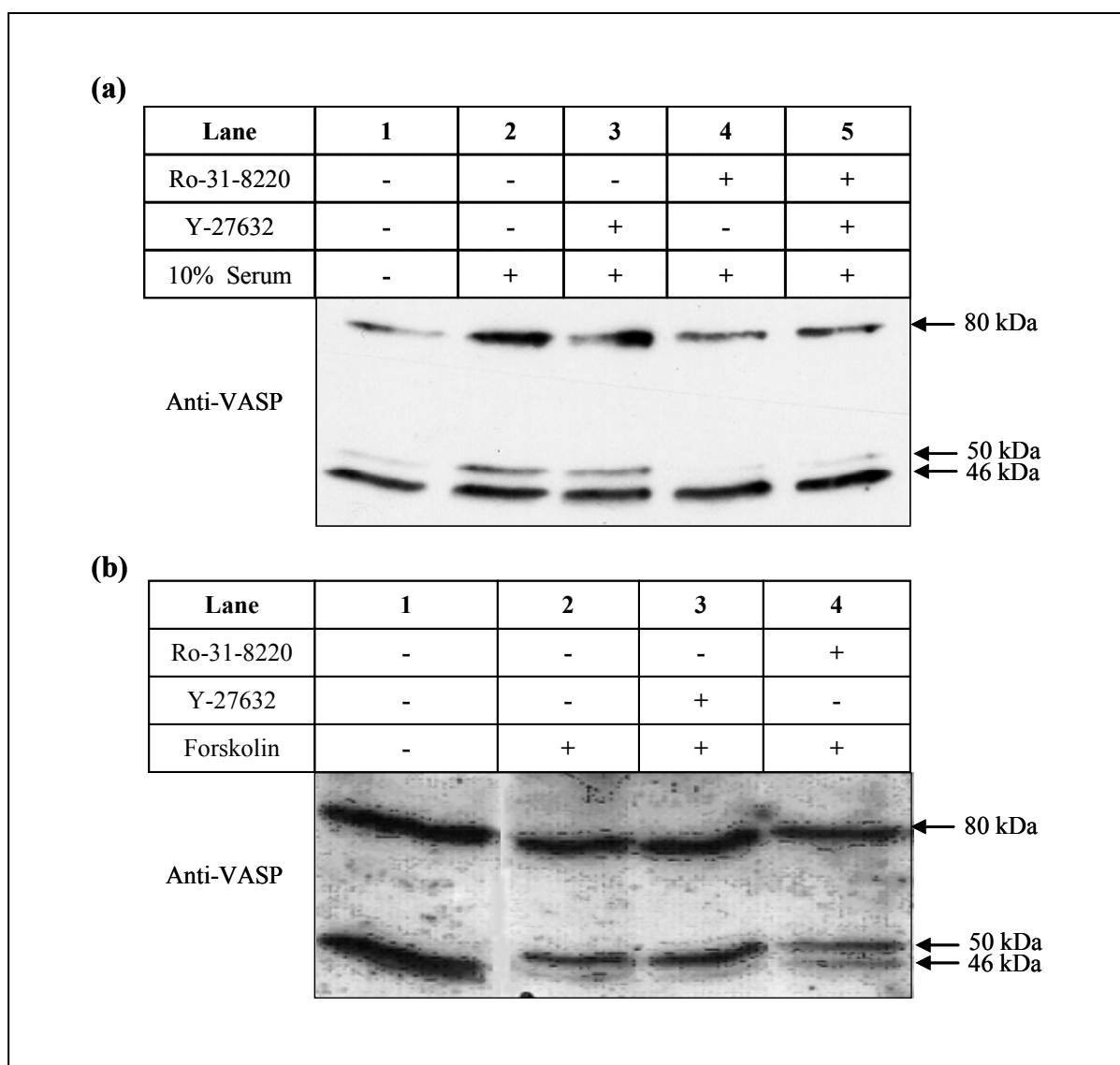


**Figure 9: The protein kinase C inhibitor but not the Rho kinase inhibitor is inhibiting serum stimulated VASP phosphorylation.** In Fig. a, shows phosphorylation of VASP detected with M4 antiserum in lysates of MCFB cells (+/+) incubated with Ro-31-8220 (10  $\mu$ M), a protein kinase C inhibitor or Y-27632 (10  $\mu$ M), a Rho kinase inhibitor or both for 30 min prior to serum stimulation for 3 hours. In Fig. b, shows the extent of VASP phosphorylation after incubating cells for 30 min with inhibitors Ro-31-8220 (10  $\mu$ M) or Y-27632 (10  $\mu$ M) followed by activation with Forskolin (10  $\mu$ M), an adenylate cyclase activator that activates PKA, for 10 min. In all the blots, 46 kDa and 50 kDa bands represent the non-phospho and phospho forms of VASP respectively and the upper band of 80 kDa which is also recognized by the M4 anti-VASP antiserum serves as a loading control. Lane 1 in both blots represent unstimulated control cell sample. Blots shown are representative of three independent experiments.

Firstly to examine the role of PKA in the serum stimulated VASP phosphorylation at Ser-157, the overnight starved cells were incubated with H89 at a concentration of 10  $\mu$ M, an inhibitor of PKA prior to stimulation with serum. Western blot analysis with M4 antiserum as shown in Fig. 10a did not show phosphorylation of VASP at Ser-157 in the presence of H89 (10  $\mu$ M) after serum stimulation as seen in lane 6. The same observation was made in lane 4 in the presence of the PKC inhibitor, Ro-31-8220 but not in lane 3 in presence of the Rho kinase inhibitor, Y-27632 which was already observed in chapter 5.1.2. In lane 5, inhibition of serum

stimulated VASP phosphorylation at Ser-157 in presence of both Ro-31-8220 and Y-27632 together is only due to the activity of Ro-31-8220, according to the results seen in lane 3 and 4 and also lanes 3 and 4 in Fig 9a. Lane 1 and 2 show unstimulated and serum stimulated controls without and with phosphorylation of VASP at Ser-157 respectively. These results show that serum stimulated VASP phosphorylation at Ser-157 is mediated by both PKC and PKA. It suggests particularly that PKA is involved in serum stimulated VASP phosphorylation at Ser-157 and that this might happen by either pathways  $[1'+2]$  or  $[2'+1]$  as depicted in Fig.8. However we suspect the former pathway to be the most probable one because PKA is well known to directly phosphorylate VASP preferentially at Ser-157 (see Fig.1). To establish the sequence of action of these two protein kinases this signalling pathway will be elucidated in further detail later on (see Chapters 5.1.6).

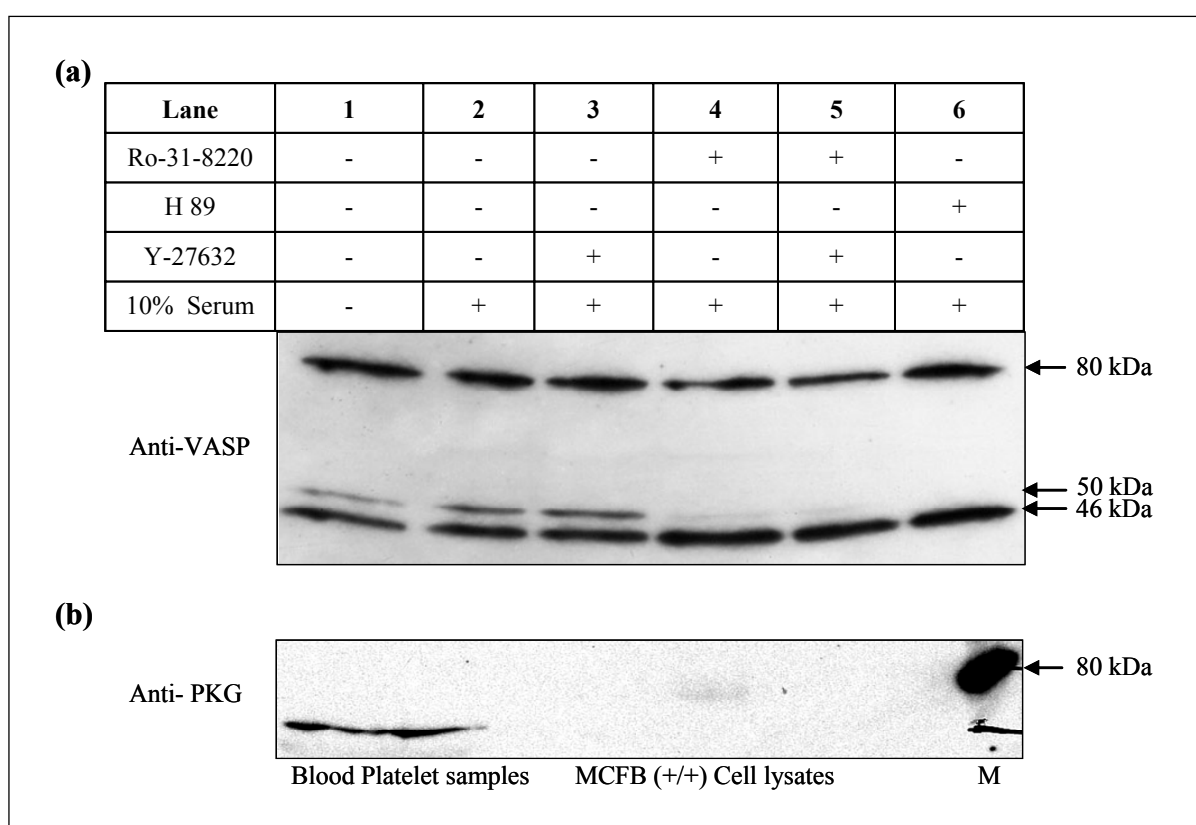


**Figure 10: (a) PKA is involved in serum stimulated VASP phosphorylation at Ser-157.** MCFB cells (+/+) were incubated with Ro-31-8220 (10  $\mu$ M), a protein kinase C inhibitor, H89 (10  $\mu$ M), a PKA inhibitor and Y-27632 (10  $\mu$ M), a Rho kinase inhibitor for 30 min prior to serum stimulation of 3 hours and blotted for VASP phosphorylation with M4 antiserum. In the blot, 46 kDa and 50 kDa bands represent non-phospho and phospho forms of VASP respectively and the upper band of 80 kDa which is also recognized by the M4 anti-VASP antiserum serves as a loading control. Lane 1 represents unstimulated control. **(b) MCFB (+/+) cells lack PKG.** The presence of PKG in MCFB (+/+) cells was examined by immunoblotting cell lysates (which are collected without any further treatments or starvation) with anti PKG antibody. Sodium nitro prusside (SNP) stimulated blood platelet samples which are rich in PKG were used as positive control for this experiment. *M* in the diagram represents protein molecular weight ladder and the thick band in the marker near 80 kDa is due to cross-reactivity with the anti-PKG antiserum. The blots shown are representative of three independent experiments.

It is known that use of an inhibitor for a single protein kinase can also affect other protein kinases within the same cell due to its limited specificity. H89 is known to inhibit many protein kinases including PKG depending on the concentration used [177]. This will be addressed in the following experiments. A reason for this unspecific mode of action is that a major group of protein kinase inhibitors are developed on the basis of their competitive inhibitory activity against the common substrate of all protein kinases that is ATP. The inhibitory activity of an antagonist for a specific protein kinase in an individual cell line is also highly concentration dependent. Therefore it is not possible in general to predict the activity spectrum of a given inhibitor type such as H89. In preliminary experiments, we have tried to inhibit PKA with other inhibitors which are more specific for PKA than H89 and which are cAMP-antagonist. All these inhibitors (for example Rp-8-Br-cAMPS) were found to be unable to inhibit PKA in our cell lines even at very high concentrations or using different batch stocks. We also failed to observe their inhibitory action in combination with different types of PKA activators (Forskolin, 8-Br-cAMPS and BIMPS, data not shown here). A reason might be that MCFB cells (+/+) might have become impermeable for these compounds or that they might have lost their ability to reach their target sites of action. Hence we will use compound H89 in further experiments only together with appropriate positive controls to make sure that a specific protein kinase inhibition with this drug is observed in every case under study.

The above results suggested that serum stimulated VASP phosphorylation at Ser-157 mediated by PKC involves of another cytoskeleton-associated protein kinase that is PKA. In general, PKA and PKG are both major protein kinases linking cyclic nucleotide-dependent signal transduction with the cytoskeleton. After we found an involvement of Ser-157 and PKA in serum stimulated VASP phosphorylation, it is therefore necessary to examine a possible participation of PKG in this process. Even though PKG preferentially phosphorylates VASP at Ser-239, it can also phosphorylate at Ser-157 [2]. Moreover the inhibitor used to inhibit PKA in the previous experiments can in principle also inhibit PKG. So, the VASP phosphorylation inhibited by H89 in the previous experiments might also be due to PKG. Furthermore, it was recently found that there is an active interaction between PKC and PKG [181]. All these observations suggest that serum stimulation could have been mediated in principle by PKG rather than PKA to result in phosphorylation of VASP at Ser-157 (i.e. via pathways  $[1''+3]$  or  $[3'+1]$  as depicted in Fig.8). To address a role of PKG in the serum stimulated VASP phosphorylation, experiments were conducted by stimulating overnight starved quiescent cells with serum in the presence of a PKG inhibitor (Rp-8-Br-cGMPS). However these experiments had shown no alteration in VASP

phosphorylation at Ser-157 after serum stimulation (data not shown). Results from the literature suggest that MCFB (+/+) cells may lack PKG [182] which led us to examine the PKG levels in these cells directly. Western blots of cell lysates with anti PKG antibody didn't detect any PKG protein (Fig.10b). SNP stimulated platelet samples used as a positive control in this western blot showed the expected expression of PKG in this cell type and thus support the activity of the antibody used. As there is no detectable PKG level in MCFB (+/+) cells and as there was no influence detectable of a PKG inhibitor on serum stimulated VASP phosphorylation, these results strongly suggest that serum stimulated VASP phosphorylation is independent of PKG in MCFB cells (+/+). Moreover results from a blot with 16C2 antibody (with specificity for VASP phospho-Ser-239) against serum stimulated cell lysates (Fig.7b) further support this conclusion.

In summary, these results suggest that along with PKC, PKA but not PKG is involved in serum stimulated VASP phosphorylation at Ser-157 and that this might happen by the sequential pathways  $[1'+2]$  or  $[2'+1]$  of the protein kinase network model depicted in Fig.8. However according to this model, it could also be possible that PKA and PKC may regulate the activity of VASP independently each other. Nevertheless based on known data we suspect the former pathway to be the most probable one because PKA is well known to directly phosphorylate VASP preferentially at Ser-157 (see Chapter 2.1.1.4 and Fig.8). To establish the sequence of action of these two protein kinases the signalling pathway was elucidated further in detail.

#### **5.1.4. Serum stimulated PKCs involved in VASP phosphorylation are members of the Bis I sensitive and phorbol ester regulated classical isoforms of protein kinase C**

PKC comprises different isozyme forms and each isozyme is expressed in different cell types with a different mode of specific activity [183] [184]. The inhibitor used in the above experiments (Ro-31-8220) to inhibit PKC activity is not specific enough to discriminate among PKC isozymes individually. An important question therefore is to find out the responsible isozyme class of PKC that is involved in serum stimulated VASP phosphorylation at Ser-157. It can be done by using isozyme class-specific inhibitors which are commercially available (see Table.6). So called classical isoforms of PKC, which are also phorbol ester sensitive, participate in cytoskeletal reorganization and serum mediated protein kinase activities [185] [179]. Hence we searched for a role of classical isozymes of PKC in serum stimulated VASP phosphorylation by using specific inhibitors for this class of PKC, which are generally accepted in the literature and proven to be potent inhibitors.

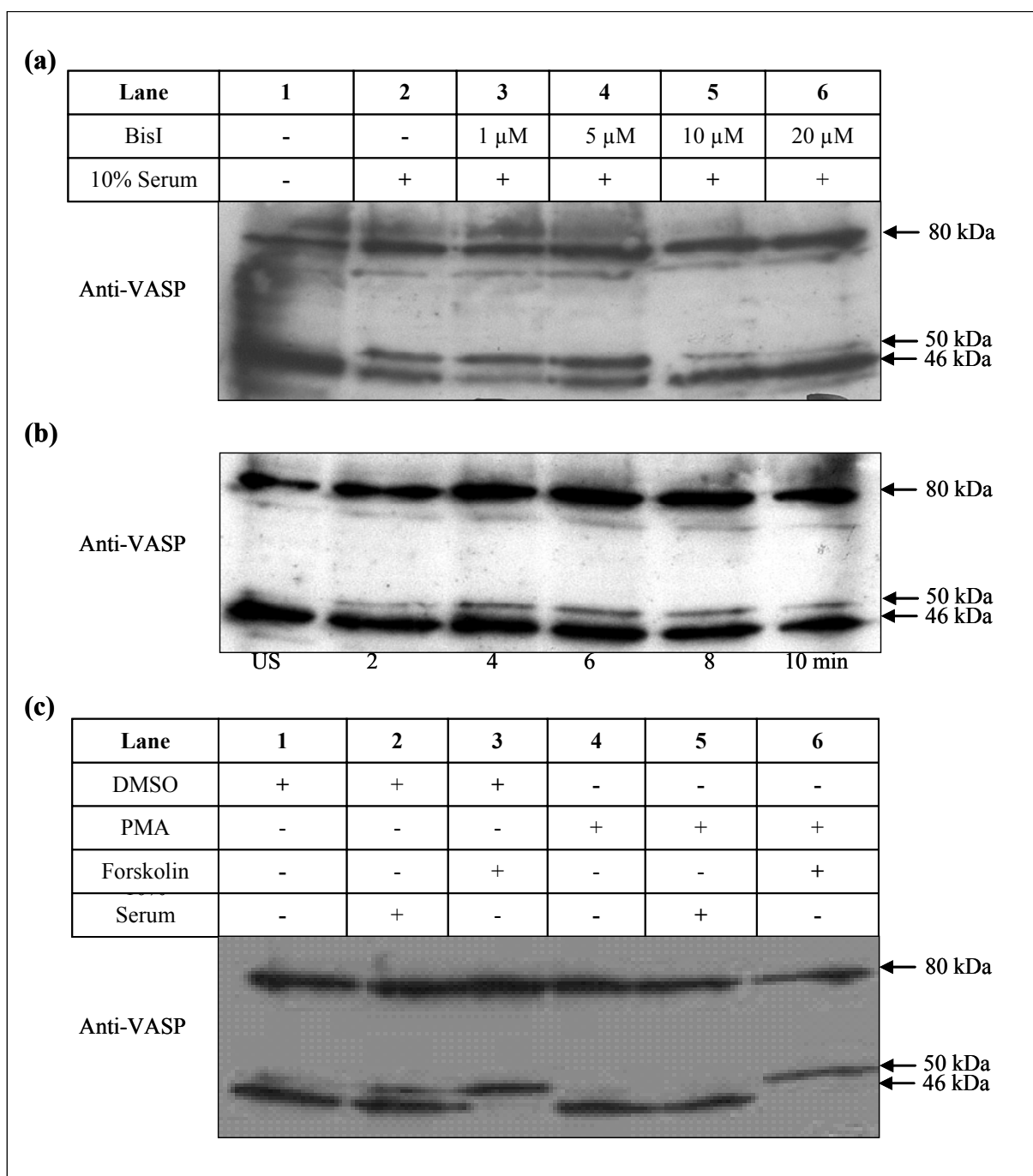


**Figure 11: Serum stimulated VASP phosphorylation is sensitive to inhibition activity of Bis I and phorbol ester treatment.** (a) MCFB cells (+/+) were incubated with different concentration of Bis I, an inhibitor of classical protein kinase C isozymes, for 30 min prior to serum stimulation for 3 hours and blotted for VASP phosphorylation with M4 antibody. (b) MCFB cells (+/+) were stimulated with PMA, an activator of classical protein kinase C isozymes, for different time periods and blotted for VASP phosphorylation with M4 antibody. (c) MCFB (+/+) cells were also stimulated with PMA either alone or prior to stimulation with 10% serum (3 hours) or 10  $\mu$ M Forskolin (10 min), an activator of adenylate cyclase and thus PKA. DMSO was used as vehicle for PMA and thus substituted for PMA in positive control experiments. In all the blots, 46 kDa and 50 kDa bands represent non-phospho and phospho forms of VASP respectively and the upper band of 80 kDa which is also recognized by the M4 anti-VASP antiserum serves as a loading control. In Fig. a, lane 1 and 2 represent unstimulated and stimulated positive controls respectively. In Fig. b, US represent an unstimulated control cell sample. Blots shown are representative of three independent experiments.

The experiments were carried out with Bis I, a potent classical PKC isoform inhibitor [175], and Bis V [176] which is an inactive version thereof serving as a negative control

for inhibition of PKC by this class of drugs. Overnight starved quiescent cells were incubated with these two types of inhibitors at different concentrations (1  $\mu$ M, 5  $\mu$ M, 10  $\mu$ M, 20  $\mu$ M) for 30 min and then stimulated with 10% serum according to the general experimental scheme as given in chapter 4.2.1.5. The cell lysates analyzed by western blotting with M4 antibody showed that the presence of the classical PKC inhibitor, Bis I inhibited the serum stimulated VASP phosphorylation at Ser-157 in a concentration dependent manner (shown in Fig. 11a). Lane 1 shows no VASP phosphorylation at Ser-157 in unstimulated cells but lane 2 does due to serum stimulation. Treatment of cells by low concentrations of Bis I did not show a prominent inhibition of VASP phosphorylation (in lanes 3 and 4 in Fig.11a). However, 10  $\mu$ M and 20  $\mu$ M concentrations of Bis I applied to these cells and assayed in lanes 5 and 6 respectively showed a prominent inhibition of serum stimulated VASP phosphorylation at Ser-157. From this experiment it could be deduced that a concentration of 10  $\mu$ M of Bis I is optimal in MCFB (+/+) cells to interrupt the activity of PKC as assayed by their phosphorylation of VASP (Fig.11a). Moreover there was no inhibition of VASP phosphorylation in samples stimulated with serum after incubating for 30 min with the corresponding inactive Bis derivative, Bis V, which serves as the required negative control compound to assess the specificity of PKC inhibition (data not shown). These results show that Bis I sensitive classical isozymes of PKC are among the participants in serum stimulated VASP phosphorylation at Ser-157 and these data further support the results obtained with the general PKC inhibitor Ro-31-8220 (see Fig.9a and 10a).

If the classical isoforms of the PKC are participating in serum stimulated VASP phosphorylation, then this pathway(s) should also respond to the effects of phorbol ester activity due to the phorbol ester sensitivity of this class of isoforms. Phorbol esters have a characteristic mode of regulating activity of PKCs and are highly time dependent in their action spectrum: they not only activate PKC for short time intervals but also inhibit the activity of PKC on the longer run upon translocation of PKCs to the membrane [185]. Incubation of cells with phorbol esters for longer time periods thus down regulates the activity of PKC [186]. Given the involvement of PKC in serum induced VASP phosphorylation it should also be affected upon modulation of PKCs with phorbol esters. Overnight starved quiescent cells were therefore stimulated with PMA, a well known phorbol ester compound, and samples were collected at every two minutes to find out the time course of PKC activation and down-regulation. Western blots with M4 antibody showed that there is VASP phosphorylation up to 8 min after phorbol ester stimulation and at later time points no further increase of VASP phosphorylation was seen (Fig.11b), possibly indicating a down regulation of PKC activity by phorbol ester treatment (data not shown for time periods after 10 min). It is interesting to note here that VASP phosphorylation occurred nearly after 90 min of

serum stimulation (Fig.6b), but an activation of PKC directly with PMA induced VASP phosphorylation as early as after 2 min with this activity not further extending beyond 8 min after PMA addition. The different time course might be due to differences in the lag time of the signal transduction cascades depending on a more proximal or distal activation of the PKC enzymes. However these kinetic aspects have not been studied further in this work.

The above result (Fig.11b) suggests that down-regulation of PKC by phorbol esters may have inhibited phosphorylation of VASP. But, for this interpretation, it has to be confirmed that the down regulation of the VASP phosphorylating protein kinase activity by phorbol ester long-term treatment is indeed only due to PKC but not PKA which is also involved in the serum stimulated VASP phosphorylation as shown above in Fig.10a. We therefore performed a control experiment in such a way to down regulate the activity of PKC by phorbol ester long-term treatment (i.e. more than 8 min) during the activation of PKA via Forskolin which activates adenylyl cyclase. In a six well plate, the cells were incubated with PMA for more than 8 min and they were then stimulated with either serum (10%) or Forskolin (10  $\mu$ M). If the phorbol ester would not affect PKA activity, then we would expect a prospective activity of this protein kinase i.e. a VASP phosphorylation in Forskolin stimulated cells pre-incubated with PMA. However no VASP phosphorylation would be expected in serum stimulated cells during phorbol ester long-term treatment as PKC activity is down regulated and the process is dependent of PKC as shown above in the results of Fig.11a and b. Cell lysate samples stimulated with either serum or Forskolin were used as positive controls in this experiment which are both known to induce VASP phosphorylation at Ser-157 as shown in lanes 2 and 3 respectively in Fig.11c and also in the previous experiments. The experimental results in Fig. 11c clearly show that there is an inhibition of VASP phosphorylation at Ser-157 after phorbol ester long-term treatment as shown in lanes 4 and 5 either with or without serum stimulation respectively (compare lanes 5 and 4 with lane 2). But there is phosphorylation of VASP at Ser-157 after Forskolin treatment in the presence of phorbol ester long-term treatment as seen in lane 6. Result in lane 3 show that the vehicle substance DMSO does not affect Forskolin stimulation and lane 1 shows the activity of the vehicle (DMSO) alone which does not induce phosphorylation of VASP at Ser-157 in the cell line under study. The absence of VASP phosphorylation at Ser-157 was observed in lanes 4 and 5 is thus due to the phorbol ester (PMA) long-term treatment which finally inactivates PKC. VASP phosphorylation at Ser-157 as observed in lane 6 due to a Forskolin treatment after long-term application of PMA suggests that the phorbol ester seems to be specific for PKC and is not affecting the PKA mediated signalling pathway leading to phosphorylation of VASP at Ser-157. Most important these results gave a first cue that PKA activity might act downstream to PKC and therefore PKC inhibition did



not oppose an activation of PKA by Forskolin. However, a sequential order of activity as suggested from these results has to be further substantiated by using combinations of activators and inhibitors as described in the following paragraph (see Chapter 5.1.5).

In summary, the results of the last three chapters have shown that PKA and Bis I sensitive, phorbol ester regulated classical isozymes of PKC are the major cytoskeleton associated protein kinases involved in serum stimulated VASP phosphorylation at Ser-157. The combined evidence rules out all the other possible pathways involving either PKG or Rho kinases shown in the interaction network model of Fig.8. However the experimental evidence obtained so far does not allow to conclusively decide between pathways  $[1'+2]$ ,  $[2'+1]$  or  $[1+2]$  of this model (Fig.8) i.e. the order of involvement of PKA and PKC in either a serial or parallel organisation of the pathway in serum-stimulated VASP phosphorylation at Ser-157 is still unresolved at this stage of the study. In signal transduction research, it is usually only a first step to identify the participating biological molecules in a pathway and it is finally important to find out the order of action of these biological players in the pathway under study.

### **5.1.5. Serum stimulated VASP phosphorylation is mediated by a sequential action of classical PKC isoforms and PKA**

From the above results, it has been shown that PKC and PKA are mediating serum stimulated VASP phosphorylation. To resolve the order of these participating protein kinases in the signalling cascade, it will be necessary to determine the output reaction i.e. VASP phosphorylation at Ser-157 in response to simultaneous activations and inhibitions of these protein kinases using informative combinations of specific activators and inhibitors during serum stimulation of cells (Fig.8). In principle serum stimulation could lead to VASP phosphorylation via PKA and PKC either by a parallel or a serial action of these protein kinases (see pathways  $[1+2]$  in comparison to pathways  $[1'+2]$  or  $[2'+1]$  in Fig.8 of our interaction network model). A sequential order of PKA and PKC action in serum stimulated VASP phosphorylation was determined by using in independent experiments instead of serum the specific activators of PKA or PKC, Forskolin or PMA in combination with the inhibitors H89 or Bis I which are specific for these protein kinases (see Fig.8 for target sites and mode of action of these drugs). Bis V was again used as an inactive derivative to control the specificity of inhibition of Bis I in case of PKC (see Table.6). Overnight starved quiescent MCFB cells (+/+) were therefore pre-incubated with the inhibitors H89 (10  $\mu$ M) or Bis I (or Bis V) (10  $\mu$ M) either separately or together in a six well plate for 30 min and then stimulated in separate experiments either with serum (10%) (Fig.12a), or the adenylyl cyclase activator Forskolin (10  $\mu$ M) (Fig. 12b) or the PKC activator PMA (1  $\mu$ M) (Fig.12c) as described in

chapter 4.2.1.5 and Fig.4 The general experimental protocol in the combination of the inhibitors and activators used in these three independent experiments (labelled as a,b,c) is further summarized in the schemes above the gel sections of Fig.12.

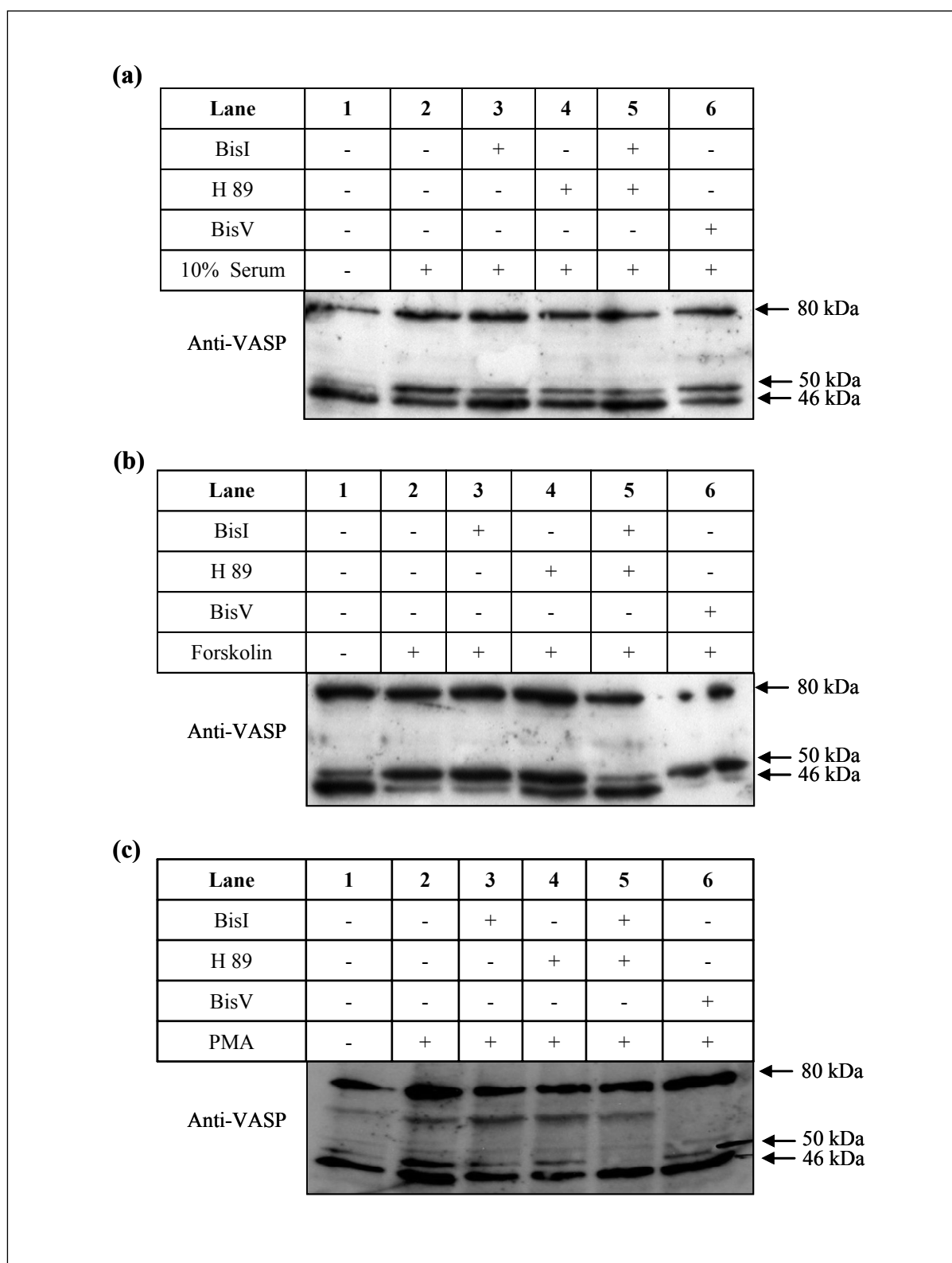


**Figure 12: Serum activated PKC passes a signal to PKA to phosphorylate VASP at Ser-157.** MCFB cells (+/+) were incubated with Bis I (10  $\mu$ M), a PKC inhibitor and/or H89 (10  $\mu$ M), a PKA inhibitor for 30 min prior to stimulation with serum (10%) (Fig. a) or Forskolin (10  $\mu$ M), an activator of adenylyl cyclases thus activates PKA (Fig.

b) or PMA (1  $\mu$ M), a PKC activator (Fig. c) for 3 hours, 10 min and 8 min respectively. Bis V is a negative specificity control for PKC inhibition. The samples were blotted for VASP phosphorylation with M4 antibody. In all the blots, 46 kDa and 50 kDa bands represent non-phospho and phospho forms of VASP respectively and the upper band of 80 kDa recognized by the M4 anti-VASP antiserum serves as a loading control. Lane 1 in all the three blots represents unstimulated control. Blots shown were representative of three independent experiments.

Upon **serum stimulation**, lane 1 in Fig. 12a represents the unstimulated control showing no VASP phosphorylation and in lane 2 there is VASP phosphorylation observed at Ser-157 as expected. Lane 3 and 4 show partial inhibition of this serum stimulated VASP phosphorylation in the presence of either Bis I or H89. In the presence of Bis I and H89 together, lane 5 shows a prominent inhibition of serum stimulated VASP phosphorylation (see lanes 3 and 4 in comparison to lane 5). Bis V treatment did not effect VASP phosphorylation (see lane 6) and thus supports the specificity of Bis I on PKC. These results show that while there is only a partial inhibition of serum stimulated VASP phosphorylation by Bis I or H89 when applied separately, a prominent inhibition of serum stimulated VASP phosphorylation is observed in the presence of Bis I and H89 together. Although from these results it cannot be safely conclude whether PKC and PKA act in serum stimulated VASP phosphorylation either in series (see pathways [1'+2] or [2'+1] in Fig.8) or in parallel (see pathways [1+2] in Fig.8), the data clearly further supports the combined involvement of PKC and PKA in this process. Experiments have therefore been carried out by using directly instead of serum as a stimulator, activators of PKC or PKA in combination with the corresponding inhibitors of these protein kinases to further test the structure of this pathway.

The results of VASP phosphorylation in the presence of the adenylyl cyclase activator **Forskolin** and the different inhibitor combinations are shown in the western blot analysis of Fig. 12b using M4 antibody. Lane 1 of Fig.12b shows almost no VASP phosphorylation without any Forskolin treatment whereas Forskolin treatment induced prominent VASP phosphorylation at Ser-157 in the cells (see lane 2). In lane 3, addition of the PKC inhibitor, Bis I did not interrupt the Forskolin activity i.e. VASP phosphorylation upon PKA activation. However in lane 4, the PKA inhibitor H89 inhibited this activity as seen by the more prominent appearance of the 46 kDa dephospho Ser-157 VASP band in this lane compared to lane 2. This inhibition of Forskolin activated PKA activity by H89 is an expected experimental result because both the drugs exert opposite effects on the same target (see Table.6 and node 'PKA' in Fig 8). Bis I treatment alone was found to have no influence on Forskolin stimulated VASP phosphorylation at Ser-157 (lane 3). Treatment of cells together with Bis I and H89 results in lane 5 in a more prominent loss of Forskolin stimulated VASP phosphorylation at Ser-157 as compared to H89 mediated inhibition alone (lane 4). In general, the activity of both inhibitors applied together (lane 5) was expected to be similar to the activity of H89 alone (lane 4) because the PKC inhibitor Bis I does not interfere

with PKA activity as proved by using Bis V (lane 6). The prominent inhibition of Forskolin stimulated VASP phosphorylation in the presence of both Bis I and H89 compared to the activity of each one alone was thus an unexpected finding. We have within our experimental limits currently no explanation for the enhanced combined action of both inhibitors together. However, the insensitivity of Forskolin stimulated VASP phosphorylation at Ser-157 to Bis I alone (lane 3) suggests that PKC does not seem to be involved in direct VASP phosphorylation which is probably mediated by PKA upon the applied Forskolin stimulation. These data are also in line with the experiments described above which showed a Forskolin stimulated VASP phosphorylation at Ser-157 being undisturbed by a long term treatment of PMA that will also finally inactivate PKC (see Chapter 5.1.4). These data therefore suggest that the possible pathway numbered as [2'+1] in our interaction network model of Fig.8 could probably be ruled out.

Further support for this interpretation is given in the following experiment where the results of VASP phosphorylation in the presence of the short term PKC activator **PMA** and different inhibitor combinations are shown in a western blot analysis of Fig. 12c. Lane 1 again represents the unstimulated control and lane 2 shows the expected PMA stimulated VASP phosphorylation by short-term activation of PKC. Lane 3 and 4 show the inhibition of PMA induced VASP phosphorylation in the presence of the inhibitors Bis I or H89 respectively. Inhibition of PMA stimulated VASP phosphorylation by Bis I as observed in lane 3 is an expected experimental result because also these drugs exert opposite effects on the same target in this case PKC (see Table.6 and Fig.8). Most important the PKA inhibitor H89 was found to inhibit the PMA stimulation of VASP phosphorylation as it was mediated by PKC (see lane 4). VASP phosphorylation after PMA stimulation in presence of both inhibitors Bis I and H89 together is completely suppressed. Activity of Bis V in lane 6 again shows the specific inhibitory activity of Bis I on PKC also under these experimental conditions. Taken together the experimental results in particular the inhibition of PMA activity by H89 in lane 4 suggest that phosphorylation of VASP at Ser-157 by PKC seems to be mediated by PKA. This interpretation explains H89 mediated inhibition of PMA stimulated VASP phosphorylation at Ser-157 by blocking the PKA activity after upstream activity of PKC. It therefore further supports the pathway structure [1'+2] of our interaction network model as depicted in Fig.8. This organisation of the pathway states the most probable order of events during phosphorylation of VASP by a combined and sequential action of PKC and PKA.

Summarizing the cumulative evidence from the experiments shown in Fig. 12, the data suggest that serum stimulated VASP phosphorylation in MCFB cells depends on serial activity of PKC and PKA in that order. The inhibitory activity of H89 against PMA stimulated VASP

---

phosphorylation supports an upstream position of PKC to that of PKA in this signalling pathway. This interpretation also fully explains the observed inability of Bis I to interrupt Forskolin stimulated VASP phosphorylation while using the complementary combination of inhibitors and activators. It is also in line with the observation that a long term treatment of cells with PMA does not perturb the Forskolin induced VASP phosphorylation. In conclusion, we suggest within the limits of the available experimental data that upon serum stimulation of MCFB cells (+/+) cells, a classical isoform of PKC receives an external stimulatory signal which is then passed to PKA to phosphorylate VASP at Ser-157. According to our data PKA is thus positioned downstream of PKC in the pathway under study and located most proximal to its substrate VASP giving a pathway structure of serum stimulated VASP phosphorylation as: serum  $\rightarrow$  PKC  $\rightarrow$  PKA  $\rightarrow$  VASP at Ser-157 (represented as [b+I'+2] in our interaction network model of Fig.8. The internal regulation of PKA in this signalling cascade has not been addressed here; so it is still unclear if it depends on a cAMP activation or an unknown signal message received indirectly from PKC.

## **5.2. In search for binding epitopes of the Spred2 EVH1 domain: Genetic screening of a cDNA expression library using a bacterial two-hybrid system**

### **5.2.1. Motivation for the experimental approach chosen**

The Spred2 EVH1 domain is a member of a new class of EVH1 domains which has initially been described in the recently discovered Spred proteins. Its atomic structure has recently been determined by NMR spectroscopy in a close collaboration with Linda J. Ball (SGC Oxford and FMP Berlin) and our Institute based on the purification of isotopically labelled protein samples after recombinant expression in *E. coli*. The Spred2 EVH1 structure shows the typical fold of an EVH1 domain with several unique features among them a characteristic putative binding cleft region containing a subfamily-specific triad of surface exposed amino acid residues which by homology are expected to be involved in ligand binding. Based on these structural data an interaction of the Spred2 EVH1 domain with unique ligand(s) probably comprising short linear peptide epitopes is expected.

Expression and purification of a natively folded Spred2 EVH1 domain in *Escherichia coli* suitable for structure determination by NMR spectroscopy prompted us to take further advantage of this host. We therefore decided to use a bacterial two-hybrid selection protocol in *E. coli* to carry out an interaction cloning approach for the identification of candidate peptide binding partner(s) of the Spred2 EVH1 domain.

### **5.2.2. Introduction to the bacterial two-hybrid system and overview of the experimental procedure**

A variety of *E. coli* two-hybrid systems have been described in the literature which utilize components of various well-characterized bacterial genetic systems as suitable reporters for bait and target protein interactions [136, 187]. For our studies in search of Spred2 EVH1 domain binding epitopes, we established the bacterial two-hybrid screening system developed by Joung et al [137, 188]. In this genetic method, detection of an *in-vivo* interaction of a bait and target protein is based on transcriptional activation of a bicistronic reporter gene cassette comprised of the yeast imidazoleglycerolphosphate dehydratase (*HIS3*) gene [189] and a bacterial aminoglycoside 3'-adenyltransferase (*aadA*) gene [190] which is located on an F' episome in a *hisB* mutated *E. coli* strain (Fig.13) [137, 189, 191]. The promoter of this reporter gene cassette is a modified *lac* promoter and contains a single  $\lambda_{OR2}$  operator replacing its endogenous cAMP receptor protein (CRP) binding site [188, 192]. Bait and target proteins are expressed separately from two compatible expression plasmids. The protein of interest (the bait, represented as X in Fig.13) is

fused C-terminally to the dimerization domain of bacteriophage  $\lambda$  cI repressor protein (237 amino acids) which tethers to the  $\lambda$ O<sub>R2</sub> operator via its DNA binding domain (Fig.13). The target proteins (represented as Y in Fig.13) are individually fused to the N-terminal domain of the  $\alpha$ -subunit of RNA polymerase. They are encoded by a cDNA expression plasmid library which is used in the search for unknown binding epitopes. When the bait and target hybrid protein encoded by separate bait (pBT) and target (pTRG) expression plasmids interact, the  $\lambda$ cI-bait hybrid protein at the  $\lambda$ O<sub>R2</sub> operator specifically recruits and stabilizes the  $\alpha$ -N target hybrid protein at the weak *lac* promoter [192-194] thereby inducing transcription of the downstream *HIS3* and *aadA* reporter genes by RNA polymerase (Fig.13) [137]. The magnitude of this transcriptional activation correlates with the strength of the interaction between the two chimeric proteins expressed [133]. Expression of the yeast *HIS3* gene will complement in an auxotrophic *E. coli* host strain its deficiency of the homologous *hisB* gene and thus allows growth on selective histidine free media even in the presence of low concentrations of a competitive inhibitor of the *HIS3* enzyme, 3-amino-1, 2, 4-triazole (3-AT) [189]. The *aadA* gene confers streptomycin resistance to the cells for further selection of any positive protein interactions [190]. This sophisticated bacterial two-hybrid system thus allows positive selection by increasing 3-AT concentrations of bacterial clones that exhibit a productive interaction between co-expressed bait and target fusion proteins. It offers the ability for rapid analysis of gene expression libraries larger than  $10^8$  cfu due to the high transformation rate possible with highly competent *E. coli* cells. Expression plasmids for the Spred2 EVH1 and the VASP EVH1 domain are constructed and absence of self-activation by these chimeric proteins alone is assayed to make sure that transcriptional activation does not take place in the B2H system without a productive protein interaction. Before screening a cDNA expression library, it is also necessary to calibrate the B2H system with known types of protein interactions for the range of required selection intensities by determining the reporter gene expression levels compatible with growth in the presence of 3-AT. Therefore, we used as a positive control the VASP EVH1 domain in combination with a set of different binding peptides derived from the ActA protein of *Listeria monocytogenes* viz., a wild type peptide and its tighter and non binding mutant peptides [24]. These interactions were used to establish and to calibrate the B2H genetic system for detection of low affinity target interactions of a well-known adaptor protein domain. A thermodynamic study of *in-vitro* binding of the VASP EVH1 domain with these ActA peptides in our laboratory had obtained binding constants ( $K_d$ ) ranging from 19 to 214  $\mu$ M for different truncated versions of the ActA ligand [24]. In *E. coli*, this value would correspond to cellular concentrations of 20,000 to 200,000 molecules per bacterial cell and expression of these levels should be achievable with the expression plasmids employed in the B2H system. The dimerization domain of the yeast

transcriptional activator Gal4 (referred to as LGF2) and a domain derived from a mutant form of the Gal11 protein called Gal11<sup>P</sup> have been shown to interact strongly in yeast [195-197] and *E. coli* [138]. Hence, this well characterised interaction pair is considered as a further positive control pair of the B2H system. After establishing suitable 3-AT selection conditions for detection of low affinity EVH1-ligand interactions, a cDNA expression library is screened under these conditions for interacting partners of the Spred2 EVH1 domain. The cDNA expression library is derived from brain tissue since Spred proteins are known to be expressed predominantly in this and other neural tissues [79]. Hence, we had chosen a human brain cDNA library cloned uni-directionally into the expression target vector pTRG to represent brain-specific proteins as  $\alpha$ -N fusions (Fig.13) for a screen of binding epitopes of the Spred2 EVH1 domain. The library screening against this query protein is initially based on *HIS3* gene transcriptional activation followed by a secondary screening based on *aadA* gene transcriptional activity. A collection of colonies obtained after dual selection is physically characterised by colony PCR with primers flanking the cloning sites of the target plasmid. Target plasmids were then isolated after genetic and physical separation from the Spred2 EVH1 bait plasmid for further characterization. These target plasmids should contain putative Spred2 EVH1 interaction partners among an unknown fraction of false positive isolates. Individual target plasmids from this collection were therefore further characterized after retransformation with appropriate bait plasmids by three different types of genetic assays in order to assess (1) their 3-AT resistant phenotype, (2) their potential for Spred2 EVH1 independent self activation and (3) their interaction specificity to the Spred2 EVH1 domain (Fig.18). After co-transformation of each target plasmid isolate with either (1) the Spred2 EVH1 bait, (2) an empty bait or (3) a non-cognate EVH1 bait plasmid the doubly transformed clones were compared with respect to their plating efficiency (PE) in the presence of 3-AT. PE determines the fraction of 3-AT resistant colonies among the total co-transformed colonies and correlates with the interaction strength at a defined selection stringency for each fusion protein pair [198]. It is calculated by counting the cfu on selective screening medium vs. non-selective screening medium normalized to the DNA amount applied for transformation. Sequencing of positive target plasmids obtained from these genetic assays would reveal consensus motifs of the peptides interacting with the Spred2 EVH1 domain.



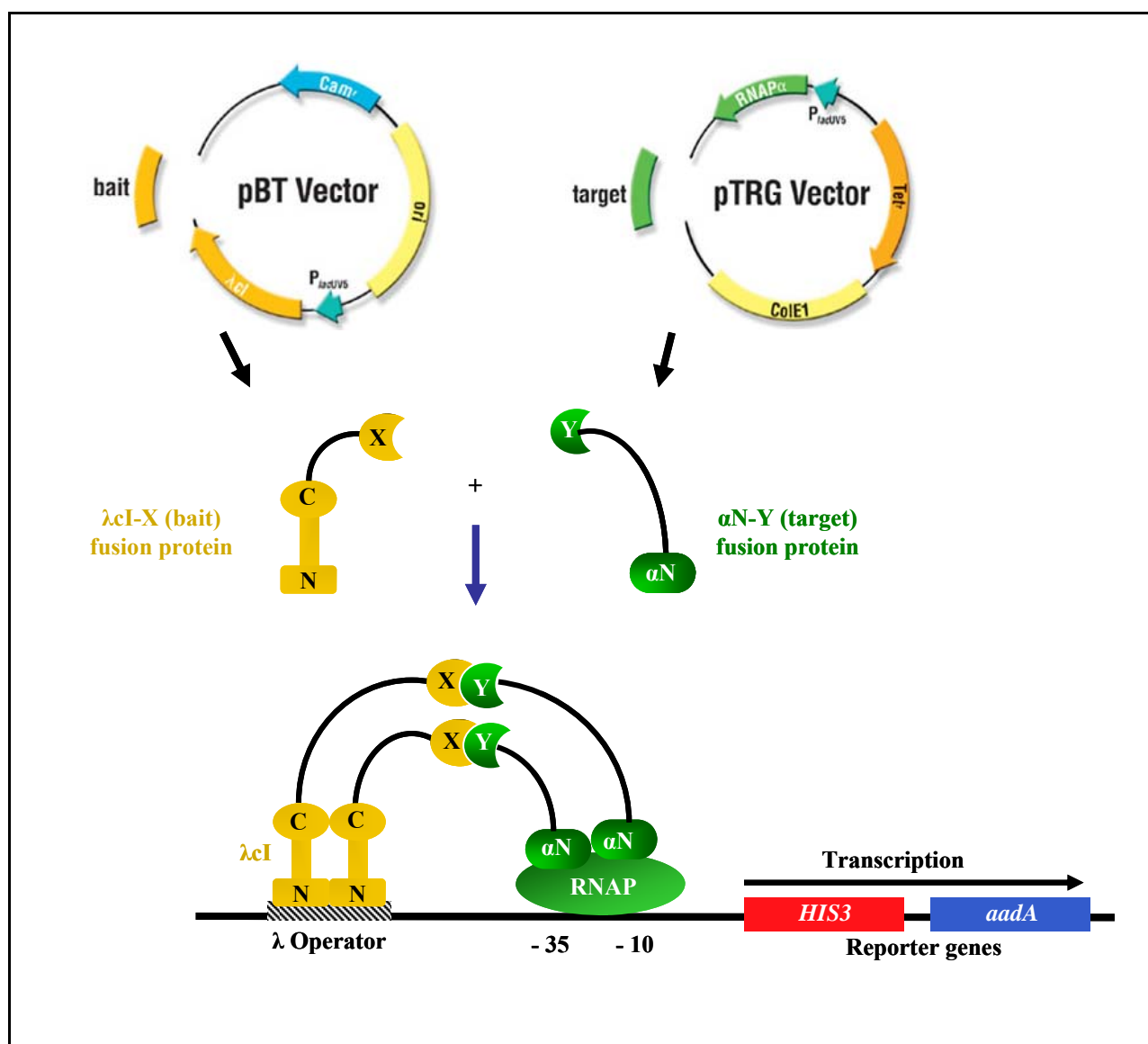


**Figure 13: An overview of bacterial two-hybrid system.** A dimeric  $\lambda$ CI-bait protein (shown as ‘X’) interacts with a RNA polymerase (RNAP)  $\alpha$ -subunit-target protein (shown as ‘Y’) containing bait binding epitope at a  $\lambda$ O<sub>R2</sub> operator, thereby recruiting RNAP to the adjacent promoter that directs expression of a *HIS3* and *aadA* reporter gene cassette. The bait and target fusion proteins are encoded on two compatible expression plasmids (pBT and pTRG), while the reporter gene cassette is located on an F’ episome.

### 5.2.3. Construction of bait and target expression plasmids and establishment of the bacterial two-hybrid system for detection of EVH1 ligand interactions

The DNA sequences encoding Spred2 (1-124) and VASP (1-115) i.e. the Spred2 EVH1 and the VASP EVH1 domains respectively were cloned into the appropriate multiple cloning sites of pBT vector by ligation of the respective amplified PCR fragments with the suitable sticky ends giving the bait plasmids pBT-Spred2 (1-124) and pBT-VASP (1-115) respectively (Table.7). Synthetic codon usage optimized oligonucleotides encoding the wild type ActA peptide  $_{332}\text{SFEFPPPPTEDEL}_{344}$  and its tighter and non-binding mutants  $_{332}\text{SFEWPPPPTEDEL}_{344}$  and  $_{332}\text{SFEAPPPPTEDEL}_{344}$  were cloned into the pTRG vector giving the target plasmids pTRG-

ActA(332-344)F, pTRG-ActA(332-344)W and pTRG-ActA(332-344)A respectively (Table.7). The commercially available plasmids pBT-LGF2 and pTRG-Gal11<sup>P</sup> expressing the LGF2 and Gal11<sup>P</sup> interaction pair were used as a further positive control. All constructs were sequenced to verify the insert coding sequence and its in-frame fusion to the acceptor ORFs. These plasmids were purified in high mass yields for experimental use.

Plasmid	Insert coding sequence	Expressed fusion product
pBT	Human Spred2 (1-124)	$\lambda$ cI-Spred2 EVH1
pBT	Human VASP (1-124)	$\lambda$ cI-VASP EVH1
pBT	LGF2	$\lambda$ cI-Gal4
pTRG	ActA [332SFE <u>F</u> PPPPTEDEL <sub>344</sub> ]	$\alpha$ N-SFE <u>F</u> PPPPTEDEL
pTRG	ActA [332SFE <u>W</u> PPPPTEDEL <sub>344</sub> ]	$\alpha$ N-SFE <u>W</u> PPPPTEDEL
pTRG	ActA [332SFE <u>A</u> PPPPTEDEL <sub>344</sub> ]	$\alpha$ N-SFE <u>A</u> PPPPTEDEL
pTRG	Gal11 <sup>P</sup>	$\alpha$ N-Gal11 <sup>P</sup>

**Table 7: Plasmid constructs used in B2H screening experiments.** The coding sequences for query bait Spred2 EVH1 and positive control bait VASP EVH1 domain were cloned into the pBT vector to express  $\lambda$ cI-bait fusion proteins. The coding sequences of different ActA peptides were cloned into pTRG target vector to express the  $\alpha$ -N RNA polymerase fusion peptides. The pBT and pTRG vectors carrying insert coding for LGF2 and Gal11<sup>P</sup> respectively were used to express the respective fusion proteins as a further positive interaction control pair.

In order to establish selection conditions of the B2H genetic system for a detection of low affinity interactions of EVH1 domains the bait and target plasmid pairs pBT-VASP (1-115) / pTRG-ActA (332-344)F, pBT-VASP (1-115) / pTRG-ActA (332-344)W, pBT-VASP (1-115) / pTRG-ActA (332-344)A were co-transformed into competent cells of the *E. coli* XL1-Blue *hisB* MRF' Kan<sup>r</sup> strain. Co-transformants were analysed for 3-AT resistant colony growth by plating on selective screening medium containing increasing concentrations of 3-AT viz., 0 mM, 0.25 mM, 0.5 mM, 1.0 mM, 2.0 mM, 3.0 mM, 4.0 mM and 5.0 mM. Colony growth was observed at 3-AT concentrations up to 5 mM for co-transformants of pBT-VASP (1-115) with the pTRG-plasmids encoding the cognate ActA peptides i.e. ActA (332-344)F and ActA (332-344)W (Fig. 14). The non-binding mutant peptide ActA (332-344)A failed to support such growth even at the lowest 3-AT concentration tested. The yeast LGF2 and Gal11<sup>P</sup> interaction pair used as a further positive control showed a similar 3-AT resistance phenotype but plated at a five fold higher plating efficiency due to their more robust interaction behaviour (Fig. 14).

Expression levels of  $\lambda$ cI-VASP EVH1 and  $\lambda$ cI-Spred2 EVH1 were analysed immunologically in western blots with an anti- $\lambda$ cI polyclonal antibody. This antibody however

could not detect an expression of  $\lambda$ C1-VASP EVH1 and  $\lambda$ C1-Spred2 EVH1 fusion proteins even after using different minimal and rich media and various host strains. Yet, the anti- $\lambda$ C1 antibody activity was confirmed by the  $\lambda$ C1-LGF2 positive control. No EVH1 antiserum was available for an independent detection of the fusion proteins. It was concluded that although the expression levels of the EVH1 fusion proteins were below the detection limit of the anti- $\lambda$ C1 antibody their local intracellular concentrations were nevertheless high enough to be detected genetically as assayed by transcriptional activation of the reporter gene cassette.

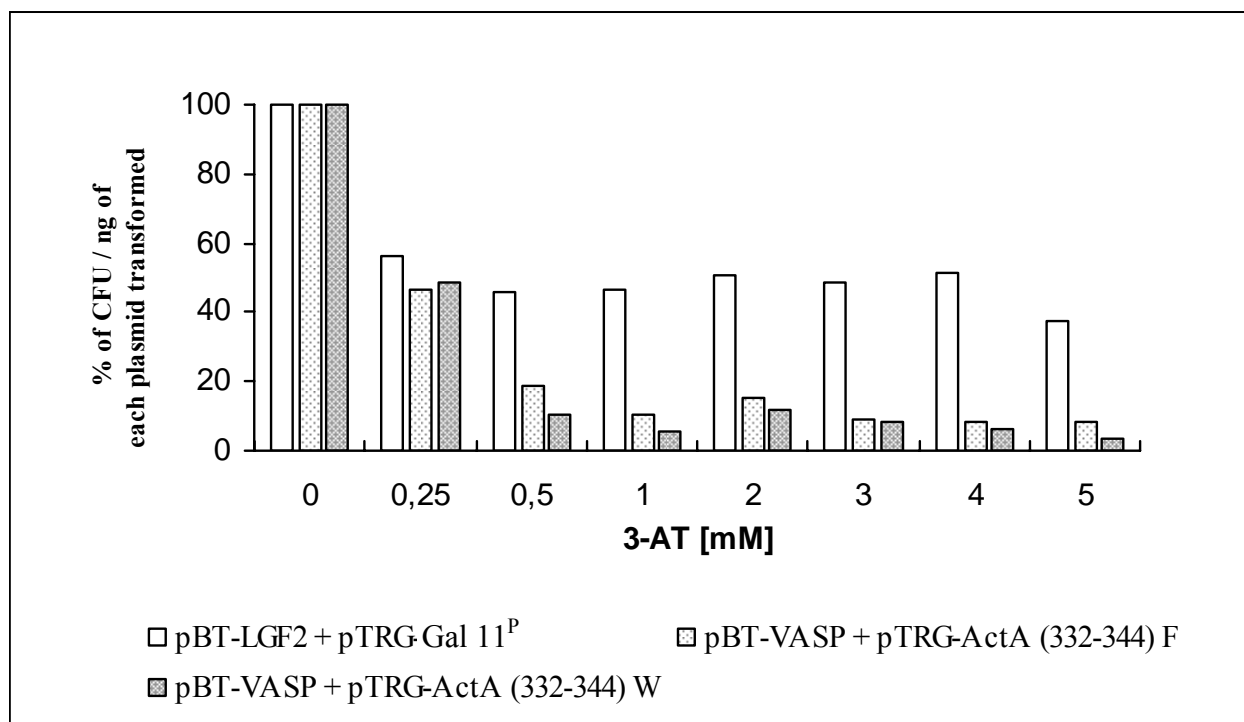


**Figure 14: Establishment of B2H system for EVH1 domain interactions.** Plating efficiency (percentage of cfu per ng of transformed plasmid) at increasing concentrations of 3-AT for co-transformants expressing appropriate fusion proteins either VASP EVH1 and two different ActA peptides ( ${}_{332}\text{SFE}\underline{\text{P}}\text{PPPT}\text{EDEL}_{344}$  (▤) or  ${}_{332}\text{SFE}\underline{\text{W}}\text{PPPT}\text{EDEL}_{344}$  (▥)) or a pair of robustly interacting yeast proteins (LGF2 and Gal11<sup>P</sup>(□)) is shown here. These data show the utility of the bacterial two-hybrid system for *in-vivo* detection of interactions between an EVH1 domain and its binding peptides that have previously [24] been well-characterized *in-vitro*.

As a further test the potential for partner-independent self activation of each of the recombinant constructs was studied by transforming into the *E. coli* XL1-Blue *hisB* MRF' Kan<sup>r</sup> reporter strain the recombinant plasmid encoding the chimeric protein together with its empty partner plasmid (pBT-X / pTRG empty plasmid; pBT empty plasmid / pTRG-Y) and assaying for colony growth on 3-AT selective and non-selective medium. Colony growth on non-selective 3-AT free medium plates confirmed that co-transformation of both bait and target plasmid confers double antibiotic resistance to the host cell to allow its growth in the presence of both antibiotics. No colony growth was observed on 3-AT selection plates showing the incapability of chimeric protein

alone to activate *HIS3* gene transcription and thus confirming the lack of self activation for each of these genetic elements.

In summary, the data from these experiments clearly demonstrate that an interaction of an EVH1 domain with its cognate binding motif which has been well-characterized *in-vitro* [24, 29] could be successfully recorded *in-vivo* in a heterologous bacterial expression system which utilizes transcriptional activation of a reporter gene cassette to monitor these interactions. Specifically the data provide evidence that in the B2H system an EVH1 domain and its ligand can be co-expressed at levels sufficiently high to detect their physical interaction inside the bacterial cell with a genetic assay. We concluded that concentrations at and above 1 mM 3-AT are suitable selection pressures for detection of EVH1 domain-peptide interactions and the B2H system of Joung et al. should be a suitable interaction cloning system for identification of unknown EVH1 domain-peptide interactions.

#### **5.2.4. Human brain cDNA library screening for candidate sequences harbouring binding epitopes of the Spred2 EVH1 domain and their physical and genetic characterization**

A commercially available pTRG expression plasmid library of human brain cDNA in *E. coli* XL1-Blue MRF' Kan<sup>r</sup> with an average insert size 1.08 kb and  $1.65 \times 10^6$  cfu of primary clones was screened for candidate sequences harbouring binding epitopes of the Spred2 EVH1 domain. Therefore the plasmid pool was isolated after amplification of the library without distortion of its sequence complexity and used for co-transformation with pBT-Spred2 (1-124) (Fig.15). Small scale pilot co-transformation experiments of pBT-Spred2 (1-124) and the pTRG clone pool from the amplified plasmid library into *E. coli* XL1-Blue MRF' Kan<sup>r</sup> reporter strain were performed to determine the scale of transformation reactions required to fully cover the library's sequence complexity for a comprehensive search of Spred2 EVH1 binding proteins.

Two primary screenings of the library co-transformed with pBT-Spred2 (1-124) were performed at a selection stringency of 1 mM and 5 mM 3-AT. Colonies were grown on selective histidine-free medium containing 3-AT. Co-transformants were also plated on non-selective 3-AT free medium to determine the co-transformation efficiency. Large number of colonies was obtained at the low stringency screen. Replica plating of several of these colonies under higher initial selection stringencies viz., 3 mM and 5 mM 3-AT again showed 3-AT resistant growth and did not lower the number of isolates significantly. Another library screening performed at higher initial selection stringency i.e. 5 mM 3-AT gave 291 colonies which were collected during the incubation at successive time periods of appearance i.e. early, intermediate and late appearing colonies. However the later result was not only due to an increased selection intensity, as

control transformations done in parallel revealed an unexpectedly low competence state of cell preparations used in this second experiment.

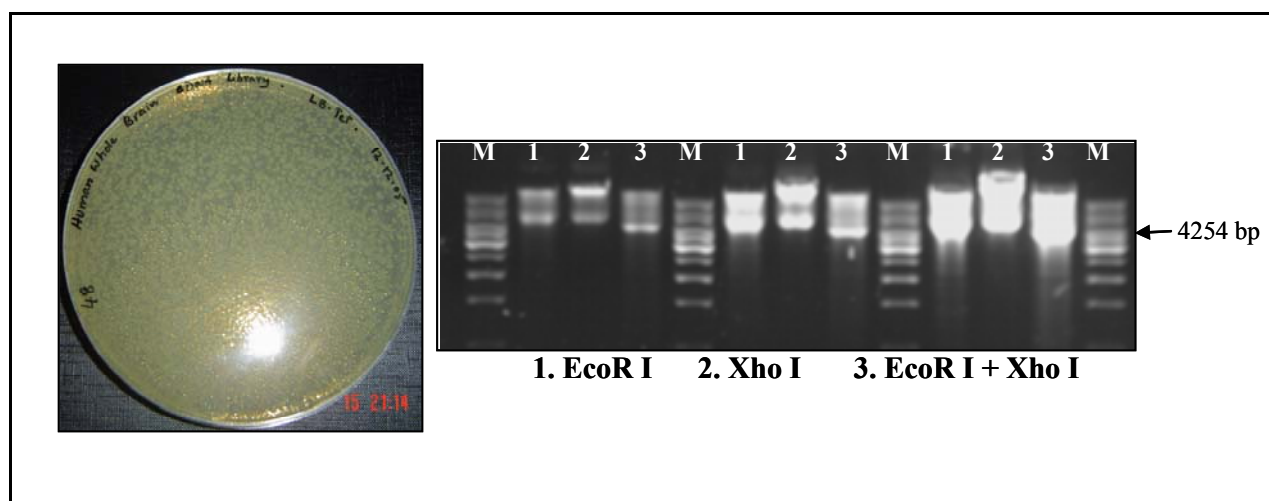


**Figure 15: Amplification and characterization of the human brain cDNA expression library.** A 150 mm LB-tetracycline plate of the amplified cDNA plasmid library after 48 hours of incubation at 37°C is shown here. The isolated pool of amplified clones is shown on a 1% agarose gel after single or double digestion with EcoRI and XhoI. The expression plasmids are shown at three different concentrations to identify the insert pool in the double digested samples (shown as lane '3' in each set of concentration) showing its broad molecular size distribution. ('M' is molecular weight markers)

The 3-AT resistant colonies selected in the primary screenings at 1 mM and 5 mM 3-AT were further analysed by a secondary screening using a dual selection pressure i.e. 5 mM 3-AT together with streptomycin (12.5 µg/ml) in histidine-free minimal medium. Replica plating of colonies from the primary library screenings again showed growth on this dual selection medium and no further differentiation of these clones with respect to their growth phenotype was possible with this strategy (Fig.16). Colonies with the positive control plasmid pairs pBT-VASP (1-115) / pTRG-ActA(332-344)F, pBT-VASP (1-115) / pTRG-ActA(332-344)W and pBT-LGF2 / pTRG-Gal11<sup>P</sup> were used throughout this protocol and confirmed the efficiency of the dual selection. Colonies which arose at different time points of incubation (early, intermediate and late) in the 5 mM primary screening showed no difference in growth behaviour in this secondary screening. Therefore, the secondary screening experiment was not found to be helpful in further selection of isolates obtained from primary screenings at 1 mM and 5 mM 3-AT. Physical characterization of 20 dual resistant colonies from each library screening by colony PCR and restriction enzyme digestion analysis of their isolated target plasmids showed the expected heterogeneity in the insert size distribution with a molecular size range from 500 bp to 2000 bp indicating the clonal origin of each isolate (Fig. 17).

Isolated target plasmids were further subjected to a genetic screening by a panel of genetic assay (Fig.18). Individual target plasmids of this clone collection were investigated against

a panel of bait expression plasmids to test linkage of the 3-AT resistance phenotype to the isolated plasmid, its EVH1 specificity of interaction and the absence of transcriptional self-activation by the target alone. Each target plasmid was co-transformed with pBT-Spred2 (1-124), pBT-VASP (1-115) and an empty pBT plasmid into the *E. coli* XL1-Blue MRF' Kan<sup>r</sup> reporter strain and analysed quantitatively for 3-AT resistant growth by determining its plating efficiency (PE value). If the growth phenotype is linked to the isolated target plasmid, the same phenotype should be observed after co-transformation of the target plasmid with pBT-Spred2 (1-124). Co-transformants of the same target plasmid with either the VASP EVH1 bait plasmid or an empty bait plasmid should not exhibit any 3-AT resistance phenotype above background if the target clone is specific for the Spred2 EVH1 domain and did not show any self activation. The plasmids pBT-LGF2 / pTRG-Gal11<sup>P</sup> and pBT-VASP (1-115) / pTRG-ActA(332-344)F were used as positive control pairs in this experiment and the empty pBT / pTRG-Gal11<sup>P</sup> plasmid combination was used to determine the background PE value in this experiment. The bait plasmid encoding the Spred2 EVH1 domain together with either a target plasmid expressing Gal11<sup>P</sup> or the ActA (332-344)F peptide were used as non-cognate interaction pairs to determine the PE values of non-specific interactions.

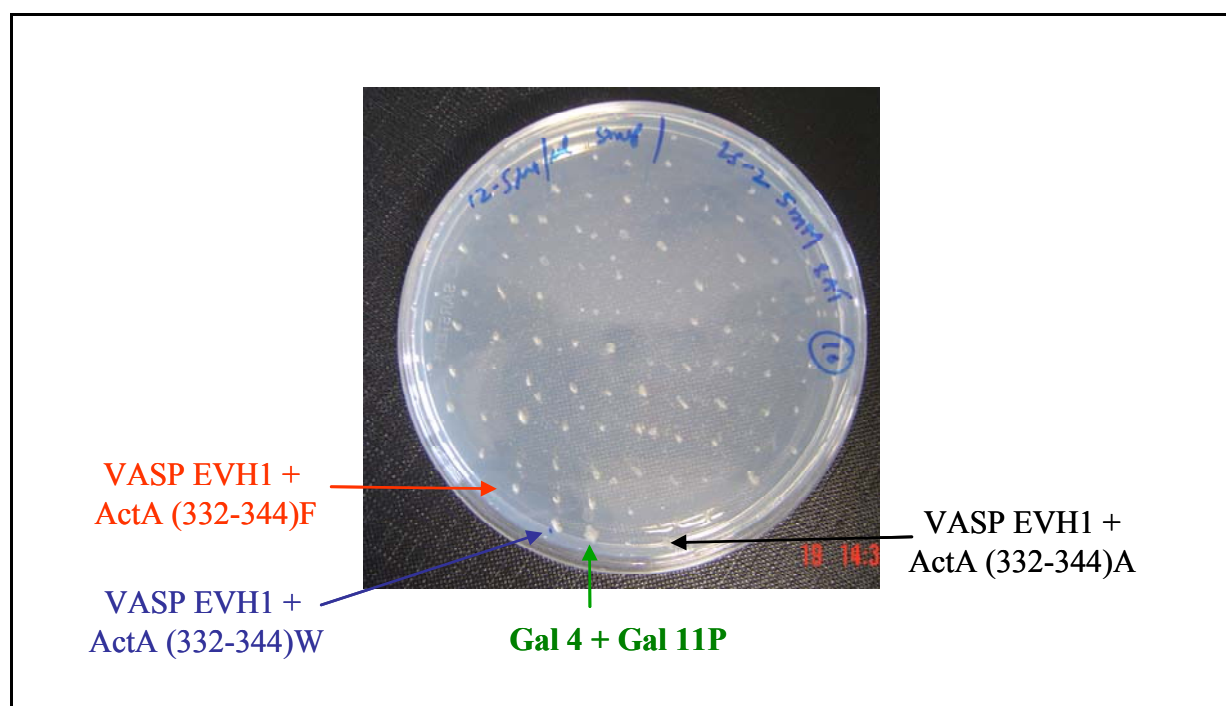


**Figure 16: Secondary screening of primary isolates from cDNA library screening.** Dual resistant colonies were obtained after replica plating on secondary screening minimal medium of the 3-AT resistant clones from the primary library screening. EVH1 control interacting pairs pBT-VASP EVH1 / pTRG-ActA(332-344)F and pBT-VASP EVH1 / pTRG-ActA(332-344)W, system positive control pair pBT-Gal4 / pTRG-Gal11<sup>P</sup> and the negative interacting pair pBT-VASP-EVH1 / pTRG-ActA (332-344)A were also spotted on the same plate.

The number of co-transformants (cfu) obtained per  $\mu\text{g}$  of DNA on non-selective 3-AT free screening medium and the number of 3-AT resistant colonies on selective screening medium were

determined to assess the efficiency of co-transformation (*XFE*) and the plating efficiency (PE). The latter is considered as a measure of the interaction strength between an interaction partner pair and was estimated by calculating the percentage of co-transformants able to grow on 5 mM 3-AT plates. PE values determined for each of the 20 target plasmid isolates should enable us to identify

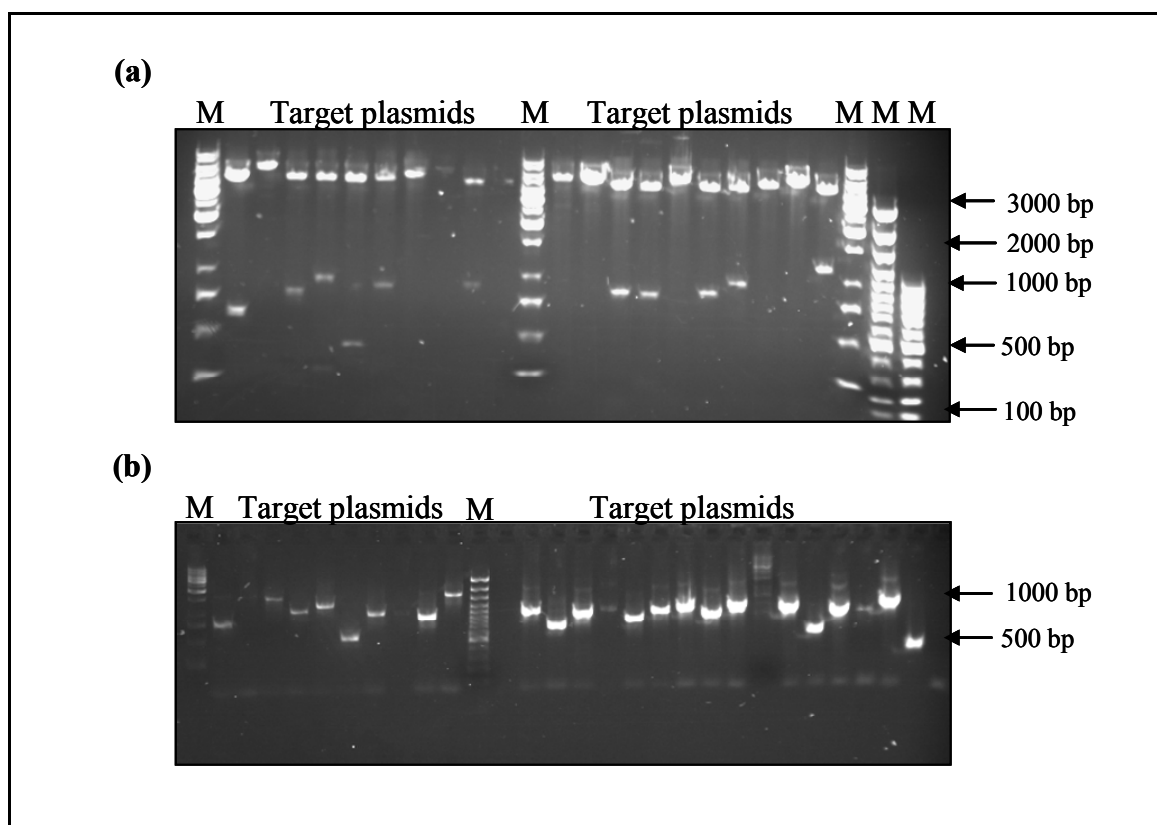


**Figure 17: Physical characterization of plasmid target isolates from the cDNA library screening.** The expression target plasmids of dual resistant colonies from secondary library screening were physically characterized by enzyme digestion (Fig. a) after separation from the bait plasmid and colony PCR (Fig. b) using the primers flanking insert cloning sites. In Fig. a and b, the expected heterogeneity in the insert size distribution is seen after 1% agarose gel electrophoresis. In fig a and b, 'M' represents the molecular weight marker.

by these genetic assays candidates for the Spred2 EVH1 binding proteins in this clone collection and give a first estimate of the false positive rate inherent to the experiment. A plasmid pair encoding interaction partners with a very high interaction strength should achieve nearly maximal PE values i.e. almost every co-transformed colony will also grow in the presence of 3-AT. A non-interacting pair should give a background PE value ideally not larger than 0.1% while a plasmid pair of intermediate interaction strength could achieve any PE value in between this range. Due to its low binding affinity, an EVH1-ligand pair is expected to give PE values in the lower range but significantly above background as it has been determined for the positive control pair of the VASP EVH1 mediated interaction. This experiment should therefore identify among the dual resistant clone collection candidate target plasmids capable of specific interaction with the Spred2 EVH1 domain which will be analysed by sequencing (Table.8). The empty pBT / pTRG-Gal11<sup>P</sup> plasmid

pair had scored at a background value of 0.5% and the pBT-LGF2 and pTRG-Gal11<sup>P</sup> plasmid pair which served as a positive control achieved PE values of 57% which is nearly 100 fold above the background. The pBT-VASP (1-115) / pTRG-ActA(332-344)F plasmid pair serving as a EVH1 interaction control scored at 9.2% which is nearly 5 fold below the maximal activity and thus nearly 20 fold above the background. None of the pTRG isolates showed evidence for transcriptional self activation. However none of the 3-AT resistant pTRG isolates showed Spred2 EVH1 specific PE values in a range similar to that observed for the VASP EVH1 domain. Only one out of 10 pTRG isolates (pTRG-II-4 in Table.8) showed a PE value sufficiently above the background and with a Spred2 EVH1 specific interaction. However it encodes an out-of-frame fragment of NADH dehydrogenase. All of the other dual resistant target plasmids were also sequenced and they did not show any in-frame inserts.

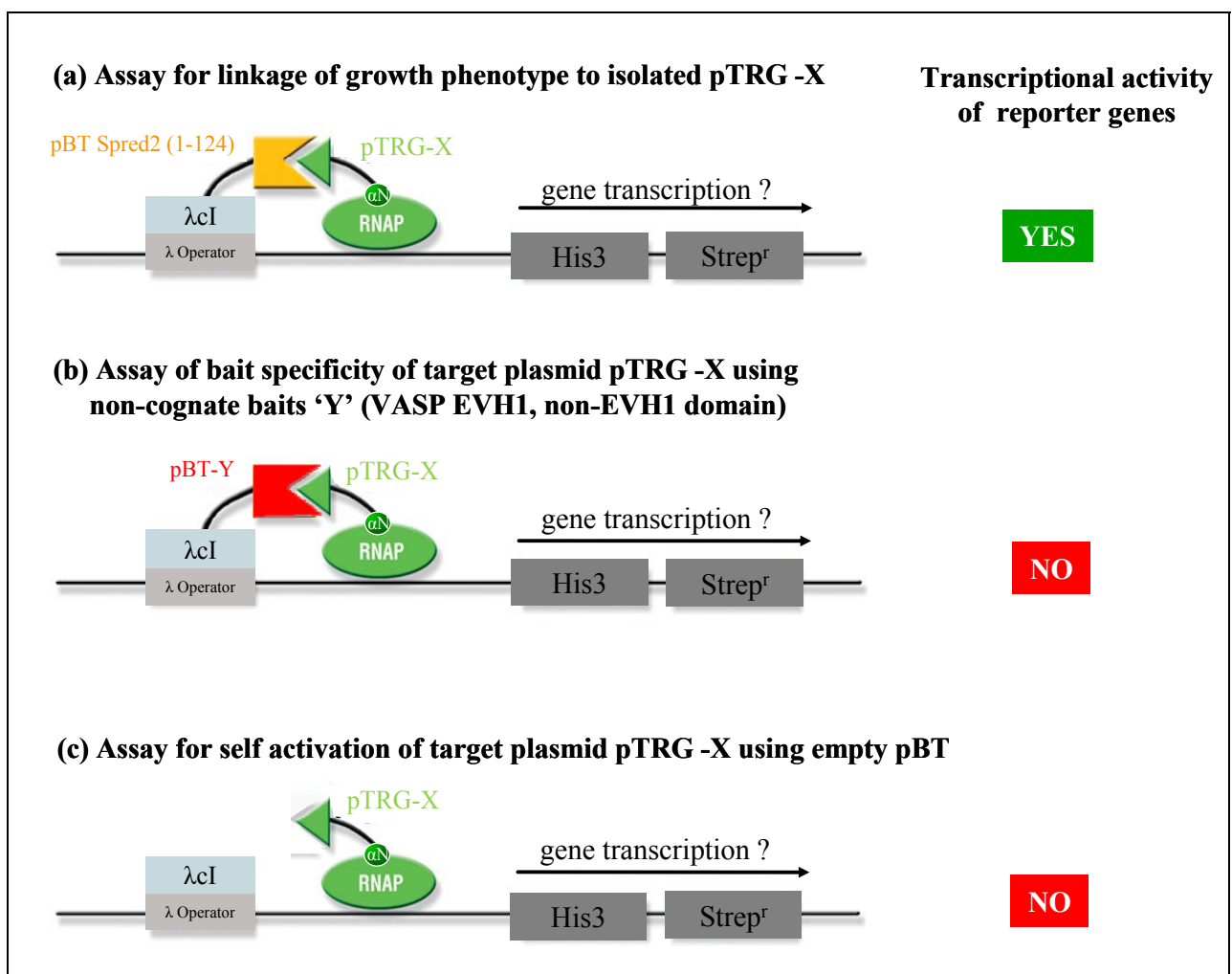


Figure 18: Validation of target plasmid isolates from library screenings by three different genetic assays.



### 5.2.5. Summary

The B2H system successfully recorded the physically well characterised interactions of the VASP EVH1 domain with its ligands by a dose-dependent 3-AT resistant growth of the respective clones which were used as positive controls throughout the experiments. Screenings of a human brain cDNA expression plasmid library for Spred2 EVH1 ligands performed at two different selection stringencies did not detect Spred2 EVH1 specific interactions among the clones characterized and thus seems to be completely dominated by false-positive isolates. These isolates which were identified as positives after the primary and secondary screenings did not show PE values significantly above background and carry target peptide sequences with stop codons. The panel of genetic assays developed in the context of validating candidate clones was found to be efficient and useful in assaying isolates of the library screening. The PE values of the target plasmid isolates clearly indicate them as false positives since the PE values of the linkage assay are in the same low range as those observed for the non-cognate interactions. Therefore it is not clear if the bacterial two-hybrid experiments had been performed at selection stringencies either too low or already too high for a detection of Spred2 EVH1 specific interactions as of course no data are available on binding affinities of this domain. Binding to this domain might well occur at affinities much lower than those known for VASP EVH1 class 1 ligands in which case it would be almost impossible to detect such interaction strengths in a B2H screen as shown by our experimental results. Searching a cDNA library with its large insert sizes for small candidate binding epitopes of an EVH1 domain might be particularly challenging due to the presence of the large background sequence information which is unrelated to the targets searched for. A biased or incorrect folding of host proteins upon heterologous expression in a bacterial cell might be another possible reason for missing any domain-specific interactions in this *in-vivo* interaction cloning approach (i.e. its suspected false-negative rate). Controlled *in-vitro* affinity selection with the purified and natively folded protein domain for short peptide target epitopes exposed on phage particles would be an alternative approach for detecting Spred2 EVH1 binding epitopes. Therefore a phage display library screening experiment was performed.

<b>Target plasmid</b>	<b>Bait plasmid</b>	<b>PE value</b>	<b>Genetic assay</b>
pTRG-Gal11 <sup>P</sup>	pBT	0.5 %	(-) control
pTRG-Gal11 <sup>P</sup>	pBT-LGF2	57 %	(+) control
pTRG-ActA (332-344)F	pBT-VASP EVH1	9.2 %	(+) control
pTRG-Gal11 <sup>P</sup>	pBT-Spred2 EVH1	0.9 %	S
pTRG-ActA (332-344)F	pBT-Spred2 EVH1	0 %	S
pTRG-I-2	pBT-Spred2 EVH1	0.3 %	L
pTRG-I-2	pBT-VASP EVH1	1.5 %	S
pTRG-I-4	pBT-Spred2 EVH1	1.0 %	L
pTRG-I-4	pBT-VASP EVH1	1.0 %	S
pTRG-II-1*	pBT-Spred2 EVH1	0.6 %	L
pTRG-II-1*	pBT-VASP EVH1	0.4 %	S
pTRG-II-4 <sup>§</sup>	pBT-Spred2 EVH1	2.4 %	L
pTRG-II-4 <sup>§</sup>	pBT-VASP EVH1	0.9 %	S
pTRG-II-5 <sup>&amp;</sup>	pBT-Spred2 EVH1	0.8 %	L
pTRG-II-5 <sup>&amp;</sup>	pBT-VASP EVH1	0.3 %	S
pTRG-II-6	pBT-Spred2 EVH1	2.0 %	L
pTRG-II-6	pBT-VASP EVH1	2.4 %	S
pTRG-II-7	pBT-Spred2 EVH1	1.4 %	L
pTRG-II-7	pBT-VASP EVH1	2.8 %	S
pTRG-II-12	pBT-Spred2 EVH1	0.4 %	L
pTRG-II-12	pBT-VASP EVH1	0.7 %	S
pTRG-II-18	pBT-Spred2 EVH1	0.7 %	L
pTRG-II-18	pBT-VASP EVH1	1.9 %	S
pTRG-II-25	pBT-Spred2 EVH1	0.4 %	L
pTRG-II-25	pBT-VASP EVH1	0.9 %	S

No target clone shows transcriptional self-activation (0.01 % < PE < 0.5 %)  
\* in-frame insert, §, & out-of-frame insert

**Table 8: Summary of genetic assays on target plasmid isolates to determine the linkage to growth phenotype [L] and EVH1 specificity of interaction [S].** Target plasmids from dual resistant clones of library screenings were isolated after physically separation from bait plasmid and assayed by a panel of genetic assays as shown in Fig. 18. In these assays, the interaction strength was determined quantitatively as the plating efficiency values (PE). No target isolates shown transcriptional self-activation (data not shown). pTRG-Gal11<sup>P</sup> / pBT-LGF2 and pTRG-ActA (332-344)F / pBT-VASP EVH1 plasmid pair were used as positive control. pTRG-Gal11<sup>P</sup> / pBT empty plasmid was used as negative control interaction pair.

### 5.3. In search for binding epitopes of the Spred2 EVH1 domain: Genetic screening using a phage display library

#### 5.3.1. Motivation for the experimental approach chosen

The identification of candidate sequences encoding Spred2 EVH1 binding proteins based on a cDNA expression library screening by the bacterial two-hybrid system of Chapter 5.2 was only of limited success despite the proper use of a control panel of interaction clones and the careful calibration of selection conditions. The results obtained were dominated by a unexpectedly high false-positive rate with a complete missing of any Spred2 EVH1 specific clones isolated as assayed by a set of genetic tests performed on random selections of these primary isolates in conjunction with a sequence characterization of their inserts. Based on our knowledge of EVH1 domain-ligand interactions (see Chapter 2.2) one possible explanation for these negative findings might be related to the rather small target sizes of the expected Spred2 EVH1 binding epitopes which have to be identified in the highly complex sequence space spanned by a cDNA expression library. Any discrimination of sequence stretches coding for such small candidate binding epitopes among these large collections of naturally occurring cDNA sequences would thus be expected to be very demanding due to the presence of the large background sequence information unrelated to the targets. A further biological problem to cope with by any *in-vivo* interaction cloning approach might be based on the limited accessibility to the domain of interest of the candidate binding epitopes which could be due to a biased or incorrect folding of their host proteins upon heterologous expression in a bacterial cell.

In recent years, phage display technology has evolved into a powerful and independent research tool providing several advantages to define natural protein-protein interactions and to delineate ligand binding motifs for different adaptor domains (see Chapter 2.3.3) [199] [200]. In contrast to B2H system technology which operates as an *in-vivo* binding assay between heterologously expressed proteins, phage display allows for an *in-vitro* screening of peptide libraries of restricted target sizes which are displayed on the surface of individual phage particles. This set-up provides not only a direct physical link between the expressed target peptides and their encoded genetic information in the viral genomes but also facilitates target accessibility to the bait protein. Libraries displayed on the phage virion surface however are repertoires of mostly non-natural peptide sequences which are generated by randomization to cover a comprehensive set of sequence combinations. It was successfully applied to identify peptide ligands for a number of SH3 domains and discovered first insights into the molecular determinants of SH3 domain affinity and selectivity [201]. Furthermore, recent studies have demonstrated the utility of this approach in

identifying the specificity profiles for proline rich motifs (PRM) of PDZ domains from phage display peptide libraries [154]. It is well-known from the other EVH1 domain classes that they bind to short proline rich epitopes. Expression and display of such short target peptides on phage virions not only restricts the target size but also favourably limits the sequence space complexity compared to the situation in a B2H system. An important feature of phage display is that conditions can be designed for screening of phage with either modest ( $K_d$  as high as 500  $\mu\text{M}$ ) or high ( $K_d$  as low as 5 pM) affinity for the target [202]. Therefore, phage display library screening was considered as a complementary and independent experimental approach for identification of Spred2 EVH1 binding epitopes which are in general expected to interact with low affinity. However *in-vitro* screening of such phage display peptide libraries by affinity selection requires a purified and biologically active bait protein. Heterologous expression of the bait domain as a fusion protein is thus a prerequisite for possible identification of its binding epitopes provided the protein is natively folded and biologically active in order to retain its binding region in a binding competent state to interact with target epitopes. The Spred2 EVH1 domain fused to a GST tag was successfully expressed and purified in our laboratory from *E. coli* in a physical state suitable for NMR structure determination of this domain. The purified Spred2 EVH1 protein has thus proven to be properly folded and is therefore expected to be in a biologically active conformation (Fig.24). Hence, the GST fused Spred2 EVH1 domain prepared according to these protocols was used for a phage display peptide library screening to search for its binding epitopes. Since the peptides displayed on phage virions may interact with different possible target regions available on the bait protein's surface including the fusion partner, appropriate control proteins have to be used in order to assess the specificity of interaction. Screening of phages populations are therefore controlled by using suitable negative and positive controls to monitor the enrichment of phage variants interacting with the Spred2 EVH1 protein.

### 5.3.2. Introduction to phage display technology and overview of the experimental procedure

Several phages are described in the literature for use as vectors with phage display experiments including filamentous phage M13 as well as the icosahedral phages such as T4 and T7. Most of the protein engineering tools using phage display are developed for filamentous phage M13. The native M13 phage particles are of thin, cylindrical shape, usually 930 nm long and 6–7 nm in diameter with a single stranded DNA genome (6,400 nucleotides in length) encoding 11 genes, of which five codes for the coat proteins. The major coat protein pVIII present in almost 2,700 copies is responsible for encapsulating the phage DNA. The distal end of the phage particle is capped by five copies each of pVII and pIX and the proximal end contains four to five copies of

each of pVI and pIII [148, 153](Fig.19). Upon infection of *E. coli* cells possessing F-pili, the single-stranded genome of M13 first replicates to a double-stranded form which serves as a template for production of viral proteins and single-stranded DNA progeny. The single stranded DNA eventually is extruded from the host cell through the inner membrane and is encapsulated by the five coat proteins residing in the outer membrane during the release [153] [148]. pIII and pVIII are most commonly used to display peptides/domains/proteins or even libraries of antibodies [149]. The repertoire of peptides expressed as N-terminal fusion partners to the phage coat protein is based on a viral gene library constructed in a phagemid vector system which enables screening of large collections of phage variants for the target of interest (Fig.19). Display of peptides on the major coat protein pVIII offers high copy numbers of target sequences for high throughput screening, though only short peptides of length up to 9 amino acids could be displayed using this fusion partner [158].

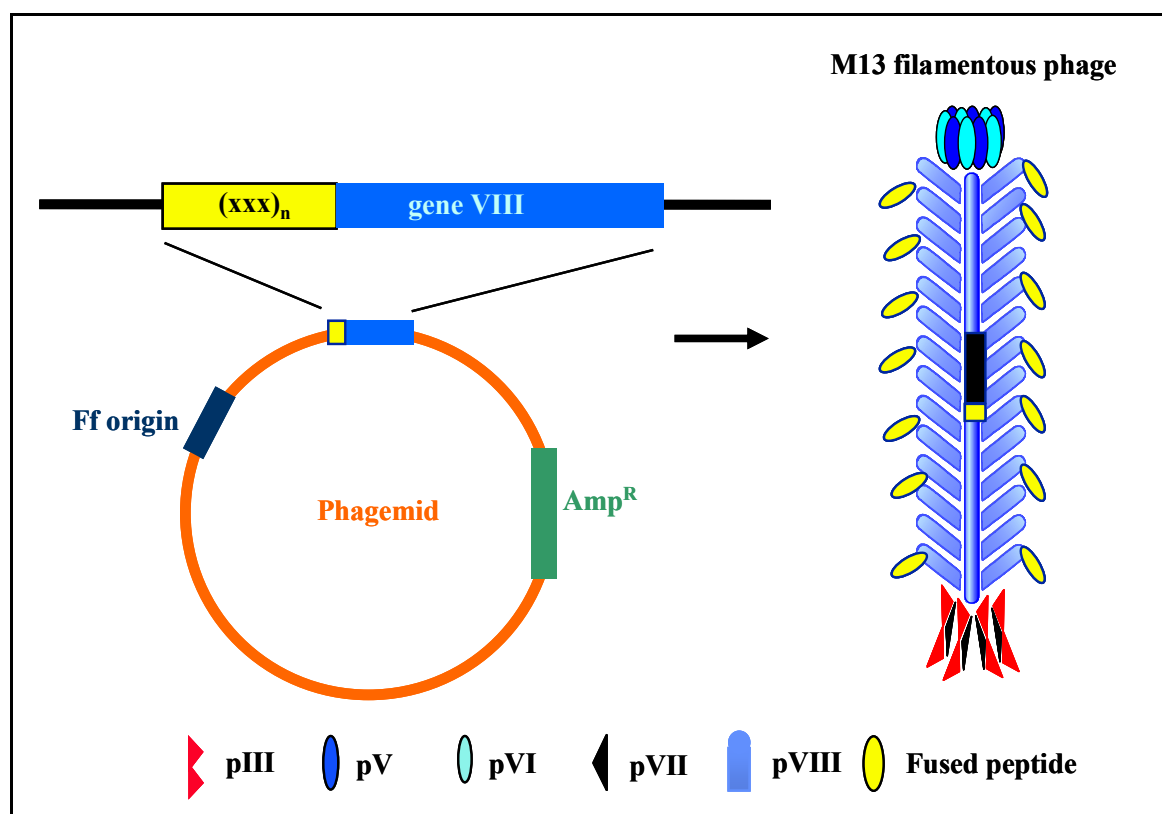


**Figure 19: Overview of the phage display system.** Peptides are displayed using plasmid based “phagemid” vectors that contain a gene encoding only one of the phage’s capsid proteins (gene VIII as shown in figure), an Ampicillin resistance gene and Ff origin to allow production of single-stranded vector DNA for subsequent encapsidation into phage particles. The gene of the peptide to be displayed (shown as  $(xxx)_n$  in figure) is cloned into the phagemid to fuse it N-terminally to the capsid protein. When *E. coli* cells containing the phagemid are infected with helper virus which lack package capability, wild type phage proteins from the helper phage genome as well as a small amount of fusion protein encoded by the phagemid are expressed and the phagemid DNA get packaged into viral particles that display both wild-type and fusion capsid proteins.

Although there are several different potential variations of the phage display approach, many investigators have used cloning systems in which the DNA sequences encoding

the coat protein target-peptide fusions are carried within a plasmid or phagemid that also contains a filamentous phage origin of DNA replication (Fig.19). Consequently, when permissive *E. coli* strains containing these plasmids/phagemids are later infected with helper phages supplying the other native phage proteins, the resulting phagemid constructs are efficiently packaged into phage particles (see Chapter 2.3.3). Protocols for affinity selection of phages on the basis of their specificity and affinity for the bait protein are focused on screening to progressively enriched phage variants. A basic affinity selection protocol for phage binding requires immobilization of the purified and biologically active bait protein via its tag to a matrix, addition of the phage variants, washing away those variants that did not bind to the bait, elution of the bound phages and their amplification by infection of host bacteria for subsequent rounds of selection. This process of selection of phages by binding, washing and elution on an immobilized bait protein is called 'panning'. For immobilization of the bait protein, there are a variety of assay formats and a number of commercially available supports including suspended resins or beads. After immobilization of the bait to the support, the remaining sites on the support are generally blocked with unrelated proteins such as BSA or powdered milk. Bound phage variants are eluted from immobilized bait in general by simply reducing pH followed by a neutralization step. Each cycle of binding, washing and elution then results in a subpopulation of phages being enriched for interaction with the bait at the expense of those variants which bind with decreased affinity. As enrichment of binding-competent phages increases in the course of selection, its stringency could be increased. By using multiple washing steps and increased washing times, phages encoding binding peptides with lower dissociation rate constants can be selected. Thus, even relatively rare binding phage variants can finally be rescued from large library repertoires by the combination of *in-vitro* affinity selection and *in-vivo* amplification. An identical selection procedure against the tag alone which is used to immobilize the bait protein serves as a negative control and any enrichment of phages against this fusion protein or the matrix is considered as a background signal. A well-characterised adaptor domain whose interacting target peptides have already been characterized by using the same library serves as a positive control to monitor panning rounds, washing and eluting procedures. After each panning round, the titers (pfu) of the phage variants eluted from either the bait protein or the tag moiety alone are determined by infection of *E. coli* to calculate an enrichment factor achieved in each panning round. The enrichment factor for a bait protein is the pfu ratio of the phages eluted from that protein to the phages eluted from the tag moiety alone. As enrichment of phages binding to the bait protein is expected to increase in successive panning rounds, the enrichment factor should also increase depicting a specific interaction of the bait protein with its cognate target peptides. Specific target binding and successful phage propagation in a phage display screening are

thus tracked by monitoring the enrichment factor and its final saturation. After several rounds of selection the eluted phage populations are cloned into single plaques for further physical analysis of phagemids encoding individual target peptides.

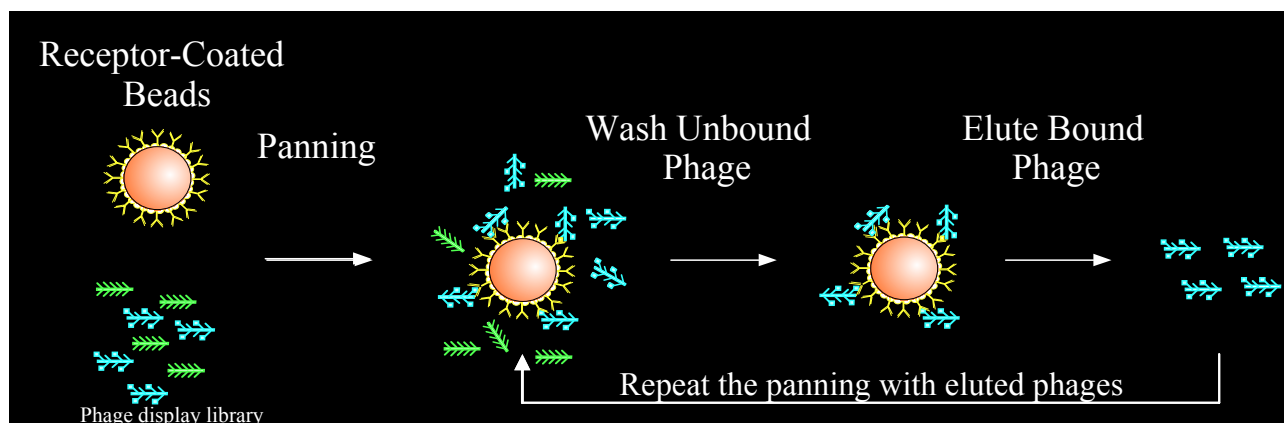


**Figure 20: Affinity selection by phage display methodology.** The most commonly used selection method in phage display is affinity based and is usually referred to as “panning”. Typically the query protein is immobilized on a solid support and the phage display library is then incubated with the support to allow binding between the immobilized query protein and the appropriate phages. Unbound phages are then removed by washing steps. Elution of the specifically bound phages can be accomplished by brief incubation at low pH. This process is repeated using the same query protein with the eluted phages for further rounds of selection to enrich more specifically bound phages.

Phage display peptide library screening for Spred2 EVH1 binding epitopes has been carried out by using a 9mer peptide library fused N-terminally to the major capsid protein, pVIII of M13 (Fig.19). It was donated by Dr. Cesareni’s group [158]. As the majority of the EVH1 domain family members are known to bind short epitopes containing proline-rich motifs of 4–6 amino acids long (see Chapter 2.2), this 9mer randomised library was expected by us to be suitable for determining peptide motif epitopes even for a new class of the EVH1 family such as the Spred2 EVH1 domain. The same library has already been used successfully in determining the short target epitopes for one of the SH3 domains [203].

### 5.3.3. Preparation and characterization of the bait fusion protein and its controls

The GST-fused Spred2 EVH1 domain was used for phage display library screening experiments. It was expressed from the recombinant pGEX-4T-2-hSpred2 EVH1 (1-124) plasmid in *E. coli* BL-21 cells in 2 X YT medium after induction with IPTG. The expressed fusion protein was isolated from the harvested cell lysates by GSH affinity column chromatography and further purified by gel filtration chromatography on a Sephadex 75<sup>®</sup> column through FPLC. The protein obtained after each chromatography step was analysed by SDS-gel electrophoresis (Fig.21). The protocols used for expression and purification of GST-Spred2 EVH1 were the same as used for preparation of isotopically labelled samples utilized in NMR structure determination of domain

(Fig.24). The natively folded conformation of freshly expressed GST-Spred2 EVH1 domain fusion protein was assayed by  $^1\text{H}$  NMR spectroscopy after treating the protein sample with  $\text{D}_2\text{O}$  in 1:10 ratio (v/v). The NMR spectrum confirmed that the sample of GST fusion protein used as bait in the phage display library screenings was natively folded and is expected thus to be biologically active (Fig.21). Target binding regions required for the interaction with a ligand should therefore be exposed on the surface of the bait protein. GST fused Fyn-SH3 domain and the GST moiety alone were expressed, purified and certified for their biologically active form according to the protocol used in Dr. C. Freund's laboratory. They were used as positive and negative control proteins respectively during phage display library screening experiments with the Spred2 EVH1 domain. The GST-Fyn-SH3 fusion protein had already been successfully screened with the same M13 X9mer peptide library [204] and it could thus be used as a well-defined positive control protein to monitor the panning rounds also against the GST-Spred2 EVH1 domain in our experiments.

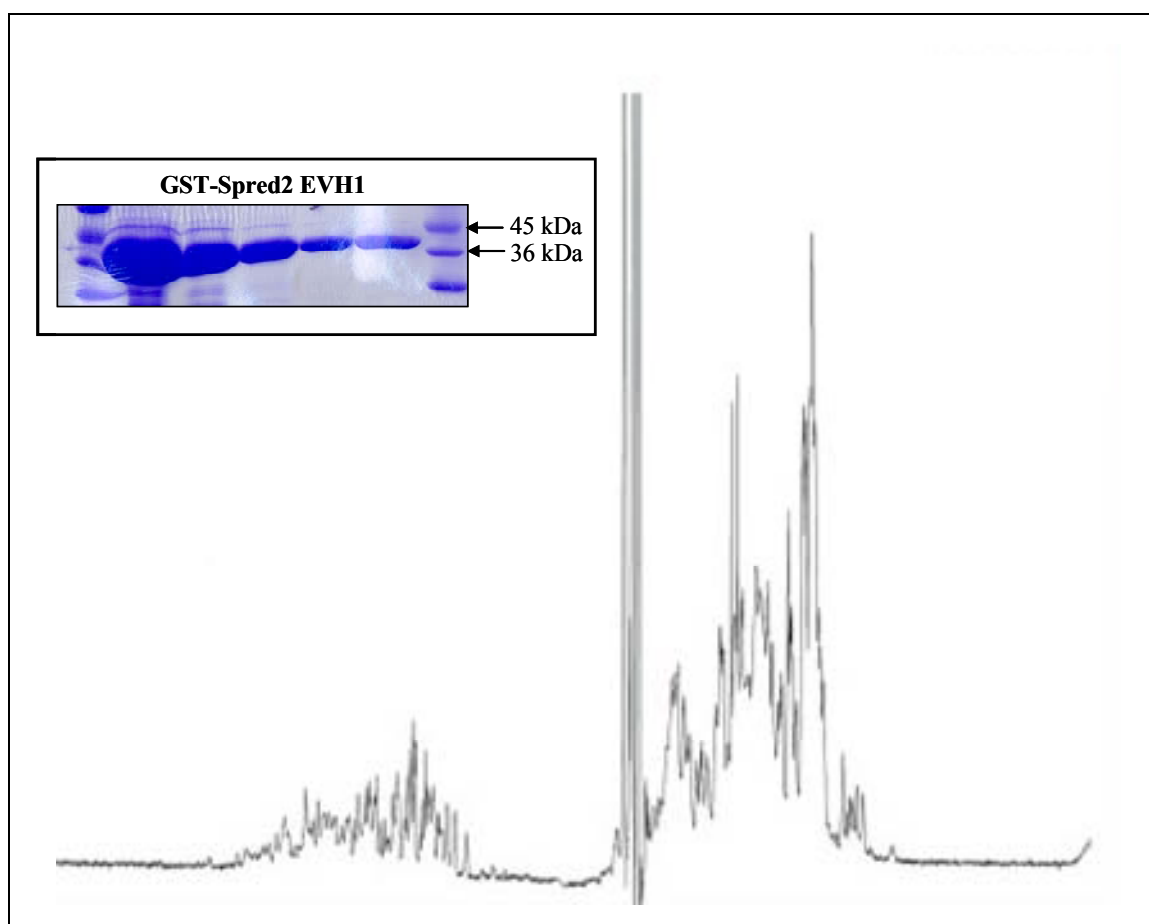


**Figure 21: Isolation and characterization of the bait fusion protein.** The  $^1\text{H}$  NMR spectrum shows the natively folded conformation of freshly purified GST-Spred2 EVH1 domain fusion protein which is expected thus to be biologically active in the experiments. **Inset figure:** A 10% SDS gel electrophoresis showing GST-Spred2 EVH1 purified consecutively by GSH-affinity column chromatography and gel filtration chromatography on a Sephadex 75<sup>®</sup> column through FPLC after expression and harvest from cell lysates. The protein was loaded after serial dilution and shows the expected molecular weight.



### 5.3.4. M13 phage display peptide library screening for binding epitopes of the Spred2 EVH1 domain and physical characterization of phagemids from the isolated phage variants

The GST-Spred2 EVH1 fusion protein had been immobilised to GSH-Sepharose beads and panning was performed by using the M13 X9mer peptide library in order to select phage variants expressing its binding epitopes [156]. GST fused Fyn-SH3 domain [204] and GST alone were used as appropriate positive and negative control protein respectively. Phages eluted after binding from each round of panning were used for a successive round against the same query protein after their amplification by infection of *E. coli* along with the packaging-defective helper phages (Fig.20). After each panning round, titers (pfu) of phages bound to the GST-Spred2 EVH1 and the GST-Fyn-SH3 fusion proteins were determined to estimate the enrichment factor achieved for the domain of interest (see Chapter.4.2.5). Three successive panning rounds were performed for the GST-Spred2 EVH1 domain in our phage display screening experiments.

Panning round	Enrichment factor	
	GST-Fyn-SH3 (Positive control)	GST-Spred2 EVH1 (Bait protein)
1	0.4	820
2	300	500
3	$5 \times 10^3$	$1 \times 10^4$
4	$2 \times 10^4$	-

**Table 9: Enrichment factors achieved during phage display experiments.** Enrichment factor for GST-Fyn-SH3 protein used as a positive control and GST-Spred2 EVH1 protein used as bait are shown until different rounds of panning against M13 X9mer phage display library.

In general as described above, the first round of panning would enrich very low numbers of specifically bound phages against any protein of interest due to the highly diverse peptide repertoire of the phage library. This value should increase in the next rounds of panning if specifically bound phages could be enriched further by eliminating non-binding and non-specifically binding phages. The positive control protein GST-Fyn-SH3 showed a continuous increase in enrichment for bound phages with every round of panning until saturation. The first round showed an enrichment factor of 0.4 and then 300 in the second round of panning. Finally, it has reached almost a saturation value after four rounds ( $5 \times 10^3$  in third and  $2 \times 10^4$  in fourth round of panning) indicating a domain-specific peptide interaction (See second column in Table. 9). These results demonstrate a successful performance of the phage display screening experiment according to the protocols used. In contrast, the GST-Spred2 EVH1 domain fusion protein showed an abnormally high enrichment factor i.e. 820 for bound phages against the same M13 X9mer peptide

library already in the first round of panning suggesting highly non-specific interactions. The next panning round for this domain showed a slightly decreased enrichment factor i.e. 500 which is however in the same range as observed for the positive control protein at this stage of the experiment (See third row in Table.9). Unexpectedly, the third round of panning against the GST-Spred2 EVH1 domain fusion protein achieved a high enrichment factor of  $1 \times 10^4$  which is in the same saturation range as observed for the GST-Fyn-SH3 protein (Table.9). Similar panning rounds of the eluate phages from the bait protein of interest against the GST moiety alone showed a declining enrichment in successive steps indicating that neither the GST tag nor the matrix unspecifically bind phages of the library used here. Phages eluted from the other two bait proteins are then physically characterised.

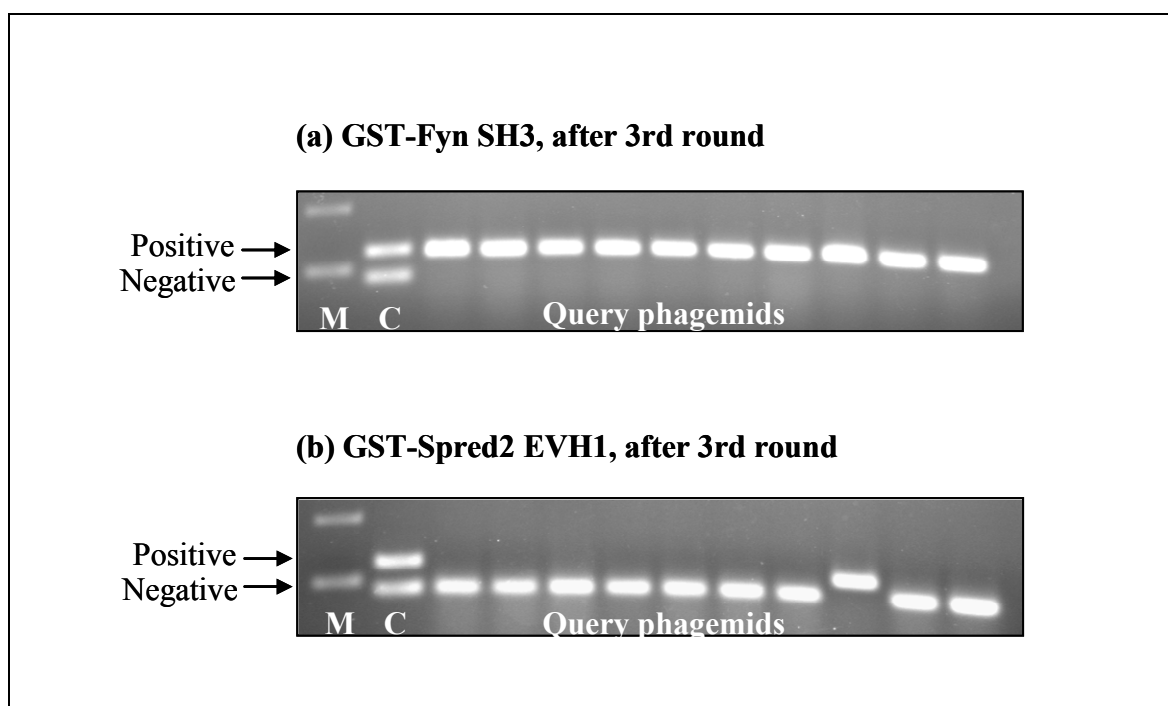


**Figure 22: Physical characterization of isolated phagemids.** Inserts of the phagemids of the elute phages after the third round of panning were amplified by colony PCR after infecting *E. coli* cells and the products were analysed on a 1% agarose gel. In lane 'C' of both Fig. a and b, upper band with nearly 50 bp higher molecular weight than the lower band represents an amplified product of a positive recombinant phagemid carrying an insert and lower band represents negative phagemids without any inserts. All the phagemids of phages selected against GST-Fyn SH3 protein (Fig. a) showed inserts of the expected size as shown in lane 'C' where as majority of the phagemids of phages selected against GST-Spred2 EVH1 protein were devoid of any inserts (Fig. b).

Therefore eluted phages after the third round of panning against both proteins were analysed by colony PCR of single plaques which amplifies the phagemid insert regions of individual isolates in order to identify phagemids with inserts encoding binding motifs. Bacteria infected with the eluted phage population were grown on LB-amp plates and plaques were used to perform colony PCR with primers flanking the insert cloning sites of the phagemid (see Chapter 4.2.5). PCR products of these phagemid isolates were analysed on a 2% agarose gel to differentiate

by a slightly higher molecular weight those isolates carrying inserts from empty phagemids without any insert. The molecular mass difference between the PCR products of a recombinant vs. an empty phagemid is less than 50 base pairs due to the short insert sizes which nevertheless can be well differentiated on a 2% agarose gel. Insert-harboring positive phagemid isolates recognised on the agarose gel were then further characterised by sequence analysis of their inserts.

Clone 3:	MLSFAAEGEF	<b><u>DAL*TLRHQ</u></b>	-----	DPAKAA
Clone 8:	MLSFAAEGEF	<b><u>KPGTPAP*T</u></b>	-----	DPAKAA
Clone 19:	MLSFAAEGEF	<b><u>RTSLSHGYT</u></b>	-----	DPA SILRA
Clone 25:	MLSFAAEGEF	<b><u>GARPVPPPVGSS</u></b>		DPAKAA
Clone 34:	MLSFAAEGEF	<b><u>P*PTARIAP</u></b>	-----	DPAKAA*
Clone 37:	MLSFAAEGEF	<b><u>*DQAACSVT</u></b>	-----	DPAKAA
Clone 40:	MLSFAAEGEF	*	-----	DPAKAA*
Clone 43:	MLSFAAEGEF	*	-----	DPAKAA*
Clone 44:	MLSFAAEGEF	<b><u>QN*NAGRFM</u></b>	-----	DPAKAA
Clone 48:	MLSFAAEGEF	<b><u>**PAVSHLR</u></b>	-----	DPAKAA
Clone 49:	MLSFAAEGEF	<b><u>LPK*PKAHL</u></b>	-----	DPAKAA

**Figure 23: Sequence alignment of insert coding sequences of the positive phagemid isolates.** The recombinant phagemids recognised as positives in the colony PCR were isolated and their inserts were sequenced. Sequence alignment of this region is shown in the figure. The amino acids shown in *bold* gave insert coding sequences of recombinant phagemids and \* represents the position of stop codons.

All the phagemid isolates obtained from a sample of eluted phages of the third round of panning against the GST-Fyn-SH3 domain showed a higher molecular weight than an empty control phagemid in this colony PCR amplification (Fig.22a). This result indicates a successful enrichment achieved in the panning with this query protein and is in line with the titration results described above. Colony PCR of clones obtained from phages of the third round of panning against the GST-Spred2 EVH1 protein however shows that the majority of their phagemids (90%) did not contain any insert to express a peptide (Fig.22b). Recombinant phagemids from colonies of the remaining 10% of insert-contained phages from the third round eluates against the Spred2 EVH1 domain were then isolated, sequenced and analysed for their insert coding sequences. The sequence results of this subpopulation showed an assortment of recombinant phagemids carrying either stop codons or short peptide encoding sequences or even empty phagemids (Fig.23). Two positive phagemids with inserts having a continuous ORF without a stop codon were found among nine negative clones (see clone 19 and 25 in Fig.23). Surprisingly one of them contained a larger than 9mer insert and shows a 13mer proline-rich sequence. The other phagemid with continuous ORF contained an unrelated sequence that exhibits no proline-rich peptide motif. Isolation of a 13mer sequence selected in this phage display peptide screening was unexpected given that the library

was initially constructed to express 9mer peptides. No further similar sequences to support this ligand motif could be enriched in our phage display library screening for Spred2 EVH1 binding epitopes.

### 5.3.5. Summary

The phage display screening experiment for Spred2 EVH1 binding epitopes was not very informative and revealed unexpected results. When compared to the positive control screening experiment using the GST-Fyn SH3 protein, the highly non-specific performance of the former screening was evident. Positive phage enrichment seems not to be possible for the Spred2 EVH1 domain due to the high number of phages obviously interacting non-specifically with this domain. The majority of phages isolated against the Spred2 EVH1 domain surprisingly either carried no insert or inserts with stop codons suggesting a dramatic lack of specificity in the interactions with this domain compared to the Fyn-SH3 domain and the GST moiety alone. The results obtained seem to suggest that the pVIII major coat protein is not an inert scaffold protein with respect to the Spred2 EVH1 protein and its N-terminal fragments might already display sticky epitopes that interact with the Spred2 EVH1 domain. No such behaviour is observed for the Fyn SH3 domain or GST alone. However, detection of a 13mer proline rich sequence from the Spred2 EVH1 screen was particularly surprising in this context as it might have been possible only if there was a sufficiently strong interaction of the Spred2 EVH1 domain with this target peptide leading to its selection. Even though the phage display peptide library screening experiment did not perform in the expected manner for the Spred2 EVH1 domain, this 13mer sequence identified in the screen might be helpful as an initial cue for further analysis by SPOT scan and amino acid substitution assays. Taken the results obtained from screening of an *in-vivo* expression library and an *in-vitro* peptide display library seriously, our working hypothesis on the peptidergic nature of a Spred2 EVH1 ligand might be questioned. Non-peptidergic interactions were therefore considered for this domain in further experiments as already described in other adaptor domains of the SH3 class [120, 205].

## 5.4. In search for binding epitopes of the Spred2 EVH1 domain: Biochemical screening using *in-vitro* binding assays for non-peptidergic interactions

### 5.4.1. Motivation of the experimental approach chosen

Two interaction cloning strategies employing a bacterial two-hybrid and a phage display system has been used in the course of this work for binding epitope identification of the Spred2 EVH1 domain. Both approaches were based on the assumption that Spred EVH1 ligands will form peptidergic epitopes. The two-hybrid system utilizes *in-vivo* co-expression of the Spred2 EVH1 domain from a low copy number expression plasmid vector together with a target cDNA expression library under conditions of growth indicative of a productive protein interaction. The phage display system in contrast relies on *in-vitro* interaction of the purified and natively folded Spred2 EVH1 protein with a repertoire of short peptides exposed on the surface of phage particles followed by enrichment of interacting phages from these display libraries. Both approaches were shown in our experiments to be capable of detecting domain: peptide interactions successfully in appropriate controls run in parallel. However the experimental results of both the bacterial two-hybrid and the phage display library screens for Spred2 EVH1 binding epitopes were found to be dominated by false-positive isolates precluding a reliable identification of candidate clones although probably for different biological reasons. The inability to find Spred2 EVH1 ligands with these genetic techniques has therefore cast some doubt on the underlying assumption that a Spred2 EVH1 ligand will form a peptide. Analysis of the newly available NMR structure of the Spred2 EVH1 domain (accession number “2JP2” and Fig.24) revealed an unusual surface charge distribution showing patches of pronounced positive charge distribution in the putative binding cleft region which is not observed in the other EVH1 classes (Fig.24). We therefore considered an interaction of this domain with a negatively charged ligand probably of non-peptidergic nature to counterbalance this unique charge pattern. Some non-EVH1 adaptor domains like the C-terminal SH3-C domain of the Adhesion and degranulation-promoting adapter protein (ADAP) [120], PDZ domains of syntenin-1 and syntenin-2 [206], the PH domain of phospholipase C- $\delta_1$  [207] also showed a positive surface charge distribution and were found experimentally to interact with phospholipid molecules. We therefore studied a possible interaction of the Spred2 EVH1 domain with several types of phospholipids using biochemical *in-vitro* binding assays.

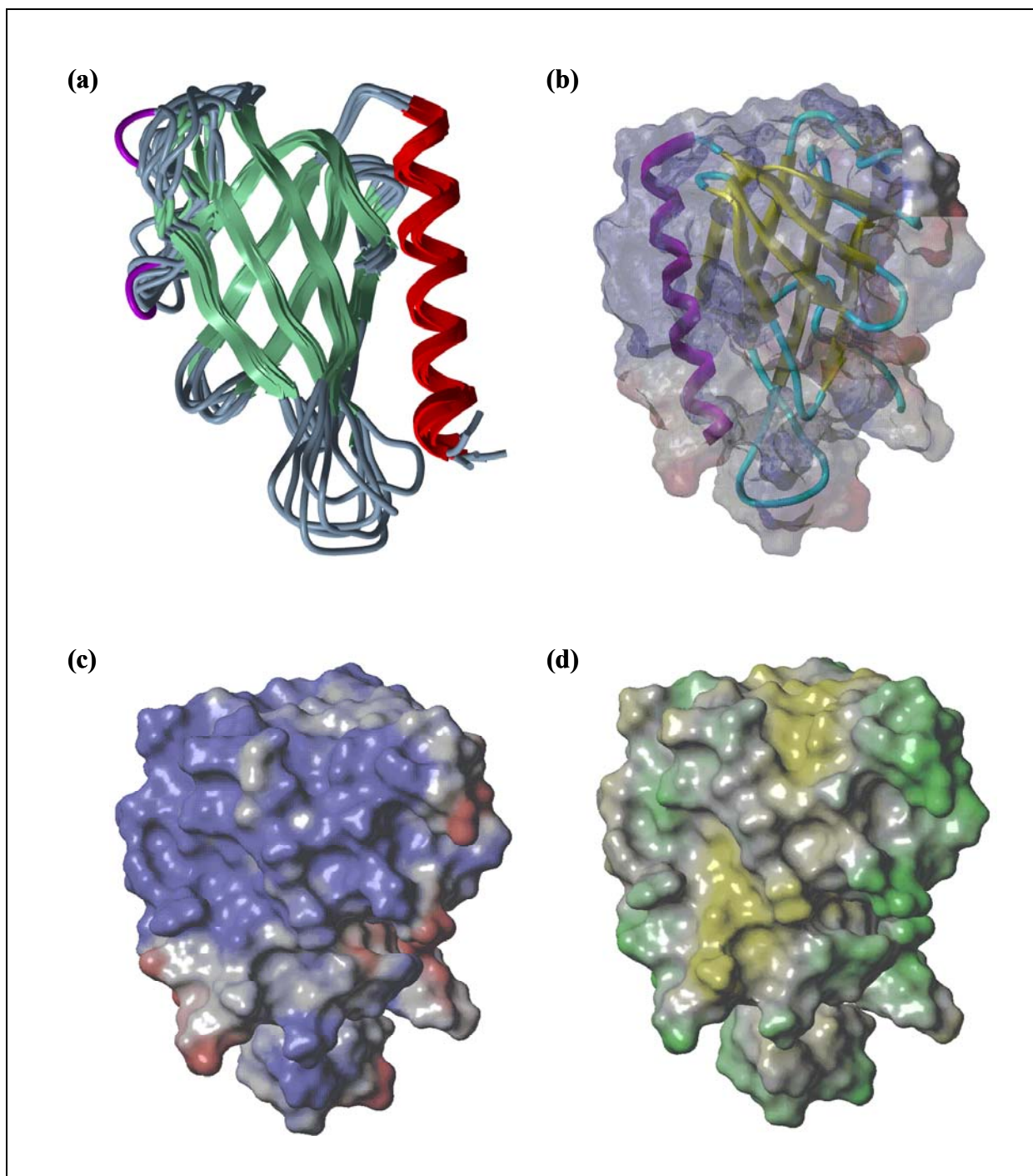


**Figure 24: NMR structure of the hSpred2 EVH1 domain.** The NMR structure of human Spred2 EVH1 domain has been resolved recently and submitted under the accession number “2JP2” by SGC (Oxford) in collaboration with our Institute. Fig. a shows a back view, Fig b, c and d show the front view of the domain highlighting its binding surface. The domain is composed of a C-terminal  $\alpha$ -helix and seven  $\beta$ -sheets. The binding groove for accommodating the still unknown ligands is seen in the front view. Electrostatic surface potential revealed patches of positive surface charge in the binding groove shown in blue colour in Fig. c. Distribution of surface hydrophobicity as shown in Fig. d points to an involvement of hydrophobic residues in the organisation of this ligand binding site. Hydrophobic patches are shown in yellow and hydrophilic patches are shown in green colour coding in Fig. d.

### 5.4.2. Introduction to protein-phospholipid binding assays and overview of the experimental procedure

Protein: phospholipid binding assays were performed in our study in a solid phase overlay format or a liquid phase binding format. The solid phase overlay assay is carried out by using a GST fusion construct of the Spred2 EVH1 domain binding to a solid phase membrane carrying different types of pre-spotted phospholipids [208] (Fig.25a), hence it is also considered as a SPOT test. This assay can determine not only the type of phospholipids but also the phosphorylation pattern of their isomers involved in interaction with a protein module of interest. Membrane-bound protein molecules interacting with a specific phospholipid are detected immunologically after blocking non-specific binding sites by an anti-GST primary antibody followed by HRP tagged secondary antibody and a chemiluminescence signal. The N-terminal SH3 domain of human ADAP protein fused to a GST tag (GST-ADAP SH3-N) was used as a negative control in our phospholipid overlay experiments since it is known to be inactive to the array of phospholipids analysed here.

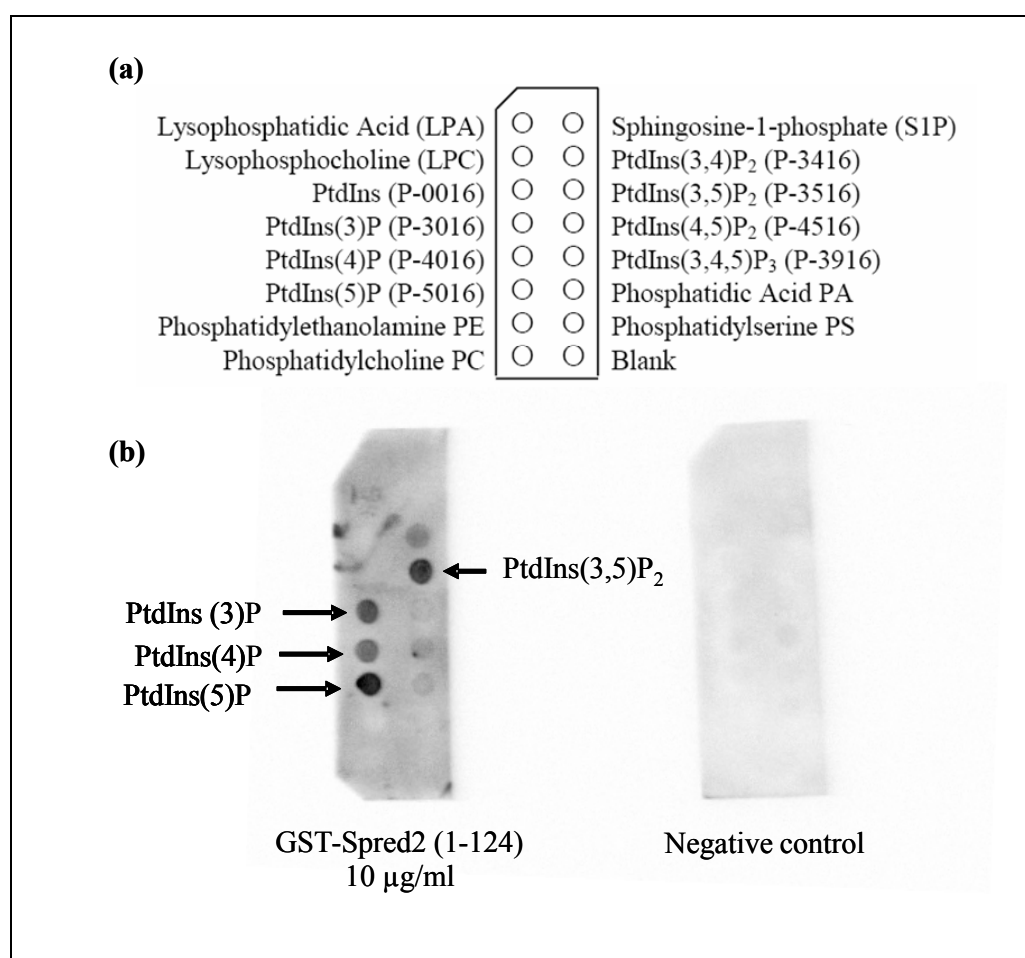


**Figure 25: Protein:phospholipid solid phase overlay experiment.** (a) Scheme depicting a membrane strip with different phospholipids spotted on it. (b) Such membrane was incubated with GST-Spred2 EVH1 protein and the bounded protein was detected by immunoblotting with a primary antibody against GST. The Spred2 EVH1 showed interaction with phosphatidyl inositol phosphorylated preferably at its 3', 4' and 5' sites. ADAP SH3-N protein used as negative control had shown no interaction with the same phospholipids.

Another assay format for studying protein:phospholipid interactions is available in liquid phase by a liposome sedimentation assay. Liposomes are artificially generated spherical vesicles dispersed in aqueous phase that consist of an aqueous core enclosed by one or more amphiphilic layers of the phospholipid to be tested along with phosphatidylcholine (PC) and phosphatidylserine (PS) to mimic plasma membrane's lipid composition. Liposomes can vary in charge and size depending on the method of preparation and the composition of the lipids used. There are different types based on their size viz., multi-lamellar vesicles (MLV, size range 0.1–5.0  $\mu\text{m}$ ), small uni-lamellar vesicles (SUV, size range 0.02–0.05  $\mu\text{m}$ ) and large uni-lamellar vesicles (LUV, size range from 0.06  $\mu\text{m}$ ). Protein: phospholipid interaction studies using liposomes have been performed to reveal biological relevant interactions like those of the ADAP SH3-C domain with phosphatidyl inositol phosphates in a mixture of phosphatidylcholine (PC)/phosphatidylserine (PS) [205] [120, 172]. This assay analyses in a quantitative manner binding of a biologically active bait protein in solution to different concentrations of liposomes containing a small fraction of a test phospholipid. Free unbound and phospholipid-bound protein fractions are separated by differential centrifugation of the reaction mixture into a liposome-free supernatant and the liposome-containing pellet respectively (Fig.26). Unbound protein remaining in the supernatant is detected by its tryptophan fluorescence or by SDS gel electrophoresis of equivalent amounts of pellet and supernatant fractions. A reaction mixture without liposomes but the same amount of bait protein as in the binding reactions is used as the blind value giving the protein concentration maximally to be present in the supernatant if no binding at all occurs. Natively folded bait protein without any fusion tag is required in a mono-disperse preparation for these experiments and Spred2 EVH1 protein was prepared accordingly. The C-terminal SH3 domain of human ADAP protein (ADAP SH3-C) which is known to interact with phosphatidyl inositol phosphorylated at 3, 4 and 5 sites was used as a positive control in our experiment [120, 205]. Not only due to the quantitative information obtained from it but also due to the physical state of its binding substrates the liposome sedimentation assay is considered as a more sensitive and less error-prone assay format compared to the semi-quantitative overlay assay which can at best only provide initial evidence for binding.

#### **5.4.3. Preparation and characterization of the Spred2 EVH1 domain and the control proteins**

The Spred2 EVH1 domain was used either as a GST- fusion protein or alone for the phospholipid interaction experiments. The GST-Spred2 EVH1 domain fusion protein was expressed and purified from the pGEX- 4T-2-hSpred2 (1-124) recombinant plasmid in *E. coli* BL-21 cells as described in Chapter. 5.3.3. The natively folded conformation of freshly expressed GST-Spred2 EVH1 domain fusion protein was assayed by  $^1\text{H}$  NMR spectroscopy after treating the



protein sample with D<sub>2</sub>O in 1:10 ratio (v/v). The NMR spectrum confirmed that the sample of GST fusion protein used as bait in the phospholipid overlay assay was natively folded and is expected thus to be biologically active (Fig.21). For the liposome sedimentation assay, Spred2 EVH1 protein was prepared by digesting the GST-Spred2 EVH1 fusion protein with Thrombin to cleave-off the GST tag and further purified by Sephadex 75<sup>®</sup> column chromatography through FPLC. The purified protein samples were verified by SDS gel electrophoresis and spectrophotometry to determine purity, molecular size and concentration. The control GST-ADAP SH3-N and ADAP SH3-C proteins were prepared in Dr. C. Freund's laboratory according to their standard expression protocols.

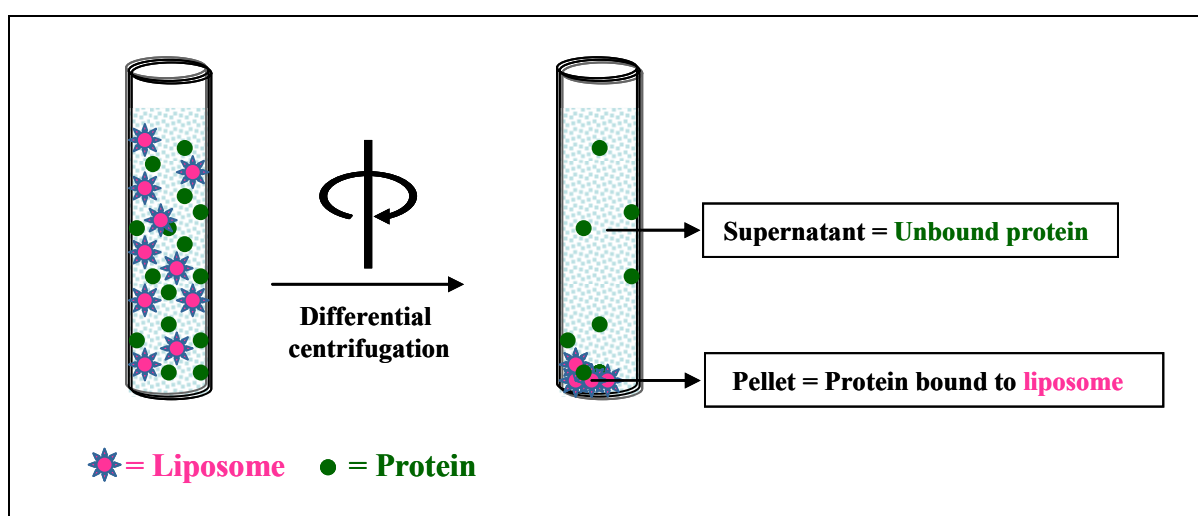


**Figure 26: Protein:phospholipid liposome sedimentation assay.** A quantitative protein-phospholipid interaction assay was performed by liposome sedimentation assay. The artificially prepared liposomes of test phospholipid at different concentrations are incubated with constant amount the query protein and the free unbound and phospholipid-bound protein are separated by differential centrifugation of the binding reaction mixture. Unbound protein remaining in the supernatant is detected by its tryptophan fluorescence or by SDS gel electrophoresis of equivalent amounts of pellet and supernatant fractions.

#### 5.4.4. Biochemical screening for phospholipid interactions of the Spred2 EVH1 domain

Phospholipid overlay experiments were performed using the purified GST-Spred2 EVH1 fusion protein and fifteen different phospholipids immobilized on a membrane strip (Fig.25a). The GST-ADAP SH3-N was used as a negative control. The results show an interaction of the Spred2 EVH1 domain at decreasing intensity with the spots of phosphatidyl inositol 5-phosphate [PtdIns(5)P], phosphatidyl inositol 3-phosphate [PtdIns(3)P], and phosphatidyl inositol 4-phosphate [PtdIns(4)P] (Fig.25b). The abundant cell membrane phospholipids, phosphatidylcholine (PC) and phosphatidylserine (PS), which are known to interact with other adaptor domains, did not interact with the Spred2 EVH1 domain. The negative control protein did not show interaction with any of the fifteen phospholipids spotted on the membrane (Fig.25b).

The results obtained with these phospholipids immobilised on a membrane were further analysed by using the liposome sedimentation assay which supplies the binding substrates under more native conditions. Large uni-lamellar vesicles were therefore prepared of those test phospholipids observed to interact in the overlay assay together with PC and PS in a composition similar to that found in the plasma membrane while taking care to equalise the total negative charge of different vesicle preparations. Increasing concentrations (100  $\mu\text{M}$  to 1200  $\mu\text{M}$ ) of vesicles were incubated with a fixed concentration (2  $\mu\text{M}$ ) of Spred2 EVH1 protein and the ADAP SH3-C was used as a positive control in this experiment. A liposome-free solution of these proteins served as a concentration standard.

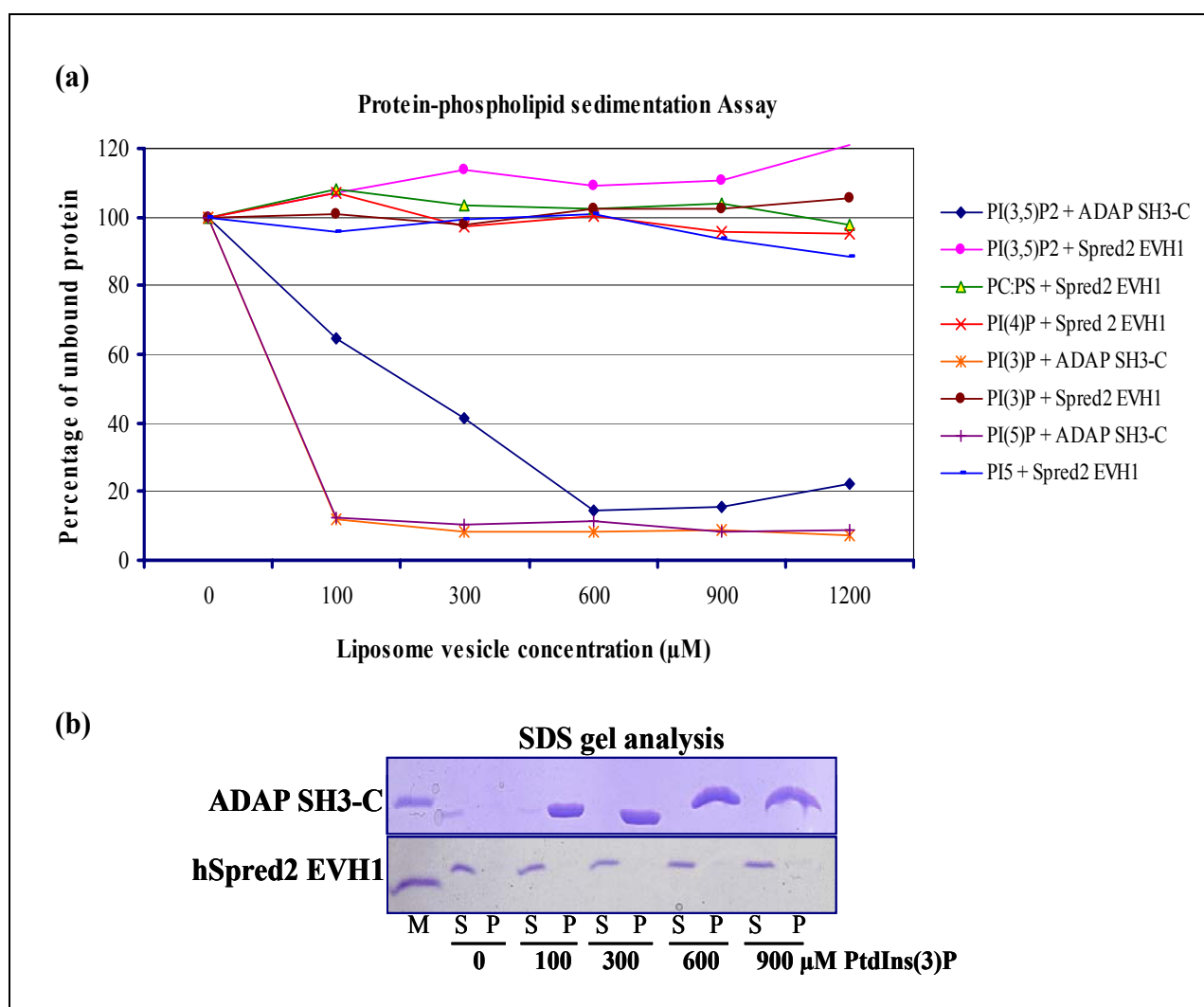


**Figure 27: Results of the liposome sedimentation assay for the Spred2 EVH1 domain.** (a) Percentage of unbound protein present in the supernatant fraction after differential centrifugation of phospholipid-protein binding reaction mixture was calculated by considering the unbound protein present in the negative control (liposome-free) as the maximal protein concentration present in the binding reaction and values are plotted in the graph against increasing liposome vesicle concentration for each phospholipid. Values higher than 100% are the experimental errors occurring during spectrophotometric measurement and pipetting steps. (b) The protein amount present in the pellet and supernatant after differential centrifugation of a binding reaction of Spred2 EVH1 and PtdIns(3)P were analysed by SDS gel electrophoresis. Positive control protein ADAP SH3-C had shown specific interaction with the phospholipid

(Fig. a) and was detected in the pellet fraction after differential centrifugation (Fig. b). In the similar assay, the Spred2 EVH1 domain was detected in the supernatant due to a lack of interaction with respective phospholipids (Fig. b).

The liposome sedimentation assay for ADAP SH3-C showed a dose-dependent interaction with vesicles of PtdIns(3)P, PtdIns(5)P and PtdIns(3,5)P<sub>2</sub> phospholipids as revealed by differential centrifugation (Fig.27a). Phosphatidyl inositol mono-phosphates PtdIns(3)P and PtdIns(5)P completely bound protein even at the lowest concentration (100 μM) studied thus depicting the high binding affinity of ADAP SH3-C. The phosphatidyl inositol bis-phosphate PtdIns(4, 5)P<sub>2</sub> showed a concentration corresponding to half-maximal binding which was three times higher (300 μM) than that observed for the mono-phosphates (Fig.27a). The qualitatively similar results were observed by SDS gel electrophoresis with the protein found in the pellet fraction after differential centrifugation (Fig.27b). These data obtained with the positive control protein showed the correct preparation of vesicles and the proper performance of the assay which was therefore used with the unknown protein. However, the liposome sedimentation assay for the Spred2 EVH1 domain did not show any interaction with vesicles containing PtdIns(3)P, PtdIns(4)P, PtdIns(5)P, PtdIns(3,5)P<sub>2</sub> and PtdIns(4,5)P<sub>2</sub> even at the highest concentration tested (up to 1200 μM) (Fig.27a). No difference in binding was observed compared to the carrier phospholipids PC and PS, used in the preparation of the liposomes (Fig.27a). The amount of protein detected in the supernatant fractions after differential centrifugation of these binding reactions was almost the same independently of the concentrations of liposomes used and did not differ from that of the liposome-free control reactions. Similar results were observed by SDS gel electrophoresis of pellet and supernatant fractions (Fig.27b). Taken together these results with the liposome sedimentation assay are at variance with the initial observations for binding of the Spred2 EVH1 domain obtained from the overlay experiments.

#### 5.4.5. Summary

Two different biochemical assays were performed to study the interaction of the Spred2 EVH1 domain with several phospholipids including phosphatidyl inositol phosphates. Whereas in a solid phase overlay assay an interaction was observed with immobilized PtdIns(3)P, PtdIns(4)P and PtdIns(5)P, no such interaction could be detected when these lipids and their bis-phosphate derivatives PtdIns(3,5)P<sub>2</sub> and PtdIns(4,5)P<sub>2</sub> were supplied in solution as vesicular preparations to study Spred2 EVH1 binding activity in a quantitative manner by a liposome sedimentation assay. The later assay format was considered to be a more sensitive and less error-prone one compared to the more qualitative overlay assay. Due to its physiological conditions supporting protein lipid interactions we therefore consider the liposome sedimentation assay to

supply the more reliable data and conclude that the Spred2 EVH1 domain does not interact in solution with vesicles containing in a small mole fraction PtdIns(3)P, PtdIns(4)P, PtdIns(5)P, PtdIns(3,5)P<sub>2</sub> and PtdIns(4,5)P<sub>2</sub> as individual test lipids (Table.10).

<b>Phospholipid</b>	<b>Protein</b>	<b>Interaction</b>
PtdIns(3)P	ADAP SH3-C	Positive
PtdIns(5)P	ADAP SH3-C	Positive
PtdIns(3,5)P <sub>2</sub>	ADAP SH3-C	Positive
PtdIns(3)P	Spred2 EVH1	Negative
PtdIns(4)P	Spred2 EVH1	Negative
PtdIns(5)P	Spred2 EVH1	Negative
PtdIns(3,5)P <sub>2</sub>	Spred2 EVH1	Negative
PtdIns(4,5)P <sub>2</sub>	Spred2 EVH1	Negative
PC:PS	Spred2 EVH1	Negative

**Table 6: Summary of phospholipid interaction experiments.** Different types of phospholipids with different phosphorylation sites were tested against control domain (ADAP hSH3<sup>C</sup>) and query domain (Spred2 EVH1) for protein-phospholipid interactions by the liposome sedimentation assay and the results are shown in the table.

In summary neither a peptide nor a phospholipid of the chemical classes studied here could be identified as a ligand of the Spred2 EVH1 domain. Experiments for ligand identification were done by genetically screening a cDNA expression library and a phage display library or by biochemically screening several phospholipid binding candidates. In each of these experimental approaches appropriate sets of positive and negative controls were used to assess their proper experimental performance. Biological consequences of these results with regard to the nature of the still elusive Spred2 EVH1 ligand(s) and its probable complementarity to a Spred2 EVH1 interaction interface described recently at an atomic scale will be addressed in the Discussion section.

## 6. DISCUSSION

### 6.1. Protein interactions of the EVH1 domain containing proteins VASP and Spred2

Protein interactions are of central importance for virtually every process in a living cell by mediating signals from the exterior to the inside of the cell. A protein may either interact with another protein just to modify it covalently (like a protein kinase adding enzymatically a phosphate group to a target protein) or proteins might interact only non-covalently to form part of a protein complex (like a modulator or suppressor protein interacting with its binding partner). During covalent modifications such as phosphorylation, phosphate groups are transferred to effector proteins under the control of secondary messengers to alter their binding activities whereas non-covalent interactions regulate the signal-dependent formation of protein complexes between interacting molecules. However, both covalent modification and non-covalent binding contribute to the signal transduction processes that trigger events inside the cell. The EVH1 domains are such protein-protein interaction adaptor modules essential for connecting their host proteins to various signalling pathways. In our study, protein interactions of the two EVH1 domain host proteins VASP and Spred2 were studied according to their involvement in different signal transduction pathways. EVH1 domains hold a unique binding pocket for their peptide epitopes and so far, the VASP EVH1 domain and its binding partners were well studied. Since VASP localizes as part of the actin cytoskeleton, it interacts specifically with different actin network proteins and also acts as a substrate for covalent modifications by PKA and PKG. The signalling pathways of many candidate protein kinases which could be involved in phosphorylation of VASP are not yet analysed. A majority of these signalling pathways can be triggered by stimulation of the cell with serum and therefore candidate protein kinases involved in phosphorylation of VASP during serum stimulation are disclosed in this study (see below). An entirely new class of the EVH1 domain family, consisting of the Spred2 EVH1 domain, carries a characteristic putative binding cleft region containing a subfamily specific triad of surface exposed aromatic amino acid residues which by homology are expected to bind unique sequences of its unknown peptide ligand(s) via non-covalent protein-protein interactions. The search for these unknown binding epitopes for the Spred2 EVH1 domain was therefore performed as a part of our study addressing protein interactions of two EVH1 domain containing proteins. The results from these interaction studies are discussed here with regard to the elucidation of candidate protein kinases involved in serum stimulated VASP phosphorylation and the identification of binding epitopes for the Spred2 EVH1 domain.

The different signalling pathways leading to a possible phosphorylation of VASP during serum stimulation were predicted from literature knowledge and summarized into an

interaction network graph model forming the theoretical basis of our study (Fig.8). The external stimulation, the expected mediators of the external signal and the target substrates of the network including the final destiny were categorised into three hierarchical levels to model the process. The key players of each layer were represented as nodes in the interaction graph. The biochemical role of multiple nodes in this interaction network graph model was assessed experimentally by using different immunological tools and a pharmacological perturbation analysis in a well-defined cell line model. After treating the cells with pharmacological drugs acting as either activators or inhibitors of the target nodes in the interaction graph that represent different candidate protein kinases, the phosphorylation of VASP at its specific phosphorylation sites was studied by using phosphosite-specific antibodies for VASP as molecular probes. By mapping the results of the perturbation analysis into the interaction network graph model, un-affected nodes could thus be excluded and a subnet of the interaction graph was subsequently developed to model those candidate protein kinases involved either directly or indirectly in the phosphorylation of VASP during serum stimulation of the cells.

The search for the unknown binding epitopes for the Spred2 EVH1 domain was performed by independent and complementary genetic and biochemical approaches using a cDNA or a peptide library together with libraries of candidate compounds. Two genetic interaction cloning strategies employing a bacterial two-hybrid and a phage display system were used for binding epitope identification of the recombinantly expressed Spred2 EVH1 domain. The atomic structure of this domain was recently solved by protein NMR spectroscopy. It revealed patches of positive surface charges on its putative binding pocket and thus raised the issue of interactions with negatively charged ligand molecules. Hence, we also searched for Spred2 EVH1 domain interactions with a panel of phospholipid candidate ligands. This study of two EVH1 domain containing proteins therefore covers both techniques and biological concepts for pathway elucidation in complete interaction networks and for an identification of direct binding partners of a single protein in such networks. However due to the different cellular function of VASP and Spred2 the networks studied belong to different and non-overlapping signal transduction pathways of the cell.

### **6.1.1. Deciphering the serum stimulated VASP phosphorylation at Ser-157**

A number of proteins such as VASP, vinculin, talin,  $\alpha$ -actin are associated with focal adhesions at the intracellular face of the plasma membrane [209]. In a functional cytoskeleton, all these molecules are forming complex connective networks with interactions at different levels either directly or indirectly. Earlier studies have shown that VASP binds to F-actin and co-localize

with stress fibres, focal contacts and highly dynamic membrane structures. It is a known fact that VASP is a major substrate for PKA and PKG, which phosphorylate VASP at Ser-157, Ser-239 and Ser-278 [2] and few recent research articles described PKC and AMP-activated protein kinase to phosphorylate VASP too [3, 4].

From our study, we made the observation utilizing a serum starvation and stimulation protocol of mouse cardiac fibroblast (+/+) and mouse mesangial cells that VASP is phosphorylated at Ser-157 on stimulation of these cells as detected in cell lysates by electrophoretic mobility shifts and phosphorylation site-specific monoclonal antibodies (Fig.6 and 7). As this conditional phosphorylation had been observed in two different cell lines, this response is considered not to be a cell specific activity. VASP phosphorylation at Ser-157 by serum induced cell stimulation is a time dependent process whose kinetics was determined with a prominent activity nearly 90 min after treatment of starved cells with serum. It persists at a steady state level even after 10 hours. These observations clearly establish that serum stimulation induces VASP phosphorylation at Ser-157 in a time dependent manner after a lag time of 90 min.

Generally, upon stimulation of cells with serum many protein kinases like MAP kinases, Rho kinases and PKC are activated which regulate cytoskeletal reorganisation in the cell. Of these three kinases, Rho kinase and PKC are known to interact with the actin cytoskeleton and focal adhesions where VASP also interacts with. An important isoform of Rho kinase, ROCK, mediates intracellular serum responses to the cytoskeleton by finally inhibiting actin polymerisation in a treadmilling process where VASP is also known to have a prominent role [210]. PKC is also one of the major protein kinases known to regulate focal adhesions and actin cytoskeleton contractions during serum stimulation [209]. Since these biological molecules show some overlap in activity and regulation with regard to serum response, we have investigated a possible role of these two protein kinases in the observed phosphorylation of VASP at Ser-157 during serum stimulation of cells. Based on published data of these and other protein kinases, an interaction network graph model of signalling pathways possibly phosphorylating VASP during serum stimulation was developed as described in Chapters 5.1.1 and 6.1 (Fig.8) with individual pathways numbered for convenient reference. In this network, the direct interaction between different nodes is in general not known and therefore we represent such interactions as multiple arrow lines keeping in mind that there might be further mediators involved in these signal passages. In our experimental work we have looked for a role of these target nodes in terms of VASP phosphorylation as shown in the network graph and internal mediators were not searched for in our study. Combinatorial treatment with activators and inhibitors of different target nodes of the network allows us in defined perturbation experiments to determine the key players involved in this cascade. A major issue which

needs to be carefully addressed in such type of experiments is the specificity profile of the pharmacological substances used to target the proteins of interest. Most of the protein kinase inhibitors have been developed based on competitive activity either against the secondary messengers that regulate the protein kinases or their common substrate ATP. The inhibitors developed for a particular kinase can therefore disturb the activity of several other protein kinases either partially or completely in a chosen concentration range due to their isomeric chemical structure. Similarly activation of one protein kinase by its respective activator should in general not interfere with other protein kinases since this response pattern would misguide results obtained by activating the targeted signalling pathway. To overcome such experimental limitations in the chemical dissection of an unknown signalling cascade, careful control experiments that complement the pharmacological approach are necessary and have been performed here.

Inhibitory targeting of the two nodes “Rho kinase” and “PKC” in the interaction network graph model by the drugs Y-27632 and Ro-31-8220 respectively had shown that only PKC but not Rho kinase participates in phosphorylation of VASP at Ser-157 upon stimulation of cells with serum (Fig.9a). These data thus rule out any pathways mediated by Rho kinase in this process i.e. those pathways numbered as [4, 4', 4''] in our interaction network model (Fig. 8). However due to their specificity profile these inhibitors may also interrupt the activity of those nodes (PKA and PKG) of the interaction network which are already known from literature data to phosphorylate VASP at Ser-157 by cyclic nucleotide dependent pathways. Hence, we examined the activity of the PKC and Rho kinase inhibitors used here with regard to their sensitivity towards PKA and PKG. We found that these inhibitors are not unspecifically interrupting a PKA and PKG mediated VASP phosphorylation (Fig.9b) and our data therefore suggests that these inhibitors act specifically to only inhibit the addressed target nodes under the experimental conditions used here. This data proved a role of PKC in phosphorylation of VASP at Ser-157 upon stimulation of cells with serum and we therefore studied its function in more detail.

It is known from the literature that activation of PKC with phorbol ester induces focal adhesions and cell contraction due to remodelling in the cell cytoskeleton [211]. The phorbol ester activates only classical isoforms of PKC that regulate the activity of the cytoskeleton. Hence, we asked whether classical isoforms of PKC mediate serum stimulated VASP phosphorylation. Activity of these phorbol ester sensitive classical isoforms could be inhibited specifically by using the compound Bis I [175]. An optimal concentration (10  $\mu$ M) of Bis I was found to prominently inhibit serum stimulated VASP phosphorylation at Ser-157 under the experimental conditions used (Fig.11a) demonstrating that Bis I sensitive classical isoforms of PKC are involved. We then



looked at the effect of the phorbol ester PMA on VASP phosphorylation. Our experimental results showed that PMA phorbol ester stimulation which activates classical isoforms of PKC induced VASP phosphorylation (Fig.11b). It is well known from the literature that phorbol ester treatment initially up-regulates PKC activity followed in the long run by its down regulation due to a translocation of PKC to the cell membrane [185]. Upon phorbol ester treatment, VASP phosphorylation showed a similar temporal pattern of activation and inactivation as that reported for activated PKC alone upon PMA stimulation. There is a transient phosphorylation of VASP at Ser-157 after 2 min of PMA stimulation which persisted no longer than 8 min after stimulation probably due to a down regulation of PKC activity by the phorbol ester (Fig.11b).

Since classical PKC isoforms were identified to mediate serum stimulated VASP phosphorylation at Ser-157, it was necessary to elucidate if this signalling cascade is also dependent on the well known protein kinases PKA and PKG which have already been found to phosphorylate VASP (See interaction graph model in Fig.8) under different experimental conditions. In consecutive experiments, we therefore looked at a role of PKA and PKG in VASP phosphorylation at Ser-157 upon stimulation of cells with serum. The PKG inhibitor Rp-8-Br-cGMPS used in our experiments was not observed to disturb serum stimulated VASP phosphorylation at Ser-157 and it was subsequently found based on immunological detection that MCFB cells (+/+) even lack PKG (Fig.10b). Hence, we concluded that PKG most probably has no role in serum stimulated VASP phosphorylation at Ser-157. This result is in line with our observations showing an absence of phosphorylation of VASP at Ser-239 during serum stimulation, which is the preferable site for PKG in this substrate (Fig.7b). These data is in accordance with previously published ones for the same cell line [182]. With this information at hand, it was possible to experimentally exclude the involvement of a further node and its associated pathway (numbered as [3] of our interaction network graph model in Fig.8) i.e. PKG was shown not be involved in serum stimulated VASP phosphorylation at Ser-157. A similarly designed experiment with H89 used as inhibitor of PKA showed a clear-cut inhibition of serum stimulated VASP phosphorylation at Ser-157 (Fig.10a). This result suggests a role for PKA in serum stimulated VASP phosphorylation at Ser-157. H89 can also inhibit PKG [177] but this is clearly not of concern here as our cells lack this enzyme. Our experiments showed that H89 can be used as a PKA-specific inhibitor in MCFB cells (+/+) at an optimal concentration of 10  $\mu$ M. Furthermore these results are consistent with previous data obtained under different conditions of cellular stimulation identifying Ser-157 of VASP as the phosphorylation site preferred by PKA (see Fig.1).

So far after excluding any involvement of Rho kinases and PKG, our experimental results have identified PKC and PKA as major protein kinases participating in VASP

phosphorylation at Ser-157 upon stimulation of MCFB cells (+/+) with serum. This phosphorylation at VASP Ser-157 by a combined action of PKC and PKA seems to utilize a signalling pathway which is clearly different from that of a PKA induced VASP phosphorylation at the same site under different stimulatory conditions. The data obtained on the two candidate protein kinases involved left us however with the question how PKA mediated VASP phosphorylation at Ser-157 upon serum stimulation relates to the serum-induced signalling cascade mediated by PKC upon phosphorylation of the same site of the VASP molecule. Control experiments with regard to specificity have also identified Bis I and PMA as useful tools for modulating in intact cells the activity of PKC by either inhibition or activation. Similar control experiments showed that for modulating the PKA activity the drugs H89 and Forskolin could be used in experiments with intact cells for either directly inhibiting or indirectly activating this enzyme. Summarizing the data obtained we therefore came up with a reduced model of the possible interaction network pathways as shown in Fig.28a with PKA and PKC identified as the main nodes together with the set of inhibitors and activators targeting each of them. The model is still ambiguous with regard to PKC and PKA participating in either a serial or a parallel order of action with regard to VASP phosphorylation in serum-stimulated cells. However with the characterized tools available it was now further elucidated experimentally by a combinatorial *in-vivo* modulation of the network target nodes involved in serum stimulated VASP phosphorylation i.e. a simultaneous activation and inhibition of these protein kinases. Specifically experiments using various drug combinations were therefore designed to activate either PKC or PKA instead by serum stimulation with their respective activators (PMA or Forskolin) in the presence of the protein kinase inhibitors (Bis I or H89) targeting either the same or the alternative node of the network.

Using a combination of Bis I and Forskolin together we found that the PKC specific inhibitor Bis I did not inhibit VASP phosphorylation at Ser-157 during Forskolin stimulation of the collateral node which activates the adenylyl cyclase and thus PKA (Fig.12b). The complementary experiment was performed with activation of PKC by short term treatment with PMA in the presence of the PKA inhibitor H89. VASP phosphorylation was found to be inhibited under these conditions (Fig. 12c). Taken together these results strongly suggest that the signalling pathway is not organised in the direction from PKA to PKC but instead PKA seems to participate in the process of VASP phosphorylation *after* initial stimulation of PKC. Thus the pathway numbered [e+2'+1] in the reduced model as shown in Fig.1a could be excluded experimentally and the data are compatible with a pathway organization summarized as [b+1'+2] in the model. The insensitivity of Forskolin stimulated VASP phosphorylation to a PKC inhibitor and the successful inhibition of PMA stimulated VASP phosphorylation by a PKA inhibitor is fully explained by the

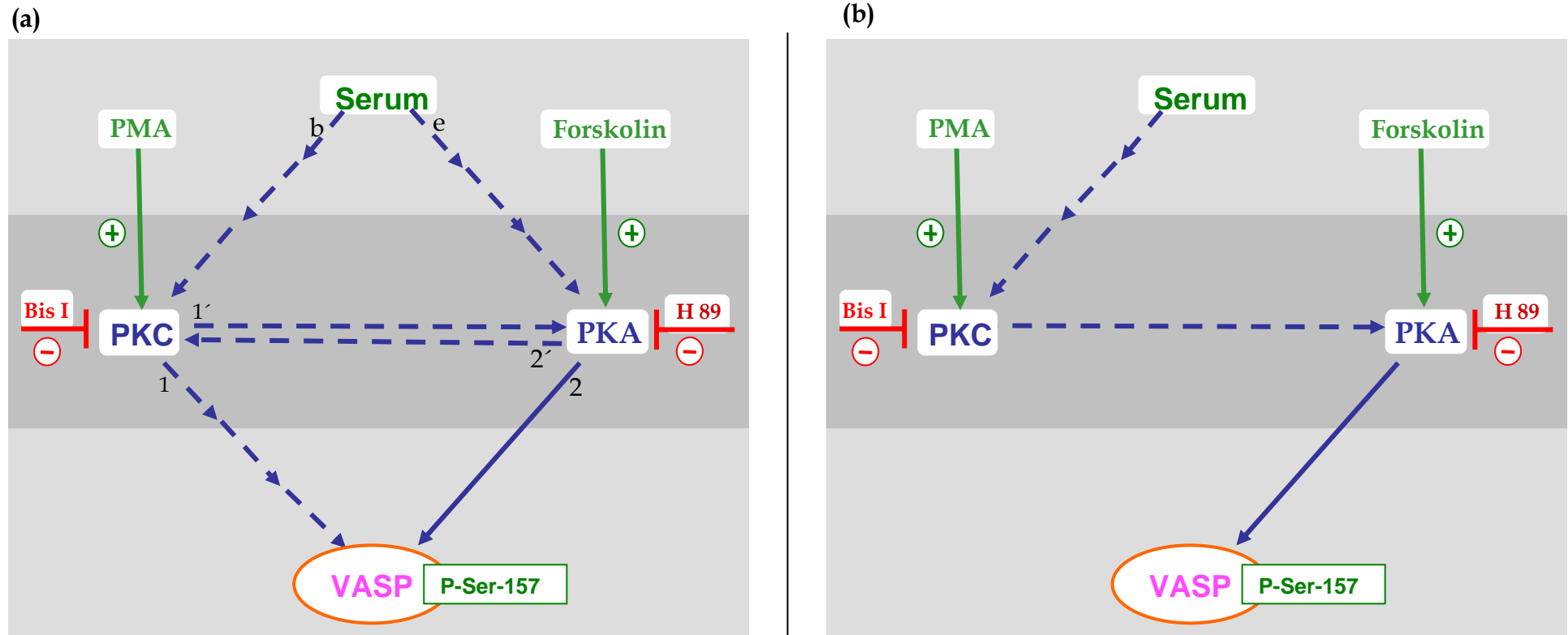


**Figure 28: Final model of the signalling pathways contributing to serum stimulated VASP phosphorylation.** Possible pathways for serum stimulated VASP phosphorylation involving the protein kinases PKC and PKA are shown in Fig. a of this experimentally reduced version of our interaction graph model. Pathways given with unbroken lines show direct interactions. The pathways involving PKC and PKA (with pathway numbers [1] and [2]) were further analysed experimentally by a combinatorial use of specific activators and inhibitors of these protein kinases to elucidate their order of action. The results of these experiments are summarized in the model of Fig. b. Cumulative data suggest that PKC acts upstream of PKA in serum stimulated VASP phosphorylation at Ser-157.

proposed pathway in the final model of Fig.28b with PKC acting *upstream* of PKA. Additional support was observed in the following experiment. After down regulation of PKC by phorbol ester long term treatment, Forskolin treated cells showed undisturbed phosphorylation of VASP at Ser-157 as mediated by PKA (Fig.11c) emphasizing again the proposed pathway organisation. Moreover, the interpretation of our experimental results given here is also in line with information from the literature showing that it is PKA that prefers Ser-157 as a phosphorylation site on VASP [2](see Fig.1). However it is still not yet understood how PKC and PKA interact under these conditions and how a signal is mediated between these two kinases. In particular the internal regulation of PKA after receiving the signal from PKC during serum stimulation either by secondary messengers or any other regulator to phosphorylate VASP at Ser-157 is not settled from the experimental results presented here. Some published studies are supporting directly and indirectly that PKC and PKA can interact during various signal transduction processes [212, 213]. PKC has been shown to activate many other cytoskeletal proteins including associated protein kinases during its activity. It is known to modulate focal adhesions and stress fibres through numerous mechanisms. The  $\alpha$  isoform of PKC is translocated to focal adhesions upon activation of the fibronectin receptor,  $\alpha_{11b}\beta_3$  after stimulation by serum or growth factors, and it is reported that PKC phosphorylates focal adhesion proteins such as vinculin and talin [214, 215]. Additionally, PKC modulates the cellular cytoskeleton through the regulation of intermediate filaments and stress-fiber related proteins, including vimentin, CPI-17, myosin light chain kinase, tau protein and numerous others [215]. It is still a matter of debate how PKC exerts its influence on VASP. Recent published data supplied preliminary information from different cell models that PMA activation of PKC induces VASP phosphorylation either directly [4, 52] or indirectly by activating PKG [216]. However this type of interaction can be excluded in MCFB cells (+/+) since they lack PKG. These discrepancies in signalling pathway organisation seem to be due to cell type or organism specific expression patterns of signalling networks.

In conclusion based on our experimental results and literature information, we hypothesize that PKC receives an external stimulatory signal upon serum stimulation of MCFB (+/+) cells which is passed either directly or indirectly to PKA which finally phosphorylates VASP at Ser-157. PKA is thus positioned downstream of PKC in serum stimulated phosphorylation of VASP and is probably located most proximal to its substrate VASP giving the following pathway: serum stimulation  $\rightarrow\rightarrow$  PKC  $\rightarrow$  PKA  $\rightarrow$  phospho Ser-157 VASP as shown in the final model of Fig.28b.

### 6.1.2. Identification of unknown binding epitopes for a new class of EVH1 domains

In a cell, modular proteins involved in signal transduction utilize a limited number of highly conserved, non-catalytic, ‘adaptor’ domains to mediate their non-covalent interactions during the formation of transient, multi-protein signalling complexes [99]. Such adaptor domains recognise surface-exposed sites on their binding partners such as proline-rich-, phosphorylated- or C-terminal motifs. For example, domain families namely EVH1, SH3, GYF, UEV and WW domains and the single domain protein profilin are known to recognise highly conserved clusters of proline rich motifs (PRM)[86]. Further, some of the modular domains (mostly in apoptotic signalling proteins) undergo homo- or heterotypic domain-domain interactions rather than binding short peptide motifs [99]. Sometimes, certain cytoskeletal modular domains like the pleckstrin homology (PH) or SH3 domains bind to different phosphorylated head groups of phospholipids [99, 120].

The EVH1 domains regulate their interactions via a unique recognition pocket exposed on their surface due to a set of three aromatic amino acids which bind to peptides that are usually 6-13 amino acids long and contain proline-rich motifs of 4-6 amino acids. The recently discovered Spred proteins harbour a new class of EVH1 domains at their N-terminus whose atomic structure was recently been determined by NMR spectroscopy [33]. The atomic structure of the domain revealed patches of positive surface charge in its putative binding cleft region and thus suggests interactions with negatively charged ligand molecules. Since the Spred2 EVH1 domain is expected to bind unique ligand(s), search for its binding epitopes had been performed in our study.

As protein-protein interactions are so important there are a multitude of high-throughput methods available to detect them [126]. Each of the approaches has its own strengths and weaknesses, especially with regard to the sensitivity and specificity of the method. These approaches may for instance select clones that have an apparently positive readout phenotype but that when further analysed are not of physiological relevance. Such clones are usually referred to as “false-positives” [217]. In some cases, expected interacting clones may escape from a library screening which are then referred to as “false-negatives”. In general a high sensitivity of a method used suggests that many of the interactions that occur in reality can be detected by the screen giving a low false-negative rate while a high specificity approach indicates a low false-positive rate with most of the interactions detected by the screen actually occurring in reality [218]. Detection of protein interactions is complicated by the fact that protein themselves are chemically distinct entities with differing charges, numerous secondary and tertiary structural folds that may include a wide variety of post translational modifications. Selection of a method suitable to detect an

interaction depends on the protein for which the interactions are to be screened and several methods are available as already described in Chapter 2.3.

The majority of protein-protein (peptidergic) interaction studies were done by *in-vivo* two-hybrid systems and *in-vitro* bacterial-based phage display methods [219]. Since few years, these methods have been scaled up in screening entire complements of proteins or peptides in large library formats. The *in-vivo* two-hybrid systems have been well-established in yeast and their more advanced developments allowed biologists to test inference about the functional aspects of entire protein networks [139]. Over the past few years, analogous to the embodiment of the yeast two-hybrid systems, similar genetic assays were developed in *E. coli* to facilitate a more rapid analysis of even larger libraries due to the higher transformation efficiency and faster growth rate of this organism [136, 137]. A bacterial two-hybrid (B2H) system thus offers a number of potentially significant advantages over analogous yeast based two-hybrid methods in identifying and characterizing protein-protein interactions from large scale cDNA expression libraries [137, 187]. In particular, it does not require a nuclear localisation of the interaction partner or any export of proteins to the cell membranes and it is possible to study proteins that are toxic to yeast [137]. Furthermore, an *E. coli* based two-hybrid screening reduces the chance that the host harbours any closely related homologues of an interacting partner. The *in-vitro* selection technique of phage display in contrast enables small protein fragments with desired properties with respect to binding of a target protein to be identified from large collections of peptide variants displayed on the surface of filamentous phages such as M13. Since phage M13 is a non-lytic phage which can be produced in high titres and secreted from the infected bacterial host cell without their killing or lysis, it also greatly simplifies phage purification steps and thus peptide identification by DNA sequencing of the isolated clones.

After considering different approaches for detection of peptidergic interactions, two interaction cloning approaches employing a bacterial two-hybrid and a M13 phage display system were used in our study for *in-vivo* screening of a cDNA library and *in-vitro* screening of a M13 9mer peptide library respectively to search for the unknown binding epitopes of the Spred2 EVH1 domain. These two genetic technologies are considered as orthogonal i.e. independent and complementary approaches suitable for a detection of protein interactions solely based on the assumption that Spred2 EVH1 ligands are of peptidergic nature. The B2H screening system used in our studies was based on a *HIS3* gene reporter system developed by Joung et al [137, 188] whereas the peptides displayed on the surface of phage are fused N-terminally to the major capsid protein, pVIII of phage M13 [158]. Both genetic systems had to be established in our study for Spred2 EVH1 binding interactions using well-characterized positive controls to survey experimental

conditions most likely to detect unknown EVH1 domain interactions. Based on those experimental conditions and guided by the control experiments performed in parallel, the search for binding epitopes of the Spred2 EVH1 domain was performed by us.

The B2H system was first of all established for a physically well characterized VASP EVH1 and ActA peptide interaction pair [24] which was used as a tool to calibrate the system for the genetic detection of low affinity interactions which are characteristic of EVH1 domains. The *HIS3* based B2H system offers the advantage to be easily regulated at different selection stringency levels by varying the concentration of 3-AT as the selection agent. This results in a 3-AT dose-dependent growth of resistant clones as reflected in their differential plating efficiency. Recombinantly expressed ActA peptides with different binding strengths as determined *in-vitro* against the VASP EVH1 domain [24] were used as target peptides in doubly transformed bacterial cells also expressing the latter protein. 3-AT resistant growth indicating VASP EVH1 and ActA peptide *in-vivo* interaction was observed for those clones expressing a wild type ActA peptide  ${}_{332}\text{SFE}\underline{\text{F}}\text{PPPPTEDEL}_{344}$  or its tighter binding mutant  ${}_{332}\text{SFE}\underline{\text{W}}\text{PPPPTEDEL}_{344}$  at 3-AT concentrations even up to 5 mM (Fig.14). The non-binding mutant peptide  ${}_{332}\text{SFE}\underline{\text{A}}\text{PPPPTEDEL}_{344}$  as observed from *in-vitro* data [24] failed to support 3-AT resistant growth of the reporter strain even at the lowest concentrations tested. These experimental results clearly showed to us that the B2H system records successfully *in-vivo* an interaction of an EVH1 domain with its cognate binding motif which has already been well-characterized *in-vitro* at the structural and energetic level [24, 29]. We thus expect the B2H system of Joung et al. to be a suitable tool for the genetic identification of unknown peptide binding epitopes of the Spred2 EVH1 domain.

A human brain cDNA expression plasmid library was then chosen for a binding epitope screen by the B2H system since the Spred protein is known to be ubiquitously expressed in brain and neural tissues [79]. The cDNA library screening performed at a selection stringency of 1 mM 3-AT using a  $\lambda$ clI fusion protein with the Spred2 EVH1 domain as the bait gave thousands of 3-AT resistant colonies. A further library screening was therefore performed by increasing the selection stringency to 5 mM 3-AT. This higher selection stringency tremendously reduced the population of 3-AT resistant colonies. However, replica plating of 3-AT resistant colonies to a secondary screening medium and thus selection based on transcriptional activation of the *aadA* gene which is located downstream of *HIS3* reporter gene and responsible for Streptomycin resistance could not further differentiate among colonies. Target plasmid isolates from resistant colonies of both screenings were physically characterized showing that these plasmids carry insert target fragments (Fig.17). Inserts selected by the Spred2 EVH1 domain from the cDNA library showed a heterogeneous molecular weight distribution demonstrating clonal heterogeneity of the

isolates obtained. Positive target plasmid isolates were then further validated genetically by a panel of genetic assays designed to assess (a) their potential for transcriptional self-activation in the absence of the bait plasmid (b) the linkage of the growth phenotype to the target plasmid isolated and (c) Spred2 EVH1 specificity of interaction by comparison against a VASP EVH1 bait plasmid (Fig.18). Positive and negative interaction control plasmid pairs were used in this panel of genetic assays during validation of the target plasmid isolates. The 3-AT resistant growth phenotype observed in these assays were analysed quantitatively by determining the plating efficiency (PE) of the clones and thus comparing these with the panel of interaction control pairs. PE values are expected to directly correlate to the interaction strength at a defined selection stringency for a fusion protein pair tested [198]. None of the target isolates showed self activation by expression of a 3-AT resistant phenotype in the absence of the bait plasmid. Surprisingly the majority of the positive target isolates assayed in these genetic assays scored at PE values not higher than the background value corresponding to a non-specific interaction with a query domain (Table.8). Sequence analysis of those few positive candidates of target isolates showing PE values similar to that of the VASP EVH1 and ActA interaction pair revealed however that they were not carrying in-frame coding sequences for expression of target peptides which would interact with the Spred2 EVH1 domain. Overall, screenings by the B2H system of a human brain cDNA expression plasmid library performed at two different selection stringencies for binding epitopes of the Spred2 EVH1 domain did not detect any Spred2 EVH1 *specific* interactions. The library screening experiments performed under these experimental conditions seemed to be completely dominated by false-positive isolates.

Although two-hybrid methods are generally considered to be highly sensitive in particular to detect domain-mediated interactions [139], our experimental results showed its reduced specificity in search for Spred2 EVH1 ligands leading to high numbers of false positives. The selection stringencies used might thus be either too low or too high for the detection of Spred2 EVH1 domain specific interactions. Of course no data about its binding affinities are available to evaluate these alternatives. If the selection stringency used here is above the threshold level for Spred2 EVH1 domain interactions, high false-negative rates are expected in these experiments and vice-versa with false-positive isolates. For an unknown interaction pair it is impossible to predict threshold selection stringency. Based on the structural information revealed from X-ray crystallography [76] and the NMR-spectroscopy of the Spred2 EVH1 domain (accession number “2JP2” and Fig.24), it was speculated that the domain might bind its ligands at affinities lower than those known for other EVH1 ligands. If this expectation is true then according to our results it would be difficult to detect such interaction strengths in a B2H based screen. If however Spred2



EVH1 ligand interactions occur at higher affinities than the well characterized EVH1 class 1 interactions probably due to binding of extended epitopes similar to those described for the WASP EVH1 class 3 ligands (see Chapter.2.2.2.3) [33], selection stringencies as applied in our library screenings are not expected to be high enough to screen for such interactions.

Several retrospective analyses of published protein-protein interaction data obtained at a genomic scale, mainly in yeast, have shown that the actual results deviate strongly from the gold standards of optimal specificity and selectivity and normally show unexpectedly high levels of false-positive and false-negative rates [142]. Binding epitope discovery can be viewed as “a needle in a haystack” problem [220] that is small target sizes of the expected Spred2 EVH1 binding epitopes are to be identified in a highly complex sequence space spanned in our case by a collection of large cDNA fragments as represented in an expression library. Discrimination of sequence stretches coding for such small binding epitopes against a huge background by cDNA sequences is thus a challenging problem. Another biological problem to cope with by any *in-vivo* interaction cloning approach using heterologously expressed proteins might be based on the limited accessibility of candidate binding epitopes. This could be due to a biased or incorrect folding of their host proteins upon heterologous expression in a bacterial cell. Furthermore heterologous eukaryotic protein expressions in a prokaryotic host cell might not accomplish the required post-translational modification which might be a necessary factor supporting the interaction. By considering a posteriori all these complications in principle inherent to a B2H system, we expected that screening of target peptide libraries under *in-vitro* conditions using a purified bait protein would be an alternative approach to identify the Spred2 EVH1 domain binding epitopes.

An *in-vitro* screening of repertoires of non-natural short target peptides exposed on the surface of phage virions seems to be superior for a precise target access and the corresponding affinity selection for Spred2 EVH1 binding epitopes. Thus, a phage display library screening for Spred2 EVH1 ligands of a M13 X9mer peptide library displayed N-terminally to the pVIII major capsid protein was performed by using purified, natively folded GST-Spred2 EVH1 protein as assessed by NMR spectroscopy. A GST-Fyn SH3 protein was used as a positive control for this library screening since its binding epitope has already been determined by screening the same phage display library which is used in our study [203]. Hence, this positive control domain would help us to calibrate the screening conditions for the GST-Spred2 EVH1 protein. Progressive enrichment of a positively interacting phage population with immobilized bait protein was calculated as a series of enrichment factors in each round of panning. For the positive control protein the enrichment factor reached saturation after four rounds of panning against this domain in our experiments. As observed by colony PCR, the phage populations enriched consists entirely of

phage particles with inserts coding for the expected size of the specific target peptide (Fig 22a). This result demonstrates a successful establishment of the experimental protocol for a phage display screening. In contrast, similar panning with the same library using the GST-Spred2 EVH1 protein revealed an irregular enrichment during successive rounds (Table.9). Analysis of phages by colony PCR after infecting to *E. coli* cells showed that the majority of the isolates did not carry any inserts and thus will not express any target peptides fused to and displayed with the capsid protein. Sequencing of those small sample set of insert containing phages identified a population mainly containing stop codons. Only two isolates harbor in-frame ORF fusions, one of which contains a 13mer proline-rich sequence. The significance of this observation is however unclear not only in the context of the non-specific overall performance of the phage display library screening experiment with the Spred2 EVH1 domain but also in light of the fact that the library used had been constructed for 9-mer insert sizes. Selection of phages containing in majority either no inserts or even stop codons suggests that already an N-terminal fragment of the pVIII major coat protein might display sticky epitopes that non-specifically interact with the Spred2 EVH1 but not with the Fyn SH3 domain. Therefore the phage display peptide library screening for identification of binding epitopes for the Spred2 EVH1 domain was of only limited over-all success despite the isolation of a promising candidate binding clone. Several factors could have been responsible for the non-specific performance of our phage display screening experiments. A partial occlusion of the Spred2 EVH1 binding surfaces by the GST moiety of the fusion construct should be considered. Although an alternative small fusion tag would be preferably such as a hexahistidine peptide, increased binding affinity of phages to a Ni-NTA matrix compared to a GSH-Sepharose matrix should be considered in view of artefacts which could arise by selection of Ni<sup>+2</sup> binding phages [157]. Since the phage display assay involves *in-vitro* affinity selection, the system can obviously not support any post-translational modifications. Finally the Spred2 EVH1 domain might be too sticky for a phage M13 based screening approach.

In general, EVH1 domains bind to proline-rich core motifs of 3-6 amino acids present in the binding epitope of target peptides. Further affinity- and specificity-increasing interactions are then formed between additional domain regions and 'core-flanking' peptide residues [85]. For this reason, we had used a 9mer peptide phage display library based on the expectation that binding epitopes for the Spred2 EVH1 domain are similar to those of the VASP EVH1 domain (see Chapter 2.2.2.1). However the Spred2 EVH1 domain does not seem to be able to bind with sufficient affinity to our phage display 9mer peptide library thus probably suggesting a requirement for still larger epitope sizes in a more stable ligand binding. The isolation of a 13mer proline-rich sequence by the Spred2 EVH1 domain from a 9mer library might suggest a preference

of this domain for 13mer peptides probably containing several core-flanking residues. But such larger peptide sequences could probably not be enriched in large amounts from this library due to its construction based which was based on short peptides. A single 13mer proline-rich isolate alone is certainly not enough to determine the binding specificity of the Spred2 EVH1 domain. However, we consider this 13mer proline-rich peptide as a first cue which could be followed up by further screening experiments like SPOT scans to identify in detail the Spred2 EVH1 domain binding motif.

The inability to find Spred2 EVH1 ligands so far not only with a B2H system but also by phage display library screening experiments raised doubts about a peptidergic nature of the ligand. It was therefore necessary to consider additionally a non-peptidergic nature of the still elusive binding ligand. The atomic structure of the Spred2 EVH1 domain showed patches of positive surface charge in the region of the expected binding epitope recognition site which are not observed in any of other EVH1 classes whose structures have been determined so far (Fig.24). It is already known from adaptor domains like pleckstrin homology (PH) or SH3 domains that positively charged surface regions bind to negatively charged phosphorylated phospholipids of different composition [99, 120]. To assess binding interactions of the Spred2 EVH1 domain with candidate phospholipids, solid phase overlay and liquid phase sedimentation assays were performed in the course of this study. The N-terminal and C-terminal SH3 domains of the ADAP protein were used as negative and positive controls respectively in our experiments to follow up their performance. As a prerequisite a natively folded conformation of the bait protein is required for assaying its interaction. Hence, the bait protein independent of the GST moiety was analysed by  $^1\text{H}$  NMR and found to be actively folded in the protein preparations used.

Protein-phospholipid solid phase overlay assays performed against natively folded Spred2 EVH1 protein with membrane strips carrying 15 different, biologically active, pre-spotted phospholipids showed a positive interaction of decreasing apparent binding intensity with phosphatidyl inositol 5-phosphate [PtdIns(5)P], phosphatidyl inositol 3-phosphate [PtdIns(3)P], and phosphatidyl inositol 4-phosphate [PtdIns(4)P] (Fig.25). Further analysis however of these binding activities by liquid phase sedimentation assay of the phospholipids including their bisphosphates phosphatidyl inositol 3,5-bisphosphate [PtdIns(3,5)P<sub>2</sub>] and phosphatidyl inositol 4,5-bisphosphate [PtdIns(4,5)P<sub>2</sub>] did *not* show any interactions of the Spred2 EVH1 domain with liposomal vesicles of up to 1.2 mM concentration (Fig.27). In contrast, the positive control domain showed a strong interaction even at the lowest concentrations tested for the expected phospholipids and thus confirmed the correct preparation of liposomes and its handling. The reason for a different interaction behaviour of a protein in two different assay formats against the same set of

phospholipids is currently unclear. Of the two tests performed, the solid phase overlay assay is considered to be at best a semi-quantitative one whereas the more sensitive liquid phase sedimentation assay is a truly quantitative assay performed at different lipid concentrations. It thus permits determination of affinities in dose dependent experiment with a low error rate in terms of binding specificity. The interactions detected in the solid phase overlay assay are considered therefore as false positives without biological relevance and are probably due to non-specific electrostatic interactions between a positively charged protein molecule and the negatively charged phospholipids spotted on the membrane. Such interactions will be excluded in the liquid phase sedimentation assay where different concentrations of liposomes are incubated with the protein assaying after separating unbound protein for its physical contact in liquid phase. Since the technically more reliable liquid phase sedimentation assay did not show any interaction of the phospholipids tested with the Spred2 EVH1 domain, we concluded from this study that the Spred2 EVH1 domain does not interact with the negatively charged phospholipids tested despite its positive surface charge. These results seem to exclude a non-peptidergic nature of the ligand for the Spred2 EVH1 domain at least with regard to the common classes of phospholipids analysed here.

## 6.2. Conclusions and open questions

In the first part of our study, the protein kinases involved in the serum stimulated VASP phosphorylation in MCFB cells (+/+) are identified as classical isoforms of PKCs and PKA. However the nature of an exchange of signals from PKC to PKA remains unclear; a direct interaction or any further mediators could be involved. The signal transmitted between these two molecules might be based on a low-molecular activator to be identified. It was not possible to address this question from the experimental setup of our study. It will also be necessary to study the newly detected signalling pathway in different cell models using further pharmacological compounds. A major limitation of any signal transduction study based on perturbation analysis is the choice of the appropriate pharmacological drugs since their specificity is often highly dependent on the biological context. If the signalling pathway detected in our study is of a more general nature, it should be reproducible in other biological models of cellular serum stimulation. We have proved so far this signalling process in two different cell models i.e. mouse cardiac fibroblast cells and mouse mesangial cells. Although we have performed our experiments with properly designed experimental controls, there is always a need to retest a pathway in future experiments whenever any new pharmacological drugs to target it may arise.

In the second part of our study, the cumulative evidence suggests to us a peptidergic nature of negatively charged Spred2 EVH1 ligands since a phospholipid mediated interaction to

this domain seems highly unlikely. In principle a peptidergic binding epitope of an adaptor domain or a receptor could form one of the following types: it could be a short or extended, linear or conformational, continuous or discontinuous, post-translationally modified or unmodified peptide sequence with or without any cofactor requirement. Although an *in-vivo* B2H and an *in-vitro* phage display system offer a wide range of library screening formats, they will not detect any post-translationally modified ligands including phosphorylated recognition motifs. Eukaryotic proteins studied in *E. coli* based library screenings are expected to lack co-factors or post-translational modifications which however could occur in yeast for determining potential interactions [134]. In general proteins can be altered by a diverse set of post-translational modifications that include phosphorylation, methylation, acetylation, ubiquitylation and hydroxylation [221]. A post-translational modification attached to one amino acid can antagonise or favour the ability of adjacent residues to recruit a binding partner. Some modular domains like SH2, PTB, WW or 14-3-3 domains recognise target core motifs containing phosphorylated residues [99, 221]. Due to the pronounced positive surface charge of the Spred2 EVH1 domain as revealed by its atomic structure, hydrophobic phosphopeptide binding motifs would be attractive candidates to think of in next steps of a study. Considering tools like phosphopeptide SPOT scans or yeast two-hybrid systems which may identify interactions of the Spred2 EVH1 domain with post-translationally modified epitopes would be an attractive option for future experiments.

## 7. References

1. Halbrügge, M. and U. Walter, *Purification of a vasodilator-regulated phosphoprotein from human platelets*. Eur J Biochem, 1989. 185(1): p. 41-50.
2. Butt, E., et al., *cAMP- and cGMP-dependent protein kinase phosphorylation sites of the focal adhesion vasodilator-stimulated phosphoprotein (VASP) in vitro and in intact human platelets*. J Biol Chem, 1994. 269(20): p. 14509-17.
3. Blume, C., et al., *AMP-activated protein kinase impairs endothelial actin cytoskeleton assembly by phosphorylating vasodilator-stimulated phosphoprotein*. J Biol Chem, 2007. 282(7): p. 4601-12.
4. Chitaley, K., et al., *Vasodilator-stimulated phosphoprotein is a substrate for protein kinase C*. FEBS Lett, 2004. 556(1-3): p. 211-5.
5. Zimmer, M., et al., *Cloning of the VASP (vasodilator-stimulated phosphoprotein) genes in human and mouse: structure, sequence, and chromosomal localization*. Genomics, 1996. 36(2): p. 227-33.
6. Halbrugge, M., et al., *Stoichiometric and reversible phosphorylation of a 46-kDa protein in human platelets in response to cGMP- and cAMP-elevating vasodilators*. J Biol Chem, 1990. 265(6): p. 3088-93.
7. Waldmann, R., M. Nieberding, and U. Walter, *Vasodilator-stimulated protein phosphorylation in platelets is mediated by cAMP- and cGMP-dependent protein kinases*. Eur J Biochem, 1987. 167(3): p. 441-8.
8. Krause, M., et al., *ENA/VASP PROTEINS: Regulators of the Actin Cytoskeleton and Cell Migration*. Annu Rev Cell Dev Biol, 2003. 19: p. 541-64.
9. Ermekova, K.S., et al., *The WW domain of neural protein FE65 interacts with proline-rich motifs in Mena, the mammalian homolog of Drosophila enabled*. J Biol Chem, 1997. 272(52): p. 32869-77.
10. Jonckheere, V., et al., *Dimerization of profilin II upon binding the (GP5)3 peptide from VASP overcomes the inhibition of actin nucleation by profilin II and thymosin beta4*. FEBS Lett, 1999. 447(2-3): p. 257-63.
11. DeMille, M.M., B.E. Kimmel, and G.M. Rubin, *A Drosophila gene regulated by rough and glass shows similarity to ena and VASP*. Gene, 1996. 183(1-2): p. 103-8.
12. Chakraborty, T., et al., *A focal adhesion factor directly linking intracellularly motile Listeria monocytogenes and Listeria ivanovii to the actin-based cytoskeleton of mammalian cells*. Embo J, 1995. 14(7): p. 1314-21.
13. Holt, M.R. and A. Koffer, *Cell motility: proline-rich proteins promote protrusions*. Trends Cell Biol, 2001. 11(1): p. 38-46.
14. Chereau, D. and R. Dominguez, *Understanding the role of the G-actin-binding domain of Ena/VASP in actin assembly*. J Struct Biol, 2006. 155(2): p. 195-201.
15. Reinhard, M., T. Jarchau, and U. Walter, *Actin-based motility: stop and go with Ena/VASP proteins*. Trends Biochem Sci, 2001. 26(4): p. 243-9.
16. Ahern-Djamali, S.M., et al., *Identification of profilin and src homology 3 domains as binding partners for Drosophila enabled*. Proc Natl Acad Sci U S A, 1999. 96(9): p. 4977-82.
17. Zimmermann, J., et al., *Relaxation, equilibrium oligomerization, and molecular symmetry of the VASP (336-380) EVH2 tetramer*. Biochemistry, 2002. 41(37): p. 11143-51.
18. Huttelmaier, S., et al., *Characterization of the actin binding properties of the vasodilator-stimulated phosphoprotein VASP*. FEBS Lett, 1999. 451(1): p. 68-74.
19. Kuhnel, K., et al., *The VASP tetramerization domain is a right-handed coiled coil based on a 15-residue repeat*. Proc Natl Acad Sci U S A, 2004. 101(49): p. 17027-32.

20. Harbeck, B., et al., *Phosphorylation of the vasodilator-stimulated phosphoprotein regulates its interaction with actin*. J Biol Chem, 2000. 275(40): p. 30817-25.
21. Grosse, R., et al., *A role for VASP in RhoA-Diaphanous signalling to actin dynamics and SRF activity*. Embo J, 2003. 22(12): p. 3050-61.
22. Zhuang, S., et al., *Vasodilator-stimulated phosphoprotein activation of serum-response element-dependent transcription occurs downstream of RhoA and is inhibited by cGMP-dependent protein kinase phosphorylation*. J Biol Chem, 2004. 279(11): p. 10397-407.
23. Ahern-Djamali, S.M., et al., *Mutations in Drosophila enabled and rescue by human vasodilator-stimulated phosphoprotein (VASP) indicate important functional roles for Ena/VASP homology domain 1 (EVH1) and EVH2 domains*. Mol Biol Cell, 1998. 9(8): p. 2157-71.
24. Ball, L.J., et al., *Dual epitope recognition by the VASP EVH1 domain modulates polyproline ligand specificity and binding affinity*. Embo J, 2000. 19(18): p. 4903-14.
25. Renfranz, P.J. and M.C. Beckerle, *Doing (F/L)PPPPs: EVH1 domains and their proline-rich partners in cell polarity and migration*. Curr Opin Cell Biol, 2002. 14(1): p. 88-103.
26. Laine, R.O., et al., *Vinculin proteolysis unmask an ActA homolog for actin-based Shigella motility*. J Cell Biol, 1997. 138(6): p. 1255-64.
27. Drees, B., et al., *Characterization of the interaction between zyxin and members of the Ena/vasodilator-stimulated phosphoprotein family of proteins*. J Biol Chem, 2000. 275(29): p. 22503-11.
28. Schick, B., et al., *Expression of VASP and zyxin in cochlear pillar cells: indication for actin-based dynamics?* Cell Tissue Res, 2003. 311(3): p. 315-23.
29. Zimmermann, J., et al., *Design of N-substituted peptomer ligands for EVH1 domains*. J Biol Chem, 2003. 278(38): p. 36810-8.
30. Niebuhr, K., et al., *A novel proline-rich motif present in ActA of Listeria monocytogenes and cytoskeletal proteins is the ligand for the EVH1 domain, a protein module present in the Ena/VASP family*. Embo J, 1997. 16(17): p. 5433-44.
31. Fedorov, A.A., et al., *Structure of EVH1, a novel proline-rich ligand-binding module involved in cytoskeletal dynamics and neural function*. Nat Struct Biol, 1999. 6(7): p. 661-5.
32. Prehoda, K.E., D.J. Lee, and W.A. Lim, *Structure of the enabled/VASP homology 1 domain-peptide complex: a key component in the spatial control of actin assembly*. Cell, 1999. 97(4): p. 471-80.
33. Ball LJ, W.U., Zimmermann J, Jarchau T *EVH1/WH1 Domains*. Modular Protein Domains. Edited by G. Cesareni MG, M. Sudol, M. Yaffe. 2005, Wiley-VCH GmbH. 73-101.
34. Reinhard, M., et al., *VASP interaction with vinculin: a recurring theme of interactions with proline-rich motifs*. FEBS Lett, 1996. 399(1-2): p. 103-7.
35. Krause, M., et al., *Fyn-binding protein (Fyb)/SLP-76-associated protein (SLAP), Ena/vasodilator-stimulated phosphoprotein (VASP) proteins and the Arp2/3 complex link T cell receptor (TCR) signaling to the actin cytoskeleton*. J Cell Biol, 2000. 149(1): p. 181-94.
36. Hoffman, L.M., et al., *Targeted disruption of the murine zyxin gene*. Mol Cell Biol, 2003. 23(1): p. 70-9.
37. Boukhelifa, M., et al., *Palladin is a novel binding partner for Ena/VASP family members*. Cell Motil Cytoskeleton, 2004. 58(1): p. 17-29.
38. Gouin, E., M.D. Welch, and P. Cossart, *Actin-based motility of intracellular pathogens*. Curr Opin Microbiol, 2005. 8(1): p. 35-45.

39. Hamon, M., H. Bierne, and P. Cossart, *Listeria monocytogenes: a multifaceted model*. Nat Rev Microbiol, 2006. 4(6): p. 423-34.
40. Bear, J.E., et al., *Antagonism between Ena/VASP proteins and actin filament capping regulates fibroblast motility*. Cell, 2002. 109(4): p. 509-21.
41. Gertler, F.B., et al., *Drosophila abl tyrosine kinase in embryonic CNS axons: a role in axonogenesis is revealed through dosage-sensitive interactions with disabled*. Cell, 1989. 58(1): p. 103-13.
42. Bashaw, G.J., et al., *Repulsive axon guidance: Abelson and Enabled play opposing roles downstream of the roundabout receptor*. Cell, 2000. 101(7): p. 703-15.
43. Gates, J., et al., *Enabled plays key roles in embryonic epithelial morphogenesis in Drosophila*. Development, 2007. 134(11): p. 2027-2039.
44. Gertler, F.B., et al., *Mena, a relative of VASP and Drosophila Enabled, is implicated in the control of microfilament dynamics*. Cell, 1996. 87(2): p. 227-39.
45. Lambrechts, A., et al., *cAMP-dependent protein kinase phosphorylation of EVL, a Mena/VASP relative, regulates its interaction with actin and SH3 domains*. J Biol Chem, 2000. 275(46): p. 36143-51.
46. Reinhard, M., Jarchau, T., Reinhard, K. & Walter, U., *Guidebook to the Cytoskeletal and Motor Proteins*, eds, eds. Kreis, T. & Vale, R. 1999, Oxford Univ. Press, Oxford. p. 168–171.
47. Horstrup, K., et al., *Phosphorylation of focal adhesion vasodilator-stimulated phosphoprotein at Ser157 in intact human platelets correlates with fibrinogen receptor inhibition*. Eur J Biochem, 1994. 225(1): p. 21-7.
48. Oelze, M., et al., *Vasodilator-stimulated phosphoprotein serine 239 phosphorylation as a sensitive monitor of defective nitric oxide/cGMP signaling and endothelial dysfunction*. Circ Res, 2000. 87(11): p. 999-1005.
49. Miralles, F., et al., *Actin dynamics control SRF activity by regulation of its coactivator MAL*. Cell, 2003. 113(3): p. 329-42.
50. Wentworth, J.K., G. Pula, and A.W. Poole, *Vasodilator-stimulated phosphoprotein (VASP) is phosphorylated on Ser157 by protein kinase C-dependent and -independent mechanisms in thrombin-stimulated human platelets*. Biochem J, 2006. 393(Pt 2): p. 555-64.
51. Chen, L., et al., *Vasodilator-stimulated phosphoprotein regulates proliferation and growth inhibition by nitric oxide in vascular smooth muscle cells*. Arterioscler Thromb Vasc Biol, 2004. 24(8): p. 1403-8.
52. Pula, G., et al., *PKCdelta regulates collagen-induced platelet aggregation through inhibition of VASP-mediated filopodia formation*. Blood, 2006. 108(13): p. 4035-44.
53. Trichet, L., et al., *VASP governs actin dynamics by modulating filament anchoring*. Biophys J, 2007. 92(3): p. 1081-9.
54. Galler, A.B., et al., *VASP-dependent regulation of actin cytoskeleton rigidity, cell adhesion, and detachment*. Histochem Cell Biol, 2006. 125(5): p. 457-74.
55. Krause, M., et al., *The Ena/VASP enigma*. J Cell Sci, 2002. 115(Pt 24): p. 4721-6.
56. Walders-Harbeck, B., et al., *The vasodilator-stimulated phosphoprotein promotes actin polymerisation through direct binding to monomeric actin*. FEBS Lett, 2002. 529(2-3): p. 275-80.
57. Rottner, K., et al., *VASP dynamics during lamellipodia protrusion*. Nat Cell Biol, 1999. 1(5): p. 321-2.
58. Garcia Arguinzonis, M.I., et al., *Increased spreading, Rac/p21-activated kinase (PAK) activity, and compromised cell motility in cells deficient in vasodilator-stimulated phosphoprotein (VASP)*. J Biol Chem, 2002. 277(47): p. 45604-10.



59. Mejillano, M.R., et al., *Lamellipodial versus filopodial mode of the actin nanomachinery: pivotal role of the filament barbed end*. Cell, 2004. 118(3): p. 363-73.
60. Samarina, S., et al., *How VASP enhances actin-based motility*. J Cell Biol, 2003. 163(1): p. 131-42.
61. Walter, U., et al., *Role of cyclic nucleotide-dependent protein kinases and their common substrate VASP in the regulation of human platelets*. Adv Exp Med Biol, 1993. 344: p. 237-49.
62. Schafer, A., et al., *Endothelium-dependent and -independent relaxation and VASP serines 157/239 phosphorylation by cyclic nucleotide-elevating vasodilators in rat aorta*. Biochem Pharmacol, 2003. 65(3): p. 397-405.
63. Aszodi, A., et al., *The vasodilator-stimulated phosphoprotein (VASP) is involved in cGMP- and cAMP-mediated inhibition of agonist-induced platelet aggregation, but is dispensable for smooth muscle function*. Embo J, 1999. 18(1): p. 37-48.
64. Hauser, W., et al., *Megakaryocyte hyperplasia and enhanced agonist-induced platelet activation in vasodilator-stimulated phosphoprotein knockout mice*. Proc Natl Acad Sci U S A, 1999. 96(14): p. 8120-5.
65. Lim, J., et al., *Sprouty Proteins Are Targeted to Membrane Ruffles upon Growth Factor Receptor Tyrosine Kinase Activation. IDENTIFICATION OF A NOVEL TRANSLOCATION DOMAIN*. J. Biol. Chem., 2000. 275(42): p. 32837-32845.
66. Wakioka, T., et al., *Spred is a Sprouty-related suppressor of Ras signalling*. Nature, 2001. 412(6847): p. 647-51.
67. Kato, R., et al., *Molecular cloning of mammalian Spred-3 which suppresses tyrosine kinase-mediated Erk activation*. Biochem Biophys Res Commun, 2003. 302(4): p. 767-72.
68. Hashimoto, S., et al., *Expression of Spred and Sprouty in developing rat lung*. Mech Dev, 2002. 119 Suppl 1: p. S303-9.
69. Nonami, A., et al., *The Sprouty-related protein, Spred-1, localizes in a lipid raft/caveola and inhibits ERK activation in collaboration with caveolin-1*. Genes Cells, 2005. 10(9): p. 887-95.
70. Nobuhisa, I., et al., *Spred-2 suppresses aorta-gonad-mesonephros hematopoiesis by inhibiting MAP kinase activation*. J Exp Med, 2004. 199(5): p. 737-42.
71. Lim, J., et al., *The cysteine-rich sprouty translocation domain targets mitogen-activated protein kinase inhibitory proteins to phosphatidylinositol 4,5-bisphosphate in plasma membranes*. Mol Cell Biol, 2002. 22(22): p. 7953-66.
72. Sasaki, A., et al., *Mammalian Sprouty4 suppresses Ras-independent ERK activation by binding to Raf1*. Nat Cell Biol, 2003. 5(5): p. 427-32.
73. Nonami, A., et al., *Spred-1 negatively regulates interleukin-3-mediated ERK/mitogen-activated protein (MAP) kinase activation in hematopoietic cells*. J Biol Chem, 2004. 279(50): p. 52543-51.
74. King, J.A., et al., *Distinct requirements for the Sprouty domain for functional activity of Spred proteins*. Biochem J, 2005. 388(Pt 2): p. 445-54.
75. King, J.A., et al., *Eve-3: a liver enriched suppressor of Ras/MAPK signaling*. J Hepatol, 2006. 44(4): p. 758-67.
76. Harmer, N.J., et al., *1.15 A crystal structure of the X. tropicalis Spred1 EVH1 domain suggests a fourth distinct peptide-binding mechanism within the EVH1 family*. FEBS Lett, 2005. 579(5): p. 1161-6.
77. Gileadi, O, S.K., Wen Hwa Lee, Brian D. Marsden, Susanne Müller, Frank H. Niesen, Kathryn L. Kavanagh, Linda J. Ball, Frank von Delft, Declan A. Doyle, Udo C. T. Oppermann, Michael Sundström, *The scientific impact of the Structural Genomics Consortium: a protein family and ligand-centered approach to medically-relevant human proteins*. Journal of Structural and Functional Genomics, 2007. (in press).

78. Miyoshi, K., et al., *The Sprouty-related protein, Spred, inhibits cell motility, metastasis, and Rho-mediated actin reorganization*. *Oncogene*, 2004. 23(33): p. 5567-76.
79. Engelhardt, C.M., et al., *Expression and subcellular localization of Spred proteins in mouse and human tissues*. *Histochem Cell Biol*, 2004. 122(6): p. 527-38.
80. Karin Bundschu, U.W.K.S., *Getting a first clue about SPRED functions*. *BioEssays*, 2007. 29(9): p. 897-907.
81. Sasaki, A., et al., *Identification of a dominant negative mutant of Sprouty that potentiates fibroblast growth factor- but not epidermal growth factor-induced ERK activation*. *J Biol Chem*, 2001. 276(39): p. 36804-8.
82. Bundschu, K., et al., *Gene disruption of Spred-2 causes dwarfism*. *J Biol Chem*, 2005. 280(31): p. 28572-80.
83. Inoue, H., et al., *Spred-1 negatively regulates allergen-induced airway eosinophilia and hyperresponsiveness*. *J Exp Med*, 2005. 201(1): p. 73-82.
84. Yoshida, T., et al., *Spreds, inhibitors of the Ras/ERK signal transduction, are dysregulated in human hepatocellular carcinoma and linked to the malignant phenotype of tumors*. *Oncogene*, 2006. 25(45): p. 6056-66.
85. Ball, L.J., et al., *EVHI domains: structure, function and interactions*. *FEBS Lett*, 2002. 513(1): p. 45-52.
86. Linda J. Ball, R.K.J.S.-M.H.O., *Recognition of Proline-Rich Motifs by Protein-Protein-Interaction Domains*. *Angewandte Chemie International Edition*, 2005. 44(19): p. 2852-2869.
87. Kwiatkowski, A.V., F.B. Gertler, and J.J. Loureiro, *Function and regulation of Ena/VASP proteins*. *Trends Cell Biol*, 2003. 13(7): p. 386-92.
88. Yu, T.W., et al., *Shared receptors in axon guidance: SAX-3/Robo signals via UNC-34/Enabled and a Netrin-independent UNC-40/DCC function*. *Nat Neurosci*, 2002. 5(11): p. 1147-54.
89. Klostermann, A., et al., *The orthologous human and murine semaphorin 6A-1 proteins (SEMA6A-1/Sema6A-1) bind to the enabled/vasodilator-stimulated phosphoprotein-like protein (EVL) via a novel carboxyl-terminal zyxin-like domain*. *J Biol Chem*, 2000. 275(50): p. 39647-53.
90. Barzik, M., et al., *The N-terminal domain of Homer/Vesl is a new class II EVHI domain*. *J Mol Biol*, 2001. 309(1): p. 155-69.
91. Irie, K., et al., *Crystal structure of the Homer 1 family conserved region reveals the interaction between the EVHI domain and own proline-rich motif*. *J Mol Biol*, 2002. 318(4): p. 1117-26.
92. Shiraishi-Yamaguchi, Y. and T. Furuichi, *The Homer family proteins*. *Genome Biology*, 2007. 8(2): p. 206.
93. Beneken, J., et al., *Structure of the Homer EVHI domain-peptide complex reveals a new twist in polyproline recognition*. *Neuron*, 2000. 26(1): p. 143-54.
94. Barzik, M., et al., *Crystallization and preliminary X-ray analysis of the EVHI domain of Vesl-2b*. *Acta Crystallogr D Biol Crystallogr*, 2000. 56 ( Pt 7): p. 930-2.
95. Kato, A., et al., *vesl, a gene encoding VASP/Ena family related protein, is upregulated during seizure, long-term potentiation and synaptogenesis*. *FEBS Lett*, 1997. 412(1): p. 183-9.
96. Volkman, B.F., et al., *Structure of the N-WASP EVHI domain-WIP complex: insight into the molecular basis of Wiskott-Aldrich Syndrome*. *Cell*, 2002. 111(4): p. 565-76.
97. Peterson, F.C., et al., *Multiple WASP-interacting Protein Recognition Motifs Are Required for a Functional Interaction with N-WASP*. *J. Biol. Chem.*, 2007. 282(11): p. 8446-8453.
98. Symons, M., et al., *Wiskott-Aldrich syndrome protein, a novel effector for the GTPase CDC42Hs, is implicated in actin polymerization*. *Cell*, 1996. 84(5): p. 723-34.
99. Pawson, T. and P. Nash, *Assembly of Cell Regulatory Systems Through Protein Interaction Domains*. *Science*, 2003. 300(5618): p. 445-452.

100. Pawson, T. and J.D. Scott, *Protein phosphorylation in signaling - 50 years and counting*. Trends in Biochemical Sciences, 2005. 30(6): p. 286-290.
101. Shoemaker, B.A. and A.R. Panchenko, *Deciphering protein-protein interactions. Part II. Computational methods to predict protein and domain interaction partners*. PLoS Comput Biol, 2007. 3(4): p. e43.
102. Linding, R., et al., *Systematic Discovery of In Vivo Phosphorylation Networks*. Cell, 2007. 129(7): p. 1415-1426.
103. Chatr-aryamontri, A., et al., *MINT: the Molecular INTERaction database*. Nucleic Acids Res, 2007. 35(Database issue): p. D572-4.
104. Salwinski, L., et al., *The Database of Interacting Proteins: 2004 update*. Nucleic Acids Res, 2004. 32(Database issue): p. D449-51.
105. Kitano, H., *Systems biology: a brief overview*. Science, 2002. 295(5560): p. 1662-4.
106. Westerhoff, H.V. and B.O. Palsson, *The evolution of molecular biology into systems biology*. Nat Biotechnol, 2004. 22(10): p. 1249-52.
107. Bruggeman, F.J. and H.V. Westerhoff, *The nature of systems biology*. Trends in Microbiology, 2007. 15(1): p. 45-50.
108. Butcher, E.C., E.L. Berg, and E.J. Kunkel, *Systems biology in drug discovery*. Nat Biotechnol, 2004. 22(10): p. 1253-9.
109. Janes, K.A. and M.B. Yaffe, *Data-driven modelling of signal-transduction networks*. Nat Rev Mol Cell Biol, 2006. 7(11): p. 820-8.
110. Cesareni, G., et al., *Comparative interactomics*. FEBS Letters, 2005. 579(8): p. 1828-1833.
111. Pawson, T. and P. Nash, *Protein-protein interactions define specificity in signal transduction*. Genes Dev., 2000. 14(9): p. 1027-1047.
112. Pawson, T. and J.D. Scott, *Signaling Through Scaffold, Anchoring, and Adaptor Proteins*. Science, 1997. 278(5346): p. 2075-2080.
113. Hlavacek, W.S., et al., *Rules for modeling signal-transduction systems*. Sci STKE, 2006. 2006(344): p. re6.
114. Pawson, T., *Dynamic control of signaling by modular adaptor proteins*. Current Opinion in Cell Biology, 2007. 19(2): p. 112-116.
115. Santonico, E., L. Castagnoli, and G. Cesareni, *Methods to reveal domain networks*. Drug Discovery Today, 2005. 10(16): p. 1111-1117.
116. Zarrinpar, A., R.P. Bhattacharyya, and W.A. Lim, *The Structure and Function of Proline Recognition Domains*. Sci. STKE, 2003. 2003(179): p. re8-.
117. Palsdottir, H. and C. Hunte, *Lipids in membrane protein structures*. Biochimica et Biophysica Acta (BBA) - Biomembranes, 2004. 1666(1-2): p. 2-18.
118. Lee, A.G., *How lipids affect the activities of integral membrane proteins*. Biochimica et Biophysica Acta (BBA) - Biomembranes, 2004. 1666(1-2): p. 62-87.
119. Lemmon, M.A., *Pleckstrin homology (PH) domains and phosphoinositides*. Biochem Soc Symp, 2007(74): p. 81-93.
120. Heuer, K., et al., *The Helically Extended SH3 Domain of the T Cell Adaptor Protein ADAP is a Novel Lipid Interaction Domain*. Journal of Molecular Biology, 2005. 348(4): p. 1025-1035.
121. Fabbro, D., et al., *Protein kinases as targets for anticancer agents: from inhibitors to useful drugs*. Pharmacology & Therapeutics, 2002. 93(2-3): p. 79-98.

122. Dubinina, G.G., et al., *In Silico Design of Protein Kinase Inhibitors: Successes and Failures*. *Anti-Cancer Agents in Medicinal Chemistry (Formerly Current Medicinal Chemistry - Anti-Cancer Agents)*, 2007. 7: p. 171-188.
123. Smolenski, A., et al., *Functional analysis of cGMP-dependent protein kinases I and II as mediators of NO/cGMP effects*. *Naunyn Schmiedebergs Arch Pharmacol*, 1998. 358(1): p. 134-9.
124. Smolenski, A., et al., *Analysis and regulation of vasodilator-stimulated phosphoprotein serine 239 phosphorylation in vitro and in intact cells using a phosphospecific monoclonal antibody*. *J Biol Chem*, 1998. 273(32): p. 20029-35.
125. Shoemaker, B.A. and A.R. Panchenko, *Deciphering protein-protein interactions. Part I. Experimental techniques and databases*. *PLoS Comput Biol*, 2007. 3(3): p. e42.
126. Phizicky, E.M. and S. Fields, *Protein-protein interactions: methods for detection and analysis*. *Microbiol Rev*, 1995. 59(1): p. 94-123.
127. Knuesel, M., et al., *Identification of novel protein-protein interactions using a versatile mammalian tandem affinity purification expression system*. *Mol Cell Proteomics*, 2003. 2(11): p. 1225-33.
128. Rigaut, G., et al., *A generic protein purification method for protein complex characterization and proteome exploration*. *Nat Biotechnol*, 1999. 17(10): p. 1030-2.
129. Ho, Y., et al., *Systematic identification of protein complexes in Saccharomyces cerevisiae by mass spectrometry*. *Nature*, 2002. 415(6868): p. 180-3.
130. Chien, C.T., et al., *The two-hybrid system: a method to identify and clone genes for proteins that interact with a protein of interest*. *Proc Natl Acad Sci U S A*, 1991. 88(21): p. 9578-82.
131. Fields, S. and O. Song, *A novel genetic system to detect protein-protein interactions*. *Nature*, 1989. 340(6230): p. 245-6.
132. Fields, S. and R. Sternglanz, *The two-hybrid system: an assay for protein-protein interactions*. *Trends Genet*, 1994. 10(8): p. 286-92.
133. Dove, S.L., J.K. Joung, and A. Hochschild, *Activation of prokaryotic transcription through arbitrary protein-protein contacts*. *Nature*, 1997. 386(6625): p. 627-630.
134. Serebriiskii, I.G., et al., *A Combined Yeast/Bacteria Two-hybrid System: Development and Evaluation*. *Mol Cell Proteomics*, 2005. 4(6): p. 819-826.
135. Fearon, E.R., et al., *Karyoplasmic interaction selection strategy: a general strategy to detect protein-protein interactions in mammalian cells*. *Proc Natl Acad Sci U S A*, 1992. 89(17): p. 7958-62.
136. Ladant, D. and G. Karimova, *Genetic systems for analyzing protein-protein interactions in bacteria*. *Research in Microbiology*, 2000. 151(9): p. 711-720.
137. Joung, J.K., E.I. Ramm, and C.O. Pabo, *A bacterial two-hybrid selection system for studying protein-DNA and protein-protein interactions*. *PNAS*, 2000. 97(13): p. 7382-7387.
138. Dove, S.L. and A. Hochschild, *Conversion of the omega subunit of Escherichia coli RNA polymerase into a transcriptional activator or an activation target*. *Genes Dev*, 1998. 12(5): p. 745-54.
139. Brent, R. and R.L. Finley, Jr., *Understanding gene and allele function with two-hybrid methods*. *Annu Rev Genet*, 1997. 31: p. 663-704.
140. Legrain, P. and L. Selig, *Genome-wide protein interaction maps using two-hybrid systems*. *FEBS Letters*, 2000. 480(1): p. 32-36.
141. Uetz, P., *Two-hybrid arrays*. *Current Opinion in Chemical Biology*, 2002. 6(1): p. 57-62.

- 
142. Fields, S., *High-throughput two-hybrid analysis. The promise and the peril.* FEBS Journal, 2005. 272(21): p. 5391-5399.
143. Ito, T., et al., *A comprehensive two-hybrid analysis to explore the yeast protein interactome.* Proc Natl Acad Sci U S A, 2001. 98(8): p. 4569-74.
144. Uetz, P., et al., *A comprehensive analysis of protein-protein interactions in Saccharomyces cerevisiae.* Nature, 2000. 403(6770): p. 623-7.
145. Wagner, A., *Does selection mold molecular networks?* Sci STKE, 2003. 2003(202): p. PE41.
146. Rual, J.-F., et al., *Towards a proteome-scale map of the human protein-protein interaction network.* Nature, 2005. 437(7062): p. 1173-1178.
147. Stelzl, U. and E.E. Wanker, *The value of high quality protein-protein interaction networks for systems biology.* Current Opinion in Chemical Biology, 2006. 10(6): p. 551-558.
148. Kehoe, J.W. and B.K. Kay, *Filamentous phage display in the new millennium.* Chem Rev, 2005. 105(11): p. 4056-72.
149. Hoess, R.H., *Protein design and phage display.* Chem Rev, 2001. 101(10): p. 3205-18.
150. McCafferty, J., et al., *Phage antibodies: filamentous phage displaying antibody variable domains.* Nature, 1990. 348(6301): p. 552-554.
151. Sidhu, S.S., *Full-length antibodies on display.* Nat Biotech, 2007. 25(5): p. 537-538.
152. Carmen, S. and L. Jermutus, *Concepts in antibody phage display.* Brief Funct Genomic Proteomic, 2002. 1(2): p. 189-203.
153. Russel, M., H. Lowman, and T. Clackson, *Introduction to phage biology and phage display.* Phage Display : A Practical Approach ed. T.C.a.H.B. Lowman. 2004, Oxford University Press. 1-26.
154. Tonikian, R., et al., *Identifying specificity profiles for peptide recognition modules from phage-displayed peptide libraries.* Nat Protoc, 2007. 2(6): p. 1368-86.
155. Kay, B.K., J. Kasanov, and M. Yamabhai, *Screening Phage-Displayed Combinatorial Peptide Libraries.* Methods, 2001. 24(3): p. 240-246.
156. Kofler, M., et al., *Novel interaction partners of the CD2BP2-GYF domain.* J Biol Chem, 2005. 280(39): p. 33397-402.
157. Dennis, M.S.a.l., H.B., *Phage selection strategies for improved affinity and specificity of proteins and peptides.* Phage Display A Practical Approach ed. T.C.a.H.B. Lowman. 2004, Oxford University Press. 61-83.
158. Felici, F., et al., *Selection of antibody ligands from a large library of oligopeptides expressed on a multivalent exposition vector.* Journal of Molecular Biology, 1991. 222(2): p. 301-310.
159. Parmley, S.F. and G.P. Smith, *Antibody-selectable filamentous fd phage vectors: affinity purification of target genes.* Gene, 1988. 73(2): p. 305-18.
160. Frank, R. and H. Overwin, *SPOT synthesis. Epitope analysis with arrays of synthetic peptides prepared on cellulose membranes.* Methods Mol Biol, 1996. 66: p. 149-69.
161. Frank, R., *The SPOT-synthesis technique: Synthetic peptide arrays on membrane supports--principles and applications.* Journal of Immunological Methods, 2002. 267(1): p. 13-26.
162. Burgoyne, N.J. and R.M. Jackson, *Predicting protein interaction sites: binding hot-spots in protein-protein and protein-ligand interfaces.* Bioinformatics, 2006. 22(11): p. 1335-1342.

- 
163. Berry, D.M., et al., *A high-affinity Arg-X-X-Lys SH3 binding motif confers specificity for the interaction between Gads and SLP-76 in T cell signaling*. *Curr Biol*, 2002. 12(15): p. 1336-41.
164. Pires, J.R., et al., *Solution structures of the YAP65 WW domain and the variant L30 K in complex with the peptides GTPPPPYTVG, N-(n-octyl)-GPPPY and PLPPY and the application of peptide libraries reveal a minimal binding epitope*. *J Mol Biol*, 2001. 314(5): p. 1147-56.
165. Wiedemann, U., et al., *Quantification of PDZ domain specificity, prediction of ligand affinity and rational design of super-binding peptides*. *J Mol Biol*, 2004. 343(3): p. 703-18.
166. Toepert, F., et al., *Combining SPOT synthesis and native peptide ligation to create large arrays of WW protein domains*. *Angew Chem Int Ed Engl*, 2003. 42(10): p. 1136-40.
167. Landgraf, C., et al., *Protein interaction networks by proteome peptide scanning*. *PLoS Biol*, 2004. 2(1): p. E14.
168. Simm, A., M. Nestler, and V. Hoppe, *PDGF-AA, a potent mitogen for cardiac fibroblasts from adult rats*. *J Mol Cell Cardiol*, 1997. 29(1): p. 357-68.
169. Laemmli, U.K., *Cleavage of structural proteins during the assembly of the head of bacteriophage T4*. *Nature*, 1970. 227(5259): p. 680-5.
170. Zimmermann, J., et al., *1H, 13C and 15N resonance assignment of the human Spred2 EVH1 domain*. *J Biomol NMR*, 2004. 29(3): p. 435-6.
171. Yamamoto, K.R., et al., *Rapid bacteriophage sedimentation in the presence of polyethylene glycol and its application to large-scale virus purification*. *Virology*, 1970. 40(3): p. 734-744.
172. Frank Szoka, J.D.P., *Comparative Properties and Methods of Preparation of Lipid Vesicles (Liposomes)*. *Ann. Rev. Biophys. Bioeng*, 1980. 9: p. 467-508.
173. Ishizaki, T., et al., *Pharmacological properties of Y-27632, a specific inhibitor of rho-associated kinases*. *Mol Pharmacol*, 2000. 57(5): p. 976-83.
174. Keller, H.U. and V. Niggli, *The PKC-inhibitor Ro 31-8220 selectively suppresses PMA- and diacylglycerol-induced fluid pinocytosis and actin polymerization in PMNs*. *Biochem Biophys Res Commun*, 1993. 194(3): p. 1111-6.
175. Toullec, D., et al., *The bisindolylmaleimide GF 109203X is a potent and selective inhibitor of protein kinase C*. *J Biol Chem*, 1991. 266(24): p. 15771-81.
176. Marmy-Conus, N., K.M. Hannan, and R.B. Pearson, *Ro 31-6045, the inactive analogue of the protein kinase C inhibitor Ro 31-8220, blocks in vivo activation of p70(s6k)/p85(s6k): implications for the analysis of S6K signalling*. *FEBS Lett*, 2002. 519(1-3): p. 135-40.
177. Burkhardt, M., et al., *KT5823 inhibits cGMP-dependent protein kinase activity in vitro but not in intact human platelets and rat mesangial cells*. *J Biol Chem*, 2000. 275(43): p. 33536-41.
178. Davies, S.P., et al., *Specificity and mechanism of action of some commonly used protein kinase inhibitors*. *Biochem J*, 2000. 351(Pt 1): p. 95-105.
179. Mochly-Rosen, D., H. Khaner, and J. Lopez, *Identification of intracellular receptor proteins for activated protein kinase C*. *Proc Natl Acad Sci U S A*, 1991. 88(9): p. 3997-4000.
180. Mosior, M. and A.C. Newton, *Mechanism of interaction of protein kinase C with phorbol esters. Reversibility and nature of membrane association*. *J Biol Chem*, 1995. 270(43): p. 25526-33.
181. Mullershausen, F., et al., *Direct activation of PDE5 by cGMP: long-term effects within NO/cGMP signaling*. *J Cell Biol*, 2003. 160(5): p. 719-27.

182. Smolenski, A., et al., *Quantitative analysis of the cardiac fibroblast transcriptome-implications for NO/cGMP signaling*. Genomics, 2004. 83(4): p. 577-87.
183. Newton, A.C. and J.E. Johnson, *Protein kinase C: a paradigm for regulation of protein function by two membrane-targeting modules*. Biochim Biophys Acta, 1998. 1376(2): p. 155-72.
184. Nishizuka, Y., *Studies and perspectives of protein kinase C*. Science, 1986. 233(4761): p. 305-12.
185. Newton, A.C., *Protein kinase C: structural and spatial regulation by phosphorylation, cofactors, and macromolecular interactions*. Chem Rev, 2001. 101(8): p. 2353-64.
186. Johnson, J.A., S. Adak, and D. Mochly-Rosen, *Prolonged phorbol ester treatment down-regulates protein kinase C isozymes and increases contraction rate in neonatal cardiac myocytes*. Life Sci, 1995. 57(11): p. 1027-38.
187. Hu, J.C., M.G. Kornacker, and A. Hochschild, *Escherichia coli One- and Two-Hybrid Systems for the Analysis and Identification of Protein-Protein Interactions*. Methods, 2000. 20(1): p. 80-94.
188. Giesecke, A.V.a.J.K.J., *Bacterial two-hybrid system for studying and modifying protein-protein interactions*. Protein-protein interactions: a molecular cloning manual, ed. E.A.G.a.P.D. Adams. 2005, Cold Spring Harbor, New York, Cold Spring Harbor Laboratory Press. 195-216.
189. Brennan, M.B. and K. Struhl, *Mechanisms of increasing expression of a yeast gene in Escherichia coli*. Journal of Molecular Biology, 1980. 136(3): p. 333-338.
190. Hollingshead, S. and D. Vapnek, *Nucleotide sequence analysis of a gene encoding a streptomycin/spectinomycin adenylyltransferase*. Plasmid, 1985. 13(1): p. 17-30.
191. Whipple, F.W., *Genetic analysis of prokaryotic and eukaryotic DNA-binding proteins in Escherichia coli*. Nucl. Acids Res., 1998. 26(16): p. 3700-3706.
192. Hochschild, A., *Transcriptional Activation: How [lambda] repressor talks to RNA polymerase*. Current Biology, 1994. 4(5): p. 440-442.
193. Dove, S.L. and A. Hochschild, *Use of artificial activators to define a role for protein-protein and protein-DNA contacts in transcriptional activation*. Cold Spring Harb Symp Quant Biol, 1998. 63: p. 173-80.
194. Nickels, B.E., et al., *Protein-Protein and Protein-DNA Interactions of [sigma]70 Region 4 Involved in Transcription Activation by [lambda]cI*. Journal of Molecular Biology, 2002. 324(1): p. 17-34.
195. Barberis, A., et al., *Contact with a component of the polymerase II holoenzyme suffices for gene activation*. Cell, 1995. 81(3): p. 359-68.
196. Hidalgo, P., et al., *Recruitment of the transcriptional machinery through GAL11P: structure and interactions of the GAL4 dimerization domain*. Genes Dev, 2001. 15(8): p. 1007-20.
197. Farrell, S., et al., *Gene activation by recruitment of the RNA polymerase II holoenzyme*. Genes Dev, 1996. 10(18): p. 2359-67.
198. Estojak, J., R. Brent, and E.A. Golemis, *Correlation of two-hybrid affinity data with in vitro measurements*. Mol. Cell. Biol., 1995. 15(10): p. 5820-5829.
199. Scott, J.K. and G.P. Smith, *Searching for peptide ligands with an epitope library*. Science, 1990. 249(4967): p. 386-90.
200. Smith, G.P., *Filamentous fusion phage: novel expression vectors that display cloned antigens on the virion surface*. Science, 1985. 228(4705): p. 1315-7.
201. Rickles, R.J., et al., *Identification of Src, Fyn, Lyn, PI3K and Abl SH3 domain ligands using phage display libraries*. Embo J, 1994. 13(23): p. 5598-604.

- 
202. Gordon, E.M., et al., *Applications of combinatorial technologies to drug discovery. 2. Combinatorial organic synthesis, library screening strategies, and future directions.* J Med Chem, 1994. 37(10): p. 1385-401.
203. Kofler, M., K. Motzny, and C. Freund, *GYF domain proteomics reveals interaction sites in known and novel target proteins.* Mol Cell Proteomics, 2005. 4(11): p. 1797-811.
204. Freund, C., et al., *Dynamic interaction of CD2 with the GYF and the SH3 domain of compartmentalized effector molecules.* Embo J, 2002. 21(22): p. 5985-95.
205. Heuer, K., et al., *Lipid-binding hSH3 Domains in Immune Cell Adapter Proteins.* Journal of Molecular Biology, 2006. 361(1): p. 94-104.
206. Zimmermann, P., *The prevalence and significance of PDZ domain-phosphoinositide interactions.* Biochimica et Biophysica Acta (BBA) - Molecular and Cell Biology of Lipids, 2006. 1761(8): p. 947-956.
207. Lemmon, M.A. and K.M. Ferguson, *Signal-dependent membrane targeting by pleckstrin homology (PH) domains.* Biochem. J., 2000. 350(1): p. 1-18.
208. Dowler, S., G. Kular, and D.R. Alessi, *Protein Lipid Overlay Assay.* Sci. STKE, 2002. 2002(129): p. pl6-.
209. Zaidel-Bar, R., et al., *Functional atlas of the integrin adhesome.* Nat Cell Biol, 2007. 9(8): p. 858-67.
210. Narumiya, S., T. Ishizaki, and N. Watanabe, *Rho effectors and reorganization of actin cytoskeleton.* FEBS Lett, 1997. 410(1): p. 68-72.
211. Blobe, G.C., et al., *Protein kinase C beta II specifically binds to and is activated by F-actin.* J Biol Chem, 1996. 271(26): p. 15823-30.
212. Chio, C.C., et al., *PKA-dependent activation of PKC, p38 MAPK and IKK in macrophage: implication in the induction of inducible nitric oxide synthase and interleukin-6 by dibutyryl cAMP.* Cell Signal, 2004. 16(5): p. 565-75.
213. Tai, T.C. and D.L. Wong, *Protein kinase A and protein kinase C signaling pathway interaction in phenylethanolamine N-methyltransferase gene regulation.* J Neurochem, 2003. 85(3): p. 816-29.
214. Ziegler, W.H., et al., *A lipid-regulated docking site on vinculin for protein kinase C.* J Biol Chem, 2002. 277(9): p. 7396-404.
215. Keenan, C. and D. Kelleher, *Protein kinase C and the cytoskeleton.* Cell Signal, 1998. 10(4): p. 225-32.
216. Hou, Y., et al., *Activation of cGMP-dependent protein kinase by protein kinase C.* J Biol Chem, 2003. 278(19): p. 16706-12.
217. Toby, G.G. and E.A. Golemis, *Using the yeast interaction trap and other two-hybrid-based approaches to study protein-protein interactions.* Methods, 2001. 24(3): p. 201-17.
218. Phizicky, E., et al., *Protein analysis on a proteomic scale.* Nature, 2003. 422(6928): p. 208-15.
219. Allen, J.B., et al., *Finding prospective partners in the library: the two-hybrid system and phage display find a match.* Trends Biochem Sci, 1995. 20(12): p. 511-6.
220. Bailey, T.L., et al., *MEME: discovering and analyzing DNA and protein sequence motifs.* Nucleic Acids Res, 2006. 34(Web Server issue): p. W369-73.
221. Seet, B.T., et al., *Reading protein modifications with interaction domains.* Nat Rev Mol Cell Biol, 2006. 7(7): p. 473-483.



## 8. Abbreviations

3-AT	3-amino-1, 2, 4-triazole
8pCPT-cGMP	8-(para-Chlorophenylthio) guanosine-3',5'-cyclic monophosphate
<i>aadA</i>	Aminoglycoside 3`adenyltransferase
Abl	Ableson tyrosine kinase
AC	Adenylate cyclase
ADAP	adhesion- and degranulation-promoting adaptor protein)
AMPK	AMP activated protein kinase
APS	Amonium persulfate
Arp 2/3	Actin related protein 2/3 complex
ATP	Adenosine triphosphate
B2H system	Bacterial two-hybrid system
Bis I	Bisindolylmaleimide I
Bis V	Bisindolylmaleimide V
DMEM	Dulbecco's Modified Eagle Medium
DMSO	Dimethyl Sulfoxide
ECL	Enhanced chemoluminescence
EDTA	Ethylendiamine tetraacetic acid
EGF	Epithelial growth factor
EVH1	Ena/VASP homology 1
EVH2	Ena/VASP homology 2
EVL	Ena/VASP-like
F-actin	Filamentous actin
FCS	Foetal Calf Serum
Fyb/SLAP	Fyn binding protein/SLP76 associated protein
G-actin	Globular actin (monomeric actin)
IP3	Inositol-1,4,5-triphosphate
IPTG	Isopropyl- $\beta$ -D-Thiogalacto(pyrano)side
KBD	c-Kit binding domain
LPA	Lysophosphatidic acid
LPP	Lipoma preferred partner
MAP Kinase	Myosin activated protein kinase
MARCKS	Myrostylated alanine-rich C-kinase substrate
MCFB	Mouse cardiac fibroblast

---

Mena	Mammalian enabled
MINT	Molecular INTeraction database
MLC	Myosin light chain
MLCK	Myosin light chain kinase
NMR	Nuclear magnetic resonance
PBS	Phosphate buffered saline
PC	phosphatidylcholine
PEG	Poly ethylene glycol
PKA	Protein kinase A
PKC	Protein kinase C
PKG	Protein kinase G
PMA	Phorbol 12-Myristate 13-Acetate
PRM	Proline rich motif
PRR	Proline rich region
PS	phosphatidylserine
PtdIns(3)P	phosphatidyl inositol 3-phosphate
PtdIns(5)P	phosphatidyl inositol 5-phosphate
RACKS	Receptor for activated C-kinases
Robo	Roundabout
Rp-8-Br-cAMPS	8- Bromoadenosine- 3', 5'- cyclic monophosphorothioate, Rp-isomer
SDS	Sodium dodecyl sulphate
SEMA6A-1	semaphoring 6A-1 protein
SGC	Structural genomic consortium
SH3	Src homology domain 3
SNP	Sodium nitro prusside
SPR	Sprouty related
Spred	Sprouty related with an EVH1 domain
SRE	Serum Response Element
SRF	Serum Response Factor
TEMED	N,N,N',N'-tetramethyldiamine
VASP	Vasodilator Stimulated phosphoprotein
WASP	Wiskott Aldrich Syndrome protein
WH1	WASP homology 1

## 9. Curriculum Vitae

**Name:** Naresh Reddy Thumati

**Date of birth:** 4<sup>th</sup> October 1976

**Place of birth:** Kodada, India

### Academic details

- |                   |  |
|-------------------|--|
| <b>1992</b>       | <b>Secondary School Education</b><br>St. Xavier's High School<br>Suryapeta, AP, India  |
| <b>1994</b>       | <b>Board of Intermediate Education</b><br>PRMS National College,<br>Vijayawada, AP, India  |
| <b>1999</b>       | <b>Bachelor of Science (Genetics)</b><br>P. B. Siddhartha College of Arts and Science<br>Vijayawada, AP, India                                     |
| <b>2001</b>       | <b>Master of Science in Biotechnology</b><br>University of Hyderabad,<br>Hyderabad, India  |
| <b>Since 2003</b> | <b>Doctoral student</b><br>Institut für Klinische Biochemie und Pathobiochemie<br>der Bayerischen Julius-Maximilians-Universität Würzburg, Germany |

### Publications and Posters:

- Chen L, Daum G, Chitale K, Coats SA, Bowen-Pope DF, Eigenthaler M, **Thumati NR**, Walter U, Clowes AW. **Vasodilator-stimulated phosphoprotein regulates proliferation and growth inhibition by nitric oxide in vascular smooth muscle cells.** *Arteriosclerosis, thrombosis, and vascular biology.* 2004 Aug; 24(8):1403-8
- **N. R. Thumati**, T. Jarchau, U. Walter. **Interaction cloning approaches in search of binding epitopes for a new group of EVH1 Domains.** Poster presented at DGKL meeting, Sept-2007, Vienna, Austria.